Tampere University

BRUNO DI BUÒ

Evaluation of the Preconsolidation Stress and Deformation Characteristics of Finnish Clays based on Piezocone Testing

Tampere University Dissertations 222

Tampere University Dissertations 222

BRUNO DI BUÒ

Evaluation of the Preconsolidation Stress and Deformation Characteristics of Finnish Clays based on Piezocone Testing

ACADEMIC DISSERTATION
To be presented, with the permission of
the Faculty of Built Environment
of Tampere University,
for public discussion in the auditorium RG202
of the Rakennustalo, Korkeakoulunkatu 5, Tampere,
on 13 March 2020, at 12 o'clock.

ACADEMIC DISSERTATION
Tampere University, Faculty of Built Environment
Finland

Responsible supervisor and Custos	Prof. Tim Länsivaara Tampere University Finland	
Pre-examiners	Prof. Emeritus Peter K. Robertson Technical Director Gregg Drilling&Testing, Inc. USA	Prof. Michael Long University College Dublin Ireland
Opponents	Prof. Laura Tonni Università di Bologna Italy	Prof. Michael Long University College Dublin Ireland

The originality of this thesis has been checked using the Turnitin OriginalityCheck service.

Cover design: Roihu Inc.

ISBN 978-952-03-1467-5 (print)
ISBN 978-952-03-1468-2 (pdf)
ISSN 2489-9860 (print)
ISSN 2490-0028 (pdf)
http://urn.fi/URN:ISBN:978-952-03-1468-2

PunaMusta Oy – Yliopistopaino
Tampere 2020

ACKNOWLEDGEMENTS

These past few years spent in Finland have been a truly life-changing experience and today, at the end of this journey, I am deeply grateful to everyone who has supported, encouraged, and believed in me. None of this would be possible without my family, colleagues and amazing friends met along the way.

First and foremost, I would like to extend my sincere gratitude to my supervisor Prof. Tim Länsivaara for his continuous support, valuable guidance and encouragement throughout my studies. I owe him my gratitude for the opportunity to join the Geotechnical Department at Tampere University, attending and presenting at international conferences, and for helping me become a better researcher.

My heartfelt thanks to Prof. Paul W. Mayne for hosting me at Georgia Institute of Technology in 2018 as a visiting student. His endless sincere support and useful advice were fundamental in this research study.

I would like to thank my pre-examiners, Prof. Emeritus Peter K. Robertson and Prof. Michael Long, and my opponent Prof. Laura Tonni for their valuable comments and suggestions. I feel honored that this dissertation has been evaluated by such relevant professionals in the geotechnical engineering field.

I warmly thank the staff at the Built Environment Department and, in particular, my "FINCONE" mates Juha and Markus for their incredible effort during the field and laboratory testing, and my colleagues Ali and Mohammed.

The time spent far from home has been very tough, especially during the cold and dark winter days. Luckily, in Finland, I have met amazing friends who have made this experience simply unforgettable. First of all, my housemate and travel mate Andrea, who has filled this journey with his contagious happiness, exuberance, enthusiasm and positive attitude. Thanks to my friend and colleague Marco for introducing me to Finland and for the help in these past years. I will miss the time

spent with Pinò, the countless nights working together at the university, the laughs and, above all, his honest friendship. To Waqar, who taught me that in life it is never too late to turn the page and move forward. Thanks to the worst roommate ever, Ugur, because, despite several misunderstandings, our discussions were always a source of personal growth. Thanks to the "forever young" and "expert of everything" Alessandro for the great life lessons he gave us during these years. Thanks to Lucio, Chiara and Donato for putting up with my endless complaints on the Finnish weather; to "soon to be" Prof. Stefano Papirio, for the amazing time spent training at GoGo gym and for the outdoor bike rides; to Gianpiero and Stefano Oscurato, for being such amazing and trustworthy friends. Thanks to my Erasmus friends, in particular Simone, Ivana, Francesco, Giulio, Mirko and Nico for their youthful vitality.

Despite being away from home, I could always count on Luca, Maurizio, and Andrea, old colleagues from UNIVPM, and Ilaria, thank you for the support in the tough time.

Last but not least, sincere deep gratitude to my family who has been dealing with my messed up life all these years. Mom and Dad, thank you for your unconditional love and for teaching me what really matters in life. Thanks to my brothers, Gianluca and Alberto, and my sister, Claudia for being there supporting me when I needed it the most. I owe you this achievement.

Finally, thank you Finland for the incredible sunsets, the northern lights, the green forests and blue lakes, the colorful autumn, and the never ending summer days. Thank you for giving me such happy days.

I will keep you all in my heart.

Tampere, December 2019

Bruno Di Buò

ABSTRACT

The design of structures and infrastructures in soft soil areas represents an important challenge in geotechnical engineering owing to the poor soil properties in terms of strength and compressibility. In this scenario, a proper geotechnical investigation plan is fundamental to evaluate geotechnical parameters for conducting stability analysis and settlement prediction. Over the past decades, in Finland, the field vane test had been widely adopted as the traditional field investigation tool. However, recent studies conducted at Tampere University (formerly Tampere University of Technology) have revealed that this test often encounters many problems in terms of accuracy, precision, and results interpretation. The present study aims to overcome these issues and improve the quality of ground investigation data in Finnish soft clays promoting the use of piezocone testing. Although this test has proven high reliability in different soil conditions, its applicability in soft sensitive clays requires high accuracy in terms of measurement and interpretation. Therefore, an extensive experimental program has been conducted on five soft clay sites located in Finland, aiming to build a high quality database of in situ and laboratory test data. In particular, seismic and resistivity piezocones have been adopted for field testing, whereas the laboratory program comprised index tests, one-dimensional constant rate of strain consolidation tests, and triaxial tests. As sample quality represents a key issue in soft sensitive clays, several sampling apparatuses and procedures have been tested to obtain high-quality undisturbed samples. Finally, the collected dataset has been exploited to establish correlations for evaluating the preconsolidation stress and deformation characteristics of the investigated clays. An analytical method based on a spherical cavity expansion theory and critical state soil mechanics solution has been adopted to derive simplified analytical equations for predicting the preconsolidation stress and the constrained modulus based on the piezocone test data. Results indicate that there is a fairly good agreement between the predicted values and the experimental data. Moreover, reliable correlations between the soil compressibility and the natural water content were established while the applicability of the piezocone testing to predict the deformation characteristics turned out to be characterized by high uncertainties.

CONTENTS

1 INTRODUCTION 15
1.1 Motivation and research objectives 15
1.2 Research outline and thesis structure 17

2 ENGINEERING PROPERTIES OF SOFT SENSITIVE CLAYS 18
2.1 Introduction 18
2.2 Origin of Finnish clay deposits 19
2.3 Mineralogical composition of Finnish clays 21
2.4 Engineering properties of soft sensitive clays 23
2.4.1 Stress history of natural soil deposits 24
2.4.2 Settlement calculation methods 25
2.4.2.1 Compression index method 26
2.4.2.2 Tangent modulus calculation method 28
2.4.2.3 CRS Swedish settlement calculation method 30

3 FIELD AND LABORATORY INVESTIGATION 32
3.1 Experimental program objectives 32
3.2 Cone penetration test (CPT) 33
3.2.1 CPTu equipment 34
3.2.2 Additional modules 36
3.2.3 Test procedure 38
3.2.4 CPTu data correction 39
3.2.5 CPTu data quality 41
3.2.6 CPTu interpretation in fine grained soils 42
3.3 Undisturbed sampling 47
3.3.1 Causes of disturbance of soft sensitive clays 48
3.3.2 Sampling equipment 51
3.3.2.1 ST:1 50 stationary piston sampler 52
3.3.2.2 Aalto 86 piston sampler 53
3.3.2.3 Mini-block sampler 54
3.3.2.4 TUT 132 tube sampler 56
3.4 Constant rate of strain (CRS) oedometer test 57

4 EXPERIMENTAL PROGRAM RESULTS 60
4.1 Introduction 60
4.2 Perniö test site 61

4.2.1 Index properties 61
4.2.2 CPTu soundings 62
4.2.3 CRS consolidation tests 65
4.3 Lempäälä test site 66
4.3.1 Index properties 66
4.3.2 CPTu soundings 67
4.3.3 CRS consolidation tests 70
4.4 Masku test site 71
4.4.1 Index properties 71
4.4.2 CPTu soundings 72
4.4.3 CRS consolidation tests 74
4.5 Paimio test site 75
4.5.1 Index properties 75
4.5.2 CPTu soundings 76
4.5.3 CRS consolidation tests 78
4.6 Sipoo test site 78
4.6.1 Index properties 78
4.6.2 CPTu soundings 79
4.6.3 CRS consolidation tests 82
4.7 Evaluation of soil properties from CRS consolidation tests 82
4.7.1 Preconsolidation stress evaluation 83
4.7.2 Evaluation of deformation properties 85
4.8 Sample quality evaluation 89
4.8.1 Performance of the different sampling methods in Finnish clays 92
4.8.2 Storage influence on sample quality 96
4.9 Conclusions 98

5 EVALUATION OF THE PRECONSOLIDATION STRESS OF FINNISH CLAYS FROM CPTu DATA 99
5.1 Introduction 99
5.2 Methods for evaluating the stress history of clays from CPTu data 100
5.2.1 Empirical models 101
5.2.2 Analytical models 103
5.3 Applicability of existing empirical correlation for evaluating the stress history of Finnish clays 105
5.4 Evaluation of the stress history of clays based on the spherical cavity expansion (SCE) and critical state soil mechanics (CSSM) theories 106
5.4.1 Introduction 106
5.4.2 Original SCE-CSSM solution 107
5.4.3 Modified SCE-CSSM solution 112
5.4.4 Evaluation of SCE-CSSM soil parameters 114
5.5 Application of the SCE-CSSM model to Finnish clays 116
5.5.1 Perniö 116

5.5.2 Lempäälä 119
5.5.3 Masku 121
5.5.4 Paimio 122
5.5.5 Sipoo 125
5.6 Validation of the SCE-CSSM analytical solutions 127
5.7 Simplified CPTu-based correlations for Finnish clays 130
5.8 Discussion 133

6 DEFORMATION PROPERTIES OF FINNISH CLAYS 135
6.1 Introduction 135
6.2 Deformation properties of Finnish clays 136
6.2.1 Constrained modulus (M_0) 137
6.2.2 Compression indices C_r and C_c 142
6.3 CPTu applicability in deriving the soil deformation characteristics 145
6.4 Aspects related to primary settlement calculation using Janbu's and Sällfors' methods 148

7 CONCLUSIONS 154
7.1 Concluding remarks 154
7.2 Recommendations for future work 156

8 APPENDICES 173

NOTATION

Latin letter

a	Area correction factor for cone resistance
a'	Attraction
b	Bias factor
c'	Effective cohesion
e	Void ratio
e_0	Initial void ratio
f_s	Sleeve friction
k	Soil permeability
k_0	Coefficient of earth pressure at rest
k_1	Correction factor applied to Sällfors' method
m	Janbu's modulus number
m_{calc}	corrected Janbu's modulus number
m_{test}	Janbu's modulus number evaluated from laboratory test
m_v	Coefficient of compressibility
m_1	Janbu's modulus number in the NC region
m_2	Janbu's modulus number in the OC region
p'	Mean effective stress
p_a	Atmospheric pressure (101.3 kPa)
q	Deviatoric stress q
q_c	Measured cone tip resistance
q_{eff}	Effective cone tip resistance
q_{net}	Net cone tip resistance
q_t	Corrected cone tip resistance
s_u	Undrained shear strength
s_u^{re}	Remolded undrained shear strength
t	Time
u	Pore pressure
u_m	measured penetration pore-water pressure
u_{ps}	Maximum negative pore pressure during sampling
u_0	Hydrostatic pore pressure

u_1	Pore pressure acting at the cone tip
u_2	Pore pressure acting behind the cone
v_s	Shear wave velocity (m/s)
w	Water content
w_L	Liquid limit
w_P	Plastic limit
A_c	Cross-sectional area of the cone
A_n	Cross-sectional area of the load cell
A_s	Sleeve area of the cone
B_q	Pore pressure ratio
C_c	Compression index
C_r	Swelling index
F_c	Axial force at the cone tip
F_r	Friction ratio
F_s	Axial force along the sleeve
G_0	Initial shear modulus (also G_{max})
I	Electric current
I_c	Soil behavior type index
I_r	Rigidity index
K	Soil conductivity
M	Constrained modulus
M_0	Constrained modulus in the OC region
M_L	Constant constrained modulus between σ'_p and σ'_L
M_{oed}	Oedometer modulus
M'	Sällfors' modulus number
N_{kt}	Cone bearing factor
Q_t	Normalized cone tip resistance
S_r	Degree of saturation
S_t	Sensitivity ($S_t = s_u/s_u^{re}$)
V	Voltage

Greek symbols

α	Constrained modulus cone factor
β	Janbu's stress exponent
β_1	Janbu's stress exponent in the NC region
β_2	Janbu's stress exponent in the OC region

Δ	Increment
ε	Strain
ε_a	Axial strain
ε_{NC}	Deformation in the normally consolidated region
ε_{OC}	Deformation in the overconsolidated region
ε_v	Vertical strain
ε_{v0}	Vertical strain at reconsolidation to σ'_{v0}
ϕ'	Effective friction angle
ϕ'_{MO}	Effective friction angle at maximum obliquity
ϕ'_{PEAK}	Effective friction angle at peak strength
γ	Soil unit weight
η	Stress ratio
κ	Modified recompression index
λ	Modified compression index
ν	Specific volume
ρ	Soil density
σ_a	Reference stress (=100 kPa)
σ_c	Cell pressure
σ_v	Vertical total stress
σ_{vy}	Yield vertical stress
σ_{v0}	Initial vertical total stress
σ'_f	Final effective stress
σ'_L	Limit stress according to Sällfors method
σ'_p	Preconsolidation stress
σ'_{pr}	Reference preconsolidation stress
$\sigma'_{p,test}$	Preconsolidation stress evaluated from laboratory test
$\sigma'_{p,calc}$	Calculated preconsolidation stress value
σ'_{ps}	Perfect sampling effective stress
σ'_v	Effective vertical stress
σ'_{v0}	Initial effective vertical stress

Acronyms

CAUC	Anisotropically consolidated undrained triaxial compression test
CIUC	Isotropically consolidated undrained triaxial compression test
COV	Coefficient of variation
CPT	Cone Penetration test
CPTu	Piezocone test
CRS	Constant rate of strain oedometer test
CSSM	Critical state soil mechanics
FTA	Finnish Transport Agency
FV	Field Vane
IL	Incrementally loaded
LI	Liquidity index
LL	Liquid limit
MASW	Multichannel analysis of surface waves
NC	Normally consolidated
NGI	Norwegian Geotechnical Institute
OC	Overconsolidated
OCR	Overconsolidation ratio
PI	Plasticity index
R-CPTu	Resistivity piezocone
S-CPTu	Seismic piezocone
SEM	Scanning electric microscopes
SCE	Spherical cavity expansion
SGI	Swedish Geotechnical Institute
S-CPTu	Seismic piezocone
SLS	Serviceability Limit State
TAU	Tampere University
TUT	Tampere University of Technology
TX	Triaxial
TXC	Triaxial compression

1 INTRODUCTION

1.1 Motivation and research objectives

Understanding the behavior of soft sensitive clays is a key aspect of geotechnical design, particularly in those regions where constructions are planned in marine clay areas. As an example, in Finland, one of the major geotechnical issues is represented by the stability and excessive settlements of railway embankments located on soft soil deposits. In particular, the need to increase the railway capacity in terms of traffic load has a negative impact in meeting the technical requirements of the serviceability limit state (SLS). Various research studies have been conducted by Tampere University (TAU), formerly Tampere University of Technology (TUT), and Finnish Transport Agency (FTA) to improve the stability calculation methods prediction (Mansikkamäki 2015; Lehtonen 2015; D'Ignazio 2016). These studies pointed out that the inaccuracy and uncertainties of both field and laboratory investigation data often lead to erroneous assumption of soil parameters, thus affecting the reliability of stability analysis. In this respect, the interpretation of field measurements as well as the quality of laboratory tests play a key role in the evaluation of soil properties used in the geotechnical design. At present, in Finland, the field vane (FV) is widely employed for in situ testing. However, a recent study conducted at Tampere University highlighted that this test often encounters many issues owing to the apparatus configuration (e.g., down-hole versus up-hole measuring system) and interpretation of measured data which is often characterized by low accuracy and repeatability (Selänpää et al. 2017). Moreover, uncertainties in laboratory testing interpretation are often encountered in low-quality undisturbed specimen retrieved in soft soils using piston sampling techniques. Both these aspects negatively affect the accuracy of the stability analysis and settlement prediction.

In 2014, Tampere University started conducting an extensive research program, referred to as "FINCONE," aiming to overcome the issues related to the investigation in Finnish geotechnical practice. To overcome the issues related to FV testing and improve the quality of field investigation, the FINCONE project aimed to promote the use of the piezocone test (CPTu). Although the CPTu is adopted

worldwide for subsoil investigation and soil characterization, its use in Finland is still at an early stage. In particular, the lack of experience and well-documented test sites did not facilitate this process. Therefore, within the framework of this project, an extensive database has been established collecting data from five different soft clay test sites located in Finland using a piezocone penetrometer equipped with seismic (S-CPTu) and resistivity (R-CPTu) modules. In parallel, a laboratory investigation program comprising index tests, oedometer, and triaxial tests on undisturbed samples has been conducted. As pointed out, the sample quality represents a key aspect in soft clays, which may negatively affect the evaluation of strength and deformation properties. For this reason, effort has been given in improving the sampling operations to retrieve high-quality undisturbed samples by adopting different apparatus and procedures. The obtained dataset has been further exploited to verify the validity of existing CPTu-based empirical and analytical models. Among them, the hybrid spherical cavity expansion (SCE) theory developed by Vesic (1972) combined with critical state soil mechanics (CSSM) solutions (Wroth 1984) have been implemented to assess the stress history of the investigated soil. Finally, the deformation characteristics have been assessed based on the results from the one-dimensional (1D) constant rate of strain (CRS) consolidation test. Three different settlement calculation methods have been adopted for the interpretation of soil compressibility, including the compression index method, tangent modulus method (Janbu 1967), and CRS Swedish method (Sällfors 1975).

The main objectives of the present study can be summarized as:

- Enhance the quality of field investigation by promoting the use CPTu and offering improvements to the data interpretation in Finnish clays;
- Investigate the performances of different undisturbed sampling techniques, including an innovative Laval-type tube sampler (Di Buò et al. 2019b), two stationary piston samplers, and the mini-block sampler (Emdal et al. 2016);
- Build an extensive database of high-quality field and laboratory tests;
- Investigate the validity of existing CPTu-based empirical correlations and establish new models for deriving the stress history and deformation characteristics of Finnish clays.

The present dissertation focuses mainly on the stress history and deformation characteristics of Finnish clays, whereas a parallel study aiming to investigate the strength properties and anisotropy is conducted by Selänpää (2020).

1.2 Research outline and thesis structure

The thesis is divided into the following six chapters:

- Chapter 1, *Introduction*.

- Chapter 2, *Engineering properties of soft sensitive clays*, discusses the Finnish clay deposits' geological origin and mineralogy as well as the fundamental aspects of their mechanical behavior including the stress history and compressibility characteristics.

- Chapter 3, *Field and laboratory investigation*, describes in detail the experimental investigation conducted at the investigated sites with particular emphasis on the CPTu test procedure, the adopted sampling techniques, and the laboratory testing program.

- Chapter 4, *Experimental program results*, presents the field and laboratory test results for each investigated site, focusing on the achieved test quality. In particular, the CPTu soundings quality is evaluated in accordance with the EN-ISO 22476-1 while the sample quality is assessed based on the Lunne et al. (1997) criterion. Moreover, the procedures adopted to evaluate the preconsolidation stress and deformation characteristics are presented.

- Chapter 5, *Evaluation of the preconsolidation stress of Finnish clays from CPTu data*, presents an overview of existing empirical and analytical methods for the evaluation of the preconsolidation stress from CPTu measurements. Among them, an established CPTu analytical solution based on the SCE-CSSM theoretical framework is employed for assessing the stress history profiles of the investigated sites. The obtained results have been exploited to derive simplified CPTu-based correlations valid for Finnish clays.

- Chapter 6, *Deformation properties of Finnish clays*, analyzes the results of CRS consolidation tests conducted on undisturbed samples and discusses in detail the compressibility of Finnish clays. In particular, the accuracy of existing settlement calculation methods is assessed, pointing out the uncertainties related to each model.

- Chapter 7, *Conclusions and future works*.

2 ENGINEERING PROPERTIES OF SOFT SENSITIVE CLAYS

2.1 Introduction

Soft sensitive clay deposits can be found in Scandinavia, Finland, and some regions of North America and Asia. In these regions, geotechnical design is often rather challenging owing to the high compressibility, low undrained shear strength (s_u), and high sensitivity (S_t) shown by the soils. In particular, sensitivity is one of the key geotechnical parameters to consider while investigating these soils. Sensitive clays are characterized by a relatively stiff response in their undisturbed state, turning into a viscous liquid when remolded (Rosenqvist 1953). The sensitivity is defined as the ratio of the s_u measured on the sample in its undisturbed state to the corresponding remolded shear strength (s_u^{re}) at the same natural water content (w). The term "quick clay" refers to highly sensitive clays characterized by S_t of over 50 and/or s_u^{re} of less than 0.4 kPa (Rankka et al. 2004). However, it is not possible to draw up an unambiguous definition of quick clays because of several classification systems are proposed in the literature (Rosenqvist 1953; Bjerrum 1954; Rankka et al. 2004).

The complex mechanical behavior of soft sensitive clays is mainly owing to the depositional and post-depositional processes that induce important transformations in terms of structure and pore-water chemistry. The depositional environment plays an important role in the development of soil sensitivity: most of these clays originated in brackish environment where the high ion concentration reduces the repulsive forces between the soil particles, allowing flocculation. The inter-particle flocculation results in an open structure characterized by high w. In contrast, among the post-depositional processes, salt leaching is considered one of the most relevant factors for soil sensitivity development (Bjerrum 1954; Torrance 1974; Rosenqvist 1978). The reduction of the salt content is mainly attributable to the isostatic uplift above the sea level of the soil deposit, which causes a direct exposure to weathering agents (e.g., rain, water seeping upward due to artesian pressure, and salt diffusion toward zones with lower ion concentrations). As a result of salinity decrease, the soil structure remains unchanged but the repulsive forces increase, which strongly affects the ability of soil particles to re-flocculate after remolding. However, since Finnish

clays mainly originated in fresh water depositional environment, the salt leaching cannot be considered the most relevant post-depositional process causing the development of soil sensitivity. Thus, these aspects would require further investigation for a better understanding of the origin of sensitive clay deposits.

Over the past decades, catastrophic landslides occurred in Canada, Norway, and Sweden, resulting in damages of over several million dollars. On the contrary, Finland has never experienced such significant failure events. The reason for this is not straightforward. First, Finnish clays are characterized by different soil morphology and geotechnical properties, which play an important role in landslides triggering. From this point of view, Finnish clays are generally characterized by higher w and plasticity compared to Scandinavian clays even though similarities between Swedish and Finnish clays have been observed. Moreover, despite the similar sensitivity and remolded shear strength values, Finnish clays require higher amount of energy to reach the remolded configuration (Thakur et al. 2017). Therefore, it should be important to consider the remolding energy in the definition of soil sensitivity. Various researchers have attempted to investigate the influence of the remolding energy in triggering large retrogressive landslides (e.g., Bishop 1971; Tavenas et al. 1983; Thakur et al. 2017). However, to date, a standard energy-based definition has not been proposed.

The present section outlines the geological formation and mineralogical composition of Finnish clays, their mechanical behavior under loading, and the existing settlement calculation methods.

2.2 Origin of Finnish clay deposits

Fine-grained soil sediments in Finland originated in the late Pleistocene, during the retreat of the continental ice sheet in the Weichselian ice age (11,700 years ago). The entire Scandinavian region was covered by a large ice sheet named Fenno-Scandian that spread out from the Scandinavian Mountains to Northwest Russia, UK, and the Netherlands. The stratigraphy of Finnish soil deposits is the result of a series of processes that occurred during the Holocene (10,000 years ago), when the Fenno-Scandian ice sheet retreated. The glacier meltwater accumulated between the front of the ice sheet and the southern shores, giving rise to what currently is the Baltic Sea. In particular, this area underwent four environmental stages in the postglacial progression of the Baltic basin, known as Baltic Ice Lake, Yoldia Sea, Ancylus Lake,

and Littorina Sea (Fig. 2.1). Despite the extensive studies conducted on this topic, the process of the formation of the Baltic Sea is not completely clear. In particular, its connection with the Atlantic Ocean during the different phases made the salinity vary with location, depth, and time. The complex origin and development of this area may explain the different geotechnical properties characterizing the clay deposits located in Finland and Sweden compared with the Norwegian ones.

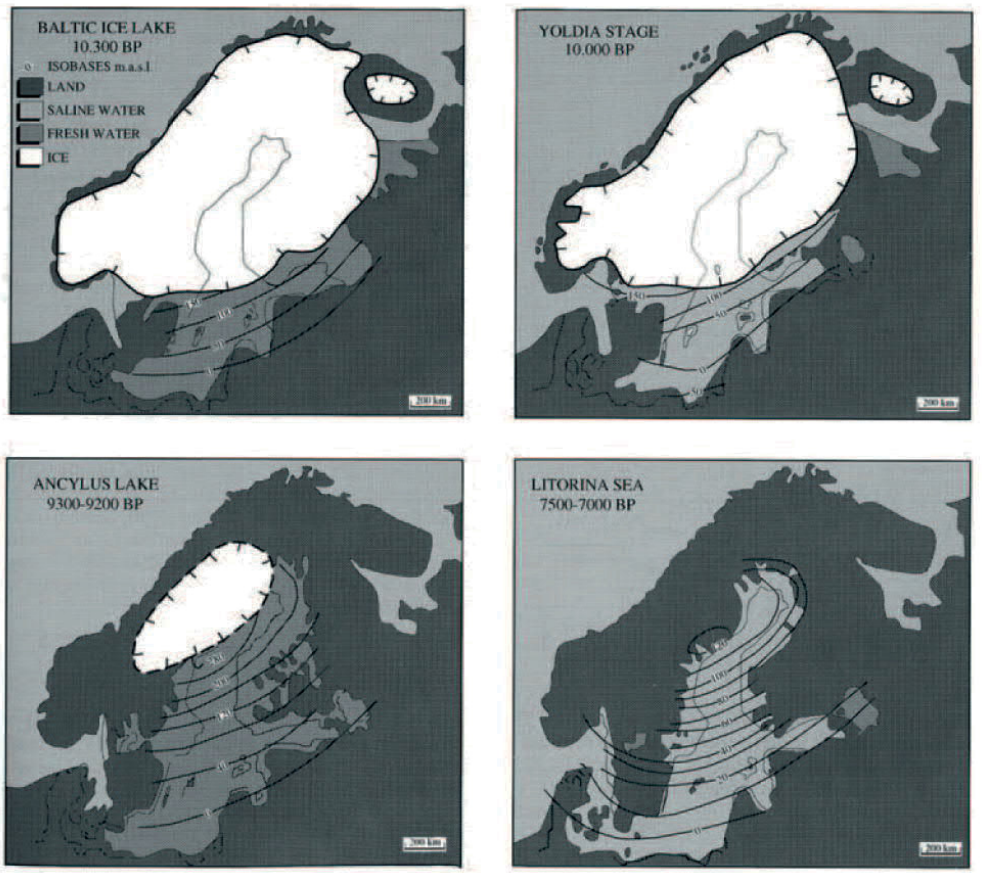

Figure 2.1. The Baltic Sea stages during the late- and post-Weichselia (Eronen et al. 2001).

The Baltic Ice Lake originated during the retreat of the Weichselian glacier, when meltwater accumulated and formed a fresh water lake. At this stage, the connections with the North Sea and the Atlantic Ocean were closed because the ground on the entire depression rose faster than the sea level. However, a short connection with the sea across central Sweden occurred during the Yoldia Sea stage. At the early

stage, the depositional environment was still characterized by low salinity owing to the heavy water flow from the continental ice sheet. The salinity increased after 200 years of the ingression of salt water, creating the condition for a brackish depositional environment. Afterward, the isostatic uplift of the Baltic basin closed the connection with the Atlantic Ocean and the Yoldia Sea turned into Ancylus Lake. This stage lasted until a new connection with the North Sea was established owing to the continuous rising of the water level of Ancylus Lake, forming the Littorina Sea. Finally, the continuous land rise made the connection with the Ocean shallower, thus creating the conditions for the formation of the current Baltic Sea, which is characterized by brackish water. A detailed study on the geological formation of fine-grained sediments in Finland was conducted by Gardemeister (1975).

It is evident that the combination of the sea water intrusion and fresh water flow from the melting glacier created a heterogeneous depositional environment characterized by variable salinity content. Although the salt leaching process is considered as the main factor explaining the high sensitivity of Scandinavian marine clays, further investigation is needed for Finnish clays.

2.3 Mineralogical composition of Finnish clays

At the present stage, the microstructural analysis results are available only for Perniö clay, whereas the investigation for the other sites is still ongoing. Although the Perniö site worked as a benchmark site for several research studies conducted on Finnish clays, dissimilarities with other clays can be observed and, therefore, additional analysis is required to have a clear overview of the mineralogical properties of Finnish soil. Details on the geotechnical properties of Perniö clay are discussed by Di Buò et al. (2019a).

The microstructural properties of the samples obtained at the Perniö site were evaluated using X-ray diffraction (XRD) tests and scanning electron microscopes (SEMs). The SEM observations were performed with Philips XL20 microscope on samples treated using air dewatering and gilding by the Emitech K550 sputter coater. In addition, energy dispersive X-ray spectroscopy (EDS) was performed at 20–30 kV voltage with the aim of identifying the main chemical compounds. Results are summarized in Table 2.1.

The mineralogical composition is evaluated by means of XRD analysis performed with a diffractometer (PW1730 X-ray generator, PW 1050/70 goniometer, and CuKα radiation). The tested sample is preliminary treated by adding hydrogen

peroxide and hydrochloric acid to remove the organic fraction and carbonates. Then, the clay fraction is isolated using the Andreasen pipette. As shown in Fig. 2.2, the sample is characterized by the presence of chlorite, mica, and quartz as the main components. It is worth observing that results obtained from Tiller (Norway) are characterized by similar mineralogical composition.

Finally, micrographs of the soil (Fig. 2.3) reveal that mica (Fig. 2.3a) and rosette-like structures of chlorite (ChL, in Fig. 2.3b) are widely distributed across the samples. In addition, diatoms are systematically detected in the observed samples (marked with letter D in Fig. 2.3c and 2.3d). In particular, these centric diatoms are typical in freshwater environments. Therefore, their presence is probably owing to the depositional history of Finnish sensitive clays and, in particular, associated with the Baltic Ice Lake phase during Pleistocene.

Table 2.1. Summary of chemical compounds, Perniö (z = 4.5 m).

Element	Mass (%)
Silicon	52
Calcium	2
Aluminum	16
Iron	14
Potassium	7.5
Magnesium	3.5
Sodium	2
Other compounds	3

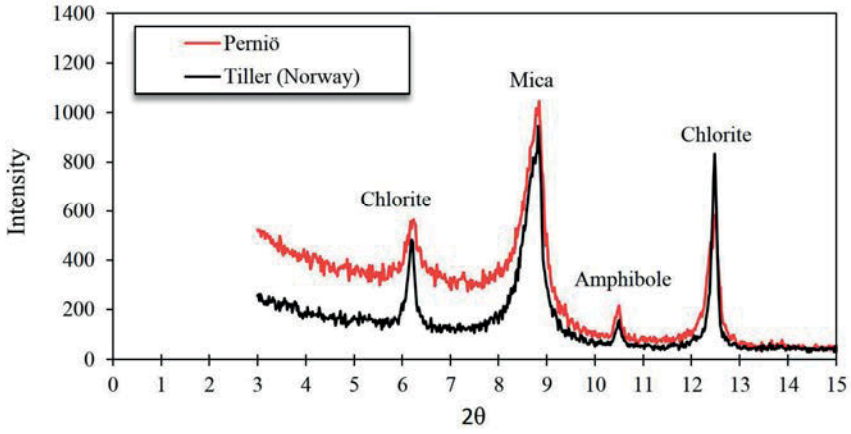

Figure 2.2. X-ray diffraction tests, Perniö.

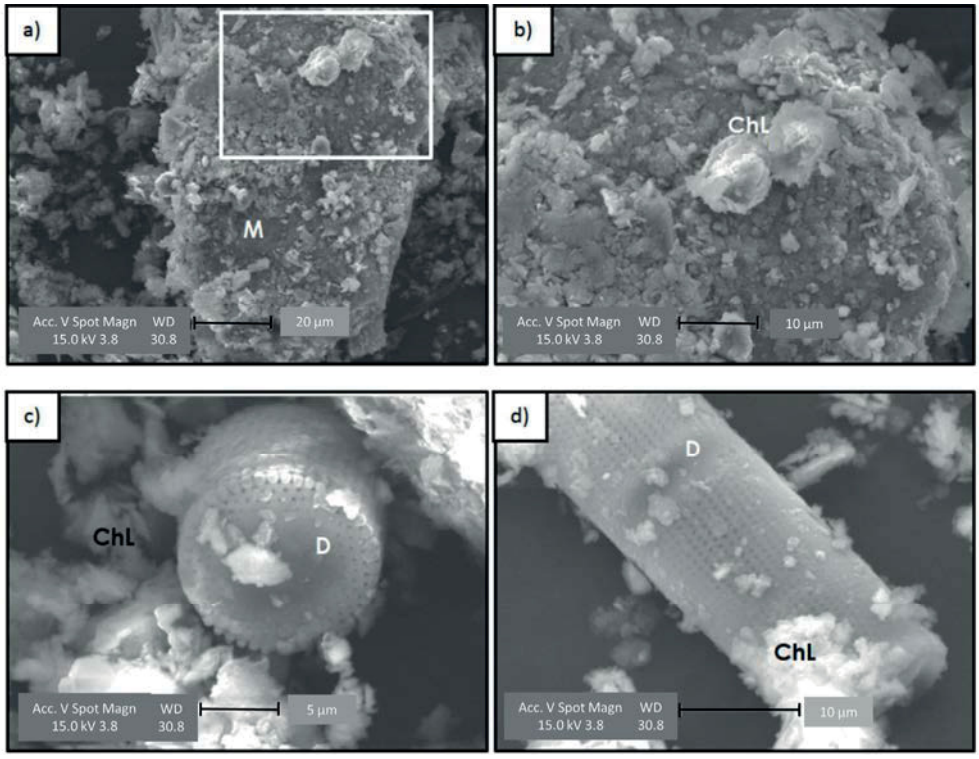

Figure 2.3. Microscopic images of Perniö clay (z = 4.5 m).

2.4 Engineering properties of soft sensitive clays

Understanding soil behavior is a crucial aspect of geotechnical design, particularly when conducting stability and settlement analyses in soft sensitive clays. In particular, these soils show a rather complex mechanical behavior owing to several aspects related to the soil structure, anisotropy, and rate dependency. Therefore, to guarantee a safe design and long-term functionality of the structures and infrastructures, the soil models adopted in the design should account for these different features. Nevertheless, simplified methods are preferred in common practice because the more advanced models require expensive and time-consuming laboratory testing.

This section discusses the different aspects related to the behavior of soft sensitive clays, with particular emphasis on yielding and compressibility. Experimental evidence from previous research studies are presented to provide a general framework for a better understanding of the geotechnical properties of these soils.

2.4.1 Stress history of natural soil deposits

Over the past decades, the yielding and compressibility properties of soft clays have been a subject of special interest. Despite the abundant literature available on this topic, the discussion among authors is still open. Several theories have been proposed to describe the stress-strain behavior of soft clays and its dependency on the strain rate.

The complex mechanical behavior shown by these clays is mainly attributable to their stress history. Herein, the term stress history refers to the geological history and loading memory that a soil deposit has experienced since its formation. It is generally represented in terms of preconsolidation stress (σ'_p), commonly defined as the maximum effective overburden stress sustained by the soil over its geological history. This value defines the transition between the overconsolidated state (OC) and the normally consolidated state (NC) of the soil behavioral response. However, the development of the σ'_p may result from depositional and post-depositional processes such as secondary compression, aging, bonding, and temperature change. In these cases, the term vertical yield stress (σ'_{vy}) is considered more appropriate (Leroueil and Hight 2003).

The depositional process for a natural soil deposit evolves along the virgin compression line (VCL), as shown in Fig. 2.4. During consolidation, the in situ vertical stress (σ'_v) increases and the void ratio (e) decreases as a consequence of the overlaying soil weight. Once the in situ vertical stress (σ'_{v0}) is reached at point A (yield point), the soil is normally consolidated and it may experience large deformation when loaded. Differently, if the soil is subject to a constant load over a long time period, the void ratio decreases (A–B_{12}) owing to the secondary compression, also referred to as "ageing" or "creep". If the soil is further loaded, it tends to behave as nearly elastic till reaching the yield stress (D_1). In some cases, the soil may exhibit additional strength due to bonding effect, resulting in higher yield stress (D_2). At this point, the soil structure collapse as a consequence of soil destracturation. Differently, in case of ageing and erosion, the yield stress is reached at point D_1*, or D_2* in case of additional bonding, and the soil is considered aged and overconsolidated.

It appears to be clear that the definition of σ'_p is rather complex and require careful investigation of these mentioned aspects. In common practice, the σ'_p is evaluated by means of 1D consolidation tests performed on undisturbed samples. Two different test procedures are adopted in the conventional geotechnical practice: incrementally loaded (IL) and continuous loading oedometer testing. In the IL

configuration, the sample is subjected to loading steps that are generally maintained constant for 24 h, or till the end of primary consolidation, while longer testing time is required in case of creep testing. In contrast, the constant rate of strain (CRS) oedometer test configuration is based on a constant strain rate applied to the tested specimen. This procedure has significantly improved the testing procedure because it provides a continuous compression curve, thus improving the accuracy in the evaluation of soil compressibility properties. Dissimilarities between the σ'_p evaluated from laboratory testing and the in situ yielding are well-documented in the literature. These are mainly attributable to the different stress paths and loading rates between field and laboratory tests. In addition, sample disturbance is a key aspect in the determination of σ'_p (Lunne at el. 1997; Di Buò et al. 2019b).

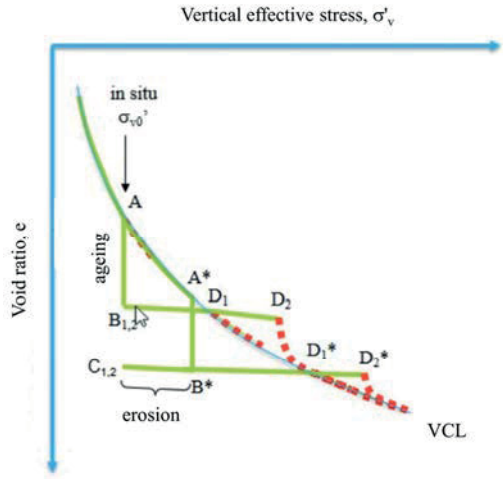

Figure 2.4. Schematization of the consolidation processes of natural soil deposits (Länsivaara 2017).

2.4.2 Settlement calculation methods

The evaluation of soil settlement is generally based on 1D consolidation properties evaluated from oedometer testing. As previously noted, the introduction of the CRS testing procedure has significantly improved the accuracy of soil deformation properties evaluation. In this section, existing settlement calculation methods are reviewed, including the compressibility index method, tangent modulus method (Janbu, 1967), and CRS Swedish settlement calculation method (Sällfors 1975), hereafter also referred to as "Janbu's method" and "Sällfors' method," respectively.

2.4.2.1 Compression index method

The compression index method is based on two parameters, the compression index (C_c) and the recompression or swelling index (C_r). These parameters are defined based on the linearization of the compressibility curve in the log τ–e plot. In particular, C_r describes the variation of the void ratio as a function of the change of effective vertical stress in the OC range, whereas C_c refers to the compressibility behavior in the NC range. Therefore, they can be obtained as follows.

$$C_r = -\frac{\Delta e_{OC}}{\Delta \log \sigma'_v} \tag{2.1}$$

$$C_c = -\frac{\Delta e_{NC}}{\Delta \log \sigma'_v} \tag{2.2}$$

Similarly, with reference to the log σ'_v–ε plot, the slope parameters are referred to as modified recompression index ($\varkappa$) and modified compression index (λ), defined as:

$$\varkappa = \frac{\Delta \varepsilon_{OC}}{\Delta \log \sigma'_v} = \frac{C_r}{1+e_0} \tag{2.3}$$

$$\lambda = \frac{\Delta \varepsilon_{NC}}{\Delta \log \sigma'_v} = \frac{C_c}{1+e_0}. \tag{2.4}$$

Table 2.2 presents a summary of some existing correlations that are widely used in common practice. It is important to consider several aspects when using the compression index method. First, the parameters C_r and C_c are arbitrary fitting values based on the consolidation test results, which have no physical meaning. Moreover, in case of low-quality samples, the evaluation of σ'_p from the stress-strain plot is rather difficult (Fig. 2.5). In relation to this, several interpretation methods have been proposed in the literature to determine the σ'_p (e.g., Casagrande, 1936; Sällfors 1975). Finally, the compression index method is characterized by several issues when applied to soft sensitive clays. These clays show highly nonlinear behavior beyond the σ'_p in the log σ'_v–e plot. Therefore, the assumption of a constant value C_c would not be representative for the entire NC range. This concept is summarized in Fig. 2.6, which presents the CRS oedometer test result from Perniö clay (Finland). Based on the experimental result, C_c is evaluated considering three different stress ranges (σ'_p + 10 kPa; σ'_p + 20 kPa; σ'_p + 50 kPa). Note that the C_c value is considerably high just beyond σ'_p, thus decreasing when the virgin compression line is reached. These aspects should be considered when performing settlement analysis in sensitive clays employing the compression index method.

Table 2.2. Existing correlations for evaluating the compression index C_c.

Proposed equation	Reference
$C_c = 0.007(w_L\text{-}10)$	Skempton and Jones (1944)
$C_c = 0.017(w_L\text{-}20)$	Shouka (1964)
$C_c = (w_L\text{-}13)/109$	Mayne (1980)
$C_c = 0.01\ w$	Koppula (1981)
$C_c = 0.85(w/100)^{1.5}$	Helenelund (1951)
$C_c = 0.01(w\text{-}7.549)$	Herrero (1983)

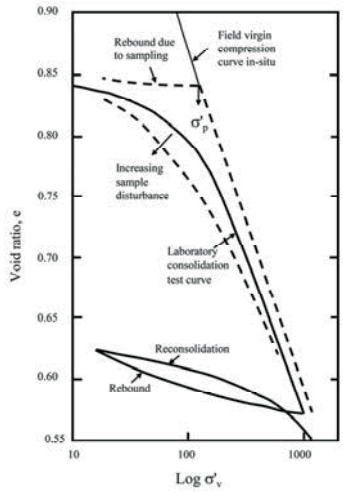

Figure 2.5. Schematization of the compressibility of natural clays.

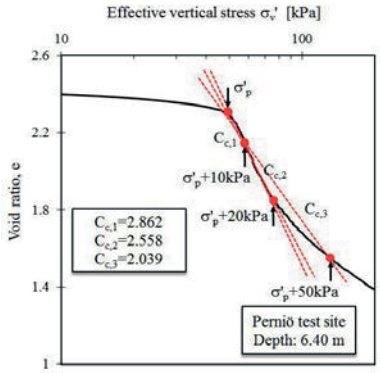

Figure 2.6. Application of the compression index method on CRS consolidation test result from Perniö, Finland (Di Buò et al. 2019c).

2.4.2.2 Tangent modulus calculation method

The tangent modulus method, also known as "Janbu method" (Janbu 1967), is widely used in soft sensitive clays. It was developed by Janbu in the early 1960s to model the stress-strain behavior of cohesive and cohesionless soils in 1D constrained conditions. By observing the behavior of different soils (Fig. 2.7), Janbu developed a method to model the constrained modulus (*M*) as a function of the effective stress based on two dimensionless parameters: a modulus number (*m*) and a stress exponent (β), as follows:

$$M = \frac{\partial \sigma}{\partial \varepsilon} = m\sigma_a \left(\frac{\sigma'_v}{\sigma_a}\right)^{1-\beta}, \tag{2.5}$$

where σ_a is the reference stress, which is equal to 100 kPa. Considering the different behavior in the NC and OC range, the constrained modulus can be expressed as:

$$M = m_2\sigma_a \left(\frac{\sigma'}{\sigma_a}\right)^{1-\beta_2} \qquad \text{for } \sigma'_{v0} < \sigma' < \sigma'_p \tag{2.6}$$

$$M = m_1\sigma_a \left(\frac{\sigma'}{\sigma_a}\right)^{1-\beta_1} \qquad \text{for } \sigma' > \sigma'_p \tag{2.7}$$

where m_1, β_1, m_2 and β_2 are the material parameters the OC and NC range, respectively. Therefore, the Janbu expression for strain can be obtained as:

$$\varepsilon = \int_{\sigma'_{v0}}^{\sigma'_f} \frac{1}{M} d\sigma', \tag{2.8}$$

where σ'_f is the final effective vertical stress reached after loading. Based on this formulation, the vertical strain can be derived by substituting (2.6) and (2.7) into (2.8), thus obtaining

$$\varepsilon_{OC} = \frac{1}{m_2\beta_2}\left[\left(\frac{\sigma'}{\sigma_a}\right)^{\beta_2} - \left(\frac{\sigma'_{v0}}{\sigma_a}\right)^{\beta_2}\right]. \qquad \text{for } \sigma'_{v0} < \sigma' < \sigma'_p \tag{2.9}$$

$$\varepsilon_{NC} = \frac{1}{m_1\beta_1}\left[\left(\frac{\sigma'}{\sigma_a}\right)^{\beta_1} - \left(\frac{\sigma'_p}{\sigma_a}\right)^{\beta_1}\right]. \qquad \text{for } \sigma' > \sigma'_p \tag{2.10}$$

Note that the value of the stress exponent defines the soil type. In particular, the dependency between the constrained modulus and the effective stress can be defined

by the value of β. As an example, by setting $\beta = 1$, the constrained modulus is assumed as a constant value:

$$M = m\,\sigma_a = m\,100. \tag{2.11}$$

This is the case of overconsolidated clays and rock. Similarly, $\beta = 0$ leads to a linear stress-dependent modulus:

$$M = m\,\sigma'_v. \tag{2.12}$$

Therefore, the Janbu method has the capability to describe several stress-strain relationships. These are summarized in Table 2.3.

Table 2.3. Schematization of the Janbu method for different soil types (according to Canadian Foundation Engineering Manual, 1992).

Soil type	β	Strain formula
OC clays and rock	1	$\varepsilon = \frac{\Delta\sigma'_v}{m\,\sigma_a}$
NC sand and silt	0.5	$\varepsilon = \frac{2}{m}\left[\sqrt{\frac{\sigma'_f}{\sigma_a}} - \sqrt{\frac{\sigma'_{v0}}{\sigma_a}}\right]$
NC clay, silt, and silty or clayey sand	0	$\varepsilon = \frac{1}{m}\ln\left(\frac{\sigma'_f}{\sigma'_{v0}}\right)$
Highly sensitive and quick clays	−0.5	$\varepsilon = \frac{2}{m}\left[\sqrt{\frac{\sigma_a}{\sigma'_{v0}}} - \sqrt{\frac{\sigma_a}{\sigma'_f}}\right]$

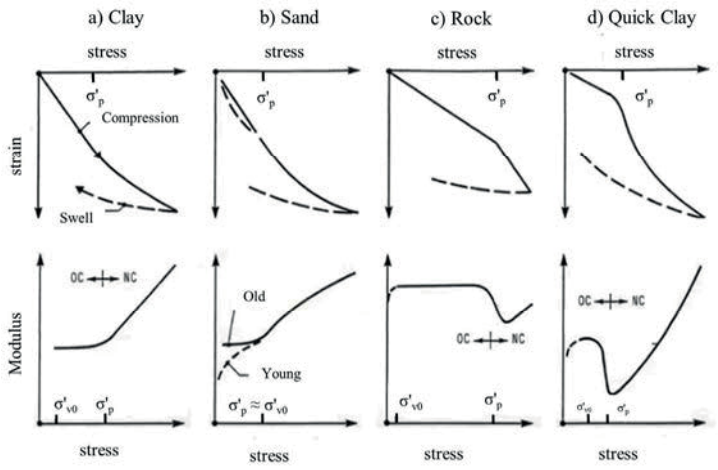

Figure 2.7. Stress-strain relationships for different soil types (Janbu 1967).

In particular, considering the behavior of soft sensitive clays, the oedometer modulus can be modeled as a constant value in the OC region while it is stress-dependent in the NC region. Therefore, the stress exponent in the OC region (β_2) can be assumed to be equal to 1, thus obtaining two different equations.

$$M_{NC} = \frac{\partial \sigma}{\partial \varepsilon} = m_1 \sigma_a \left(\frac{\sigma'}{\sigma_a}\right)^{1-\beta_1} \qquad \text{for } \sigma' > \sigma'_p \qquad (2.17)$$

$$M_{OC} = \frac{\partial \sigma}{\partial \varepsilon} = m_2 \sigma_a \left(\frac{\sigma'}{\sigma_a}\right)^{1-\beta_2} = m_2\, 100 \qquad \text{for } \sigma'_{v0} < \sigma' < \sigma'_p \qquad (2.18)$$

Typical values of the modulus number m_2 for different soil types are summarized in Table 2.4. The variability is wide, from 1000 to values close to 1 for very soft clays or peats.

Table 2.4. Values of modulus number for different soil types (according to Canadian Foundation Engineering Manual, 1992).

Soil type	Modulus number, *m*
Very dense till, glacial till	1000–300
Gravel	400–40
Dense sand	400–250
Loose sand	150–100
Dense silt	200–80
Loose silt	60–40
Very stiff clay	60–20
Medium to stiff clay	20–10
Soft marine clays	20–5
Organic clays	20–5
Peats	5–1

2.4.2.3 CRS Swedish settlement calculation method

Similarly to the Janbu method, the CRS Swedish settlement calculation method proposed by Sällfors (1975) is based on a continuous M derived from the CRS consolidation test. As observed from CRS oedometer testing on soft sensitive clays, the constrained modulus can be assumed as a constant value (M_0) up to σ'_p. Once the σ'_p is reached, the constrained modulus drops to a minimum value (M_L), which remains constant until the limit stress σ'_L. After a further increase in stress, the modulus starts increasing linearly with the stress ($M' = \Delta M/\Delta\sigma$). This formulation divides the constrained modulus curve into three parts (Fig. 2.8), defined as follows.

$$M = M_0 \qquad \text{for } 0 < \sigma' < \sigma'_p \qquad (2.19)$$

$$M = M_L \qquad \text{for } \sigma'_p < \sigma' < \sigma'_L \qquad (2.20)$$

$$M = M_L + M'(\sigma' - \sigma'_L) \qquad \text{for } \sigma' > \sigma'_L \qquad (2.21)$$

Based on the formulation provided, the vertical strain can be derived as follows.

$$\varepsilon_v = \frac{\sigma' - \sigma'_0}{M_0} \qquad \text{for } 0 < \sigma' < \sigma'_p \qquad (2.22)$$

$$\varepsilon_v = \frac{\sigma'_p - \sigma'_0}{M_0} + \frac{\sigma' - \sigma'_p}{M_L} \qquad \text{for } \sigma'_p < \sigma' < \sigma'_L \qquad (2.23)$$

$$\varepsilon_v = \frac{\sigma'_p - \sigma'_0}{M_0} + \frac{\sigma'_L - \sigma'_p}{M_L} + \frac{1}{M'} \ln\left[\frac{M'(\sigma' - \sigma_L)}{M_L} + 1\right] \qquad \text{for } \sigma' > \sigma'_L \qquad (2.24)$$

The Sällfors method has been mainly adopted in the Swedish geotechnical practice. However, for the purpose of this thesis, comparisons between the different methods based on the CRS experimental results are made. These aspects are analyzed in detail in chapter 6.

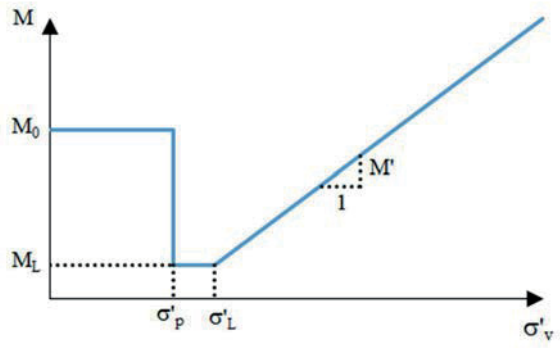

Figure 2.8. Schematization of the CRS Swedish method.

3 FIELD AND LABORATORY INVESTIGATION

3.1 Experimental program objectives

The present study is based on an extensive experimental program conducted at five soft clay sites located in the southern region of Finland. These sites have been selected based on the indications provided by the FTA among the sites along the Finnish railway track affected by stability and settlement issues. Despite similar geological origin and formation, the sites are characterized by different geotechnical properties in terms of S_t, w, PI, and clay fraction. A database of clays characterized by a wide range of geotechnical properties is therefore established.

As mentioned earlier, one of the main objectives of this study is to promote the use of the piezocone test in Finnish geotechnical practice. To this end, collecting data from several Finnish sites is fundamental to assess existing CPTu-based correlations proposed in the literature and to develop new analytical models for evaluating the soil stress history and deformation properties. Indeed, existing correlations have to be validated when applied to different geological contexts. These aspects have been extensively investigated in the present study. At the same time, the anisotropy and strength properties have been investigated during a parallel research study conducted by Selänpää et al. (2020).

The experimental program conducted at Tampere University comprises a preliminary field investigation followed by extensive laboratory testing. To obtain high-quality undisturbed samples from the tested sites, particular attention has been paid to the sampling operations. It is widely acknowledged that sample disturbance has a key role in the determination of reliable geotechnical parameters. Several studies have highlighted the difficulties encountered in obtaining high-quality undisturbed samples from soft sensitive clay sites (Lunne et al. 1997; Lunne et al. 2006; Di Buò et al. 2019b). Therefore, in this study, several sampling methods have been employed and their performance is assessed based on the Lunne et al. (1997) criteria applied to oedometer and triaxial test results. This section outlines the equipment and procedures adopted during the field and laboratory testing program and the sampling operations conducted at the sites to retrieve high-quality samples.

3.2 Cone penetration test (CPT)

Among the vast number of traditional investigation methods, CPT represents one of the most versatile, economical, and reliable in situ tests. By recording near-continuous measurements with depth, it provides excellent stratigraphic details and information for estimating a wide range of geotechnical parameters. The most significant breakthrough in the CPT was represented by the introduction of the pore-water pressure transducer in the penetrometers, resulting in the modern piezocone configuration. Therefore, the standard piezocone sounding includes the measurement of three parameters: the cone tip resistance (q_c), the sleeve friction (f_s), and the excess pore-water pressure (u_2). Recently, a number of research studies have focused on the development of sensors to be installed within the penetrometers, including electrodes, geophones, temperature, and pH sensors, to collect additional data. Among them, the seismic and resistivity modules have been widely employed for dynamic and geo-environmental applications.

The role of the piezocone in field investigation depends on the project requirements and associated risks. In particular, the evaluation of geotechnical risk is based on the hazards, probability of occurrence, and consequences (Robertson 1998). As suggested by Hight and Leroueil (2003), the level of sophistication for a site characterization program is based on the local experience, design objectives, project-associated risks, and potential cost saving. As an example, for high-risk projects, the CPT is generally used for the preliminary screening to determine the sub-surface stratigraphy and identify the soil type, thus providing useful information for the sampling program. However, for moderate- to low-risk projects, the CPTu data can be used for evaluating the geotechnical parameters and, in particular cases, for direct geotechnical design. The perceived applicability of CPTu in deriving the soil parameters depends on several factors, including the soil type and the confidence level within the geological context. Clearly, CPTu-based predictions must be verified and validated to match the local soil conditions. Therefore, especially in a complex geological context, where interpretation of CPTu data is rather difficult, it should be followed by selective high-quality sampling and advanced laboratory testing.

In Scandinavia, the piezocone is one of the most employed tools for field investigation, employed for both onshore and offshore research projects. In contrast, in Finland, the use of CPTu is still in an early stage. There are several possible explanations for this. First, in Finnish geotechnical practice, the FV test has been widely used as the traditional in situ test; therefore, FV-based correlations for the evaluation of s_u are considered reliable for the geotechnical design. Moreover,

the lack of experience in piezocone testing leads to uncertainties when applying the existing correlations in Finnish soil conditions. Therefore, this study has been conducted to derive CPTu-based correlations valid for Finnish clays and hence promote the use of the piezocone in geotechnical investigation and design.

3.2.1 CPTu equipment

A CPT system includes an electrical penetrometer, a hydraulic pushing system with rods, cable, or transmission device, a depth encoder, and a data acquisition system. The pushing equipment comprises push rods of 1-m length, thrust mechanism, and reaction system. In particular, a CPT penetrometer rig based on a crawler undercarriage (Fig 3.1) has been used to perform the CPTu soundings at the sites investigated in the present study. The crawler is equipped with three jacking cylinders for raising the apparatus up to 0.5 m for leveling before testing. A hydraulic jacking system supplied from the engine is used to transfer the total load on the top of the push rods by a thrust head. The CPT crawler itself has a relatively high self-weight (12 tons) and serves as a counterweight to provide the required penetrative force.

Figure 3.1. A.P. van den Berg CPT crawler employed for the investigation.

The standard cone penetrometer (Fig. 3.2), designed by A.P. van den Berg and referred to as Icone, includes a three-channel instrumented steel probe that measures the cone tip resistance (q_c), sleeve friction (f_s), and pore-water pressure (u_m). The filter element for measuring the pore-water pressure is located at the shoulder, just behind the cone tip (u_2, type 2). The instrumented probe comprises a 60° apex conical tip, with a cross-sectional area (A_c) of 10 cm^2 and a sleeve area (A_s) of 150

cm2. An inclinometer sensor is embedded within the cone for measuring the probe inclination during penetration. Two electrical cones of different capacities have been used during the field investigation: a high capacity cone (75 MPa) and a lower capacity cone (7.5 MPa), hereinafter referred to as "sensitive" cone. The sensitive cone is characterized by higher measurement accuracy and is therefore considered more suitable in soft soil conditions. The cones are temperature-compensated in the range between 10° and 40°. The technical features of the instrumented cones are summarized in Table 3.1. The equipment used for the field investigation, as well as the test procedure, meet the requirements of the European Standards (EN ISO 22476-1). However, it is worth observing that the f_s measurement accuracy is 2 kPa for the sensitive cone and 3 kPa for the high-capacity cone. In soft clays, the f_s is generally very low, with values lower than 1 kPa and, therefore, higher accuracy is needed. Unfortunately, in this study, the use of the f_s measurements was very limited due to the above mentioned issues. An ongoing study conducted by Di Buò et al. (2020) highlights the influence of the sleeve sensor inaccuracy on the evaluation of soil parameters. These aspects are addressed later in the thesis.

Figure 3.2. A.P. van den Berg piezocone.

Table 3.1. Technical features of the high-capacity and sensitive piezocones.

	High-capacity cone			
	q_c	f_s	u_2	**Inclination**
Maximum capacity	75 MPa	1 MPa	2 MPa	20°
Accuracy	0.13% (100 kPa)	0.3% (3 kPa)	0.25% (5 kPa)	0.5°
	Sensitive cone			
	q_c	f_s	u_2	**Inclination**
Maximum capacity	7.5 MPa	0.15 MPa	2 MPa	20°
Accuracy	0.2% (15 kPa)	0.7% (2 kPa)	0.25% (5 kPa)	0.5°

3.2.2 Additional modules

The field investigation has been conducted using two additional modules connected directly behind the cone (high capacity or sensitive) with a small coupling piece.: the seismic and resistivity modules. The seismic piezocone test (S-CPTu) has been largely employed to evaluate the small strain shear modulus (G_0) based on the shear wave velocity (v_s) measurement. G_0 is an important dynamic soil property used in different applications in geotechnical and earthquake engineering, including seismic site response analysis, soil-structure interaction, foundation design for vibrating equipment, and dynamic behavior analysis of offshore structures during wave loading. Typically, the v_s profile is evaluated using different techniques, including down-hole, cross-hole, and multichannel analysis of surface waves (MASW). The basic principle is to measure the wave travel time by placing a source on the ground surface and geophones into a borehole (down-hole configuration) or by measuring the velocity of seismic waves between boreholes (cross-hole configuration). The S-CPTu offers an economical down-hole solution as the v_s is recorder during the sounding. In particular, the seismic module contains three accelerometers arranged in three perpendicular directions (X, Y, and Z) to receive horizontal and vertical waves. The seismometer is oriented transverse to the signal source to detect the horizontal component of the shear wave arrivals. The test is performed at 1-m intervals while the cone penetration is stopped. Shear and compression waves are generated by striking a metal plate rigidly placed at the ground surface. The plate is hit with the hammer in two opposite directions to generate "right" and "left" polarized shear waves and in the vertical direction to generate compression waves. To ensure that the seismic measurements are not affected by any background noise, the CPT rig is stopped during the test execution. The v_s value is calculated by dividing the incremental traveling distance to the geophone by the incremental arriving time between successive recorded shear waves (Campanella et al. 1986).

$$v_s = \frac{L_2 - L_1}{t_2 - t_1} = \frac{\Delta L}{\Delta t} \tag{3.1}$$

Here, L_1 and L_2 are the distances between the source beam and the cone sensor for the first and second depth, respectively, and t_2 and t_1 are the shear wave arrival time for the first and second depth, respectively (Fig. 3.3). The exact time of the strike is obtained by an electronic trigger attached to the metal plate. In this study, the cross-over (or reverse polarity) method has been adopted to compute the travel time (Δt). By hitting the metal plate in two opposite directions, two reversed shear wave signals

are generated. The arrival time of the shear wave is evaluated by identifying the first cross-over point where the main shear wave arrives and changes sign. Therefore, the time interval is determined by subtracting the arrival time for the first depth from that of the second depth (Robertson et al. 1986; Liao and Mayne 2006). The reliability of the method is ensured using two shear wave measurements to determine the cross-over shear wave velocity. However, the evaluation of the time intervals based on only a single point is time consuming and can be affected by personal judgment.

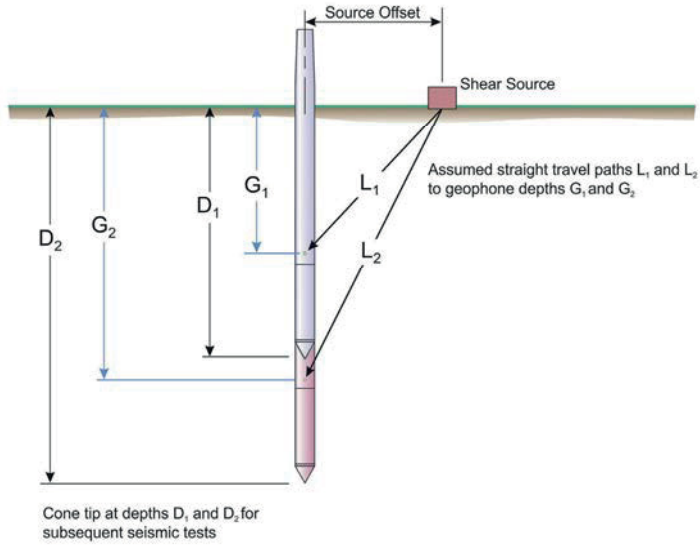

Figure 3.3. S-CPTu measurement schematization (from conetec.com).

The conductivity module is used for measuring variations of the soil electrical conductivity. It have been used for many purposes, e.g., evaluation of soil properties such as porosity and density, identification of contaminated soils, and evaluation of water content. In Scandinavia, considerable research interest is attracted by the conductivity module for soil mapping and detecting the presence of quick clay layers (Bazin and Pfaffhuber 2013; Solberg et al. 2008). Indeed, the conductivity module is considered as a powerful tool to evaluate the presence of salt or fresh water, which can be related to the presence of leached marine clays within the deposit.

The conductivity module comprises four electrode rings, isolated from each other by ceramic insulators. A known current (I) is generated through the soil between the outer electrodes using a controlled voltage source embedded in the module. The current varies during penetration to maintain a constant value of voltage difference

(*V*) across the inner electrodes. The conductivity (*K*) is expressed in milliSiemens per meter (mS/m) and is calculated as follows:

$$K = \frac{C\,I}{V}, \tag{3.2}$$

where *C* is the calibration factor.

3.2.3 Test procedure

This section details the procedures adopted for performing CPTu soundings at the investigated sites. The operations were performed to meet the requirements established in the ISO 22476-1. To ensure the highest quality class, the calibration and maintenance of the penetrometers were ensured by the manufacturer on a regular basis and before each investigation campaign.

To obtain reliable pore-pressure response during cone penetration, the saturation of the filter element has to be ensured. In piezocone testing, this represents one of the most important issues affecting the quality of the measured data. Indeed, poor preliminary saturation or desaturation of the filter element may occur while penetrating stiff layers. The filter element used in the investigation is made of stainless steel, and it was replaced after each sounding to avoid clogging problems, which are common in plastic clays. The saturation procedure consists in submerging the cone tip into a silicon oil bath in a fully closed environment provided by a vacuum device (Fig. 3.4). The deaeration operation was performed in different stages by opening and closing the aeration valve. This procedure is suggested to fully saturate the space between the pressure sensor inside the cone and the outside of the filter, particularly when the penetrometer is characterized by a female plug on the tip unit. In addition, to avoid possible desaturation when penetrating the dry crust layer, a predrilling borehole is made. This procedure has been adopted for all the soundings performed at the test sites.

Before and after the sounding, "zero-readings" of each measuring channel were recorded. The difference between these values, also called "zero-shift," is important to detect possible damages and calibration errors as well as to define the quality class of each test. Once the preliminary stage is complete, the test can be started. The standard rate of testing is at a constant push of 20 mm/s applied in 1-m increments owing to the standard cone rod length. Therefore, every one meter, the test is stopped and the next rod is added. During this break, intermittent testing can be

conducted, including the dissipation test and down-hole shear wave velocity measurement. Finally, once the final depth is reached, the test is stopped and the piezocone is recovered by pulling it upward and dissembling each rod.

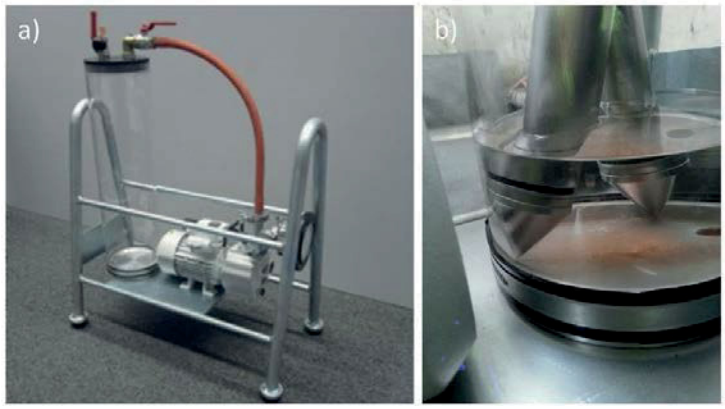

Figure 3.4. Details of piezocone saturation: a) A.P. van den Berg vacuum device; b) silicon oil bath.

3.2.4 CPTu data correction

The axial force at the cone tip (F_c) is measured using an internal load cell, whereas the axial force along the sleeve (F_s) is recorded by an additional load cell. Therefore, the cone tip resistance is obtained by dividing the measured axial force by the cross sectional area ($q_c = F_c/A_c$). However, this value must be corrected to take into account the pore-water pressures acting on unequal tip areas of the cone. This correction is significant in soft to stiff clayey soils (Jamiolkowski et al. 1985; Robertson and Campanella 1988; Lunne et al. 1997). The corrected cone tip stress, indicated as q_t, is determined as follows.

$$q_t = q_c + u_2(1 - a) \tag{3.3}$$

Here, a is the net cone area ratio, which is equal to the ratio of the cross-sectional area of the load cell or shaft (A_n) divided by the projected area of the cone (A_c), as shown in Fig. 3.5. This parameter is generally provided by the cone manufacturer based on geometrical considerations and a calibration procedure. However, to determine the proper value of the parameter a, a proper calibration test was repeated in the laboratory. This procedure involves applying an all-round water pressure to

the cone suspended in the chamber triaxial device. Readings of q_c are taken as the cell pressure increases. By plotting the cone resistance against the applied cell pressure, the cone area ratio can be determined as the slope value of the plotted line. The results of the calibration procedure of the cones used for the investigation related to the cone tip resistance and pore-water pressure are shown in Fig. 3.6. Results show that the cone factor provided by the manufacturer appears to be inaccurate and therefore, the piezocone data interpretation was conducted by considering a = 0.83. For the high-capacity cone, the suggested value of a = 0.75 is used because the calibration procedure has not been performed.

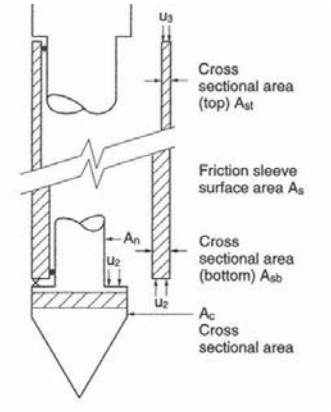

Figure 3.5. Pore-water pressure effects on measured parameters (Lunne et al. 1997).

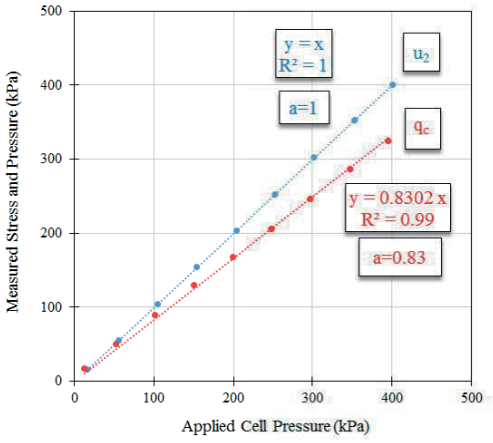

Figure 3.6. Results of the Van den Berg sensitive cone calibration procedure for the evaluation of the parameter "a."

3.2.5 CPTu data quality

Before using the CPTu data for the interpretation of soil parameters, it is fundamental to evaluate the quality of each sounding. Most modern cones involve temperature-compensated strain gauge load cells that provide high accuracy and excellent repeatability with relatively little non-linearity and hysteresis. These aspects are illustrated in Fig. 3.7. However, tests have shown that the output of the sensors at zero load can be different than zero, thus creating a zero load drift as shown in Fig. 3.7. This value can significantly affect the measurement accuracy in soft clays. Therefore, in common practice, zero load readings are recorded at the start and end of each sounding.

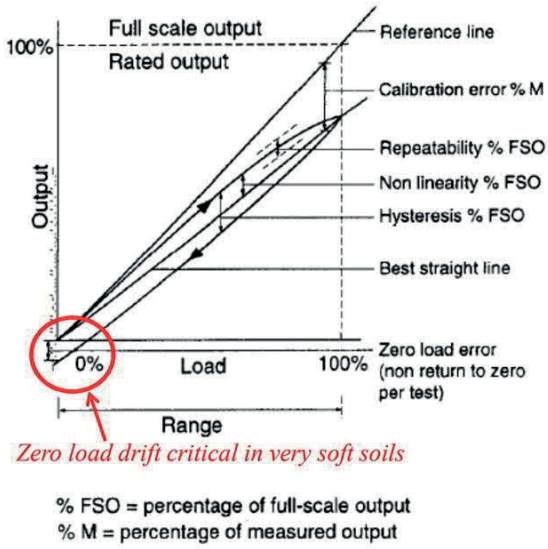

Figure 3.7. CPTu measurement quality with indication of the zero load drift (Robertson 2013a).

To assess the quality of CPT measurements, the EN-ISO 22476-1 standards specify four different application classes defining allowable minimum values for each parameter that should not be exceeded. In this study, the application class of each CPTu sounding is evaluated based on the requirement of EN-ISO 22476-1 (Table 3.2). The maximum total error related to each parameter is determined as the sum of the zero load drift and the sensor accuracy and compared to the allowable value of the relative application class. Results are presented in chapter 4.

Table 3.2. CPTu application classes with allowable minimum accuracy according to the EN-ISO 22476-1.

Application class	Test type	Measured parameter	Allowable minimum accuracy [a]	Maximum measurement interval	Soil [b]	Use interpretation [c]
1	TE2	Cone resistance Sleeve friction Pore pressure Inclination Penetration length	35 kPa or 5% 5 kPa or 10% 10 kPa or 2% 2º 0.1 m or 1%	20 mm	A	G,H
2	TE1 TE2	Cone resistance Sleeve friction Pore pressure Inclination Penetration length	100 kPa or 5% 15 kPa or 15% 25 kPa or 3% 2º 0.1 m or 1%	20 mm	A B C D	G,H* G,H G,H G,H
3	TE1 TE2	Cone resistance Sleeve friction Pore pressure Inclination Penetration length	200 kPa or 5% 25 kPa or 5% 50 kPa or 5% 5º 0.2 m or 2%	50 mm	A B C D	G G,H* G,H G,H
4	TE1	Cone resistance Sleeve friction Penetration length	500 kPa or 5% 50 kPa or 20% 0.2 m or 1%	50 mm	A B C D	G* G* G* G*

Notification:

a The allowable minimum accuracy of the measured parameter is the larger value of the two quoted. The relative accuracy applies to the measured value and not the measuring range.

b According to ISO 14688-2 [1].
A: homogeneously bedded soils with very soft to stiff clays and silts (typically $q_c < 3$ MPa)
B: mixed bedded soils with soft to stiff clays (typically $q_c \leq 3$ MPa) and medium dense sands (typically 5 MPa $\leq q_c < 10$ MPa)
C: mixed bedded soils with stiff clays (typically 1.5 MPa $\leq q_c < 3$ MPa) and very dense sands (typically $q_c > 20$ MPa)
D: very stiff to hard clays (typically $q_c \geq 3$ MPa) and very dense coarse soils ($q_c \geq 20$ MPa)

c G: profiling and material identification with low associated uncertainty level
G*: indicative profiling and material identification with high associated uncertainty level
H: interpretation in terms of design with low associated uncertainty level
H*: indicative interpretation in terms of design with high associated uncertainty level

d Pore pressure can only be measured if TE2 is used.
TE1: cone penetration tests with measurement of cone resistance (q_c) and sleeve friction (f_s)
TE2: cone penetration tests with measurement of cone resistance (q_c), sleeve friction (f_s), and pore pressure (u_2)

3.2.6 CPTu interpretation in fine grained soils

In geotechnical practice, the CPTu has three main applications: (i) stratigraphic profiling, (ii) estimation of the geotechnical parameters, and (iii) direct geotechnical design. By providing near-continuous data measurement, the CPTu is particularly suitable for the preliminary profiling of the investigated site and identification of the soil type. Then, additional information is collected from other field and laboratory

tests. However, it has been shown that a wide range of parameters can be derived from CPTu data, including strength, stiffness, and permeability (k) of the investigated soil. A unified approach in the interpretation of CPTu data is presented by Robertson (2009), where a variety of soil parameters is addressed. In particular, Robertson (2013b) investigated the perceived applicability of CPTu in deriving geotechnical parameters in different soil conditions (Table 3.3).

Table 3.3. Applicability of the CPT in deriving soil properties (Robertson 2013b)

Soil type	Initial state parameters				Strength parameters			Deformation characteristics*			Permeability	
	γ	ψ	K_0	OCR	S_t	s_u	ϕ'	E,G	M	G_0	k	c_h
Fine-grained	2-3		2-3	1	2-3	1-2	4	2-3	2-3	2-3	2-3	2-3
Coarse-grained	2-3	2	4-5	4-5			2-3	2-3	2-3	2-3	3	3-4

*improved when using S-CPTu
Applicability: 1, high reliability; 2, high to moderate; 3, moderate; 4, moderate to low; 5, low reliability

The CPTu has been widely used for estimating the stress history and s_u of fine-grained soils. Indeed, the CPT is performed in clayey soils in undrained condition; therefore, the prediction of the effective parameters (e.g., effective friction angle) is not accurate. In addition, the stiffness parameters are characterized by high uncertainty. However, improvements can be achieved using additional sensors, such as the seismic module, which allow for the measurements of v_s.

Since its introduction in geotechnical practice, the CPT has been used for profiling and identifying the soil type. Several authors proposed classifications systems that link the cone parameters (q_c and f_s or F_r) to the soil type (Begemann 1965; Robertson et al. 1986; Robertson 1990). It was observed that fine-grained soils generally show high F_r and low q_c, whereas coarse-grained soils are characterized by high q_c and low F_r. These classification charts have been used over the past decades and subjected to modifications and improvements. Among them, the soil behavior type (SBT) chart proposed by Robertson et al. (1986) has become quite popular. The chart shown in Fig. 3.8 identifies 12 types of soil based on the q_t and F_r values. Robertson (1990) pointed out that this classification system depends on the in situ soil behavior and is based on the strength, stiffness, and soil compressibility. In contrast, the unified soil classification system (USCS) is based on the grain-size distribution and soil plasticity; therefore, it is not capable of considering the soil mechanical behavior. However, in most cases, there is a fairly good agreement between the USCS-based classification and the CPT-based SBT (Molle 2005).

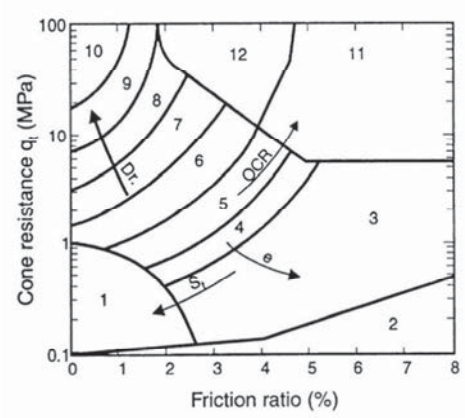

Zone	Soil Behavior Type
1	Sensitive fine grained
2	Organic material
3	Clay
4	Silty Clay to clay
5	Clayey silt to silty clay
6	Sandy silt to clayey silt
7	Silty sand to sandy silt
8	Sand to silty sand
9	Sand
10	Gravelly sand to sand
11	Very stiff fine grained*
12	Sand to clayey sand*

* Overconsolidated or cemented

Figure 3.8. Soil behavior type (SBT) chart (Robertson et al. 1986).

Recently, normalized SBT charts have been introduced to consider the influence of the increasing vertical stress on the CPT parameters. It is clear that the measured q_c tends to increase with the increasing overburden pressure. Similarly, when the cone is pushed at great depth, the measured excess pore pressure can be very high. The normalization should also account for the influence of the horizontal effective stress (σ'_{h0}), even though this aspect is generally neglected in common practice. Nowadays, these charts are widely used because the available pushing equipment allows CPT soundings to be performed at a depth of over 100 m. In particular, the differences between not normalized and normalized charts are evident when the value of σ'_{v0} exceeds 150 kPa. Based on the theoretical work of Wroth (1984), Robertson (1990) developed two charts based on the normalized parameters Q_t, F_r, and B_q, defined as follows.

$$Q_t = \frac{q_t - \sigma_{v0}}{\sigma'_{v0}} \tag{3.4}$$

$$F_r = \left(\frac{f_s}{q_t - \sigma_{v0}}\right) \text{x } 100 \tag{3.5}$$

$$B_q = \frac{u_2 - u_0}{q_t - \sigma_{v0}} = \frac{\Delta u}{q_t - \sigma_{v0}} \tag{3.6}$$

Here, σ_{v0} is the in situ vertical total stress, σ'_{v0} in the in situ effective vertical stress, u_0 is the hydrostatic pore-water pressure, and Δu_2 is the excess pore-water pressure. The charts are illustrated in Fig. 3.9.

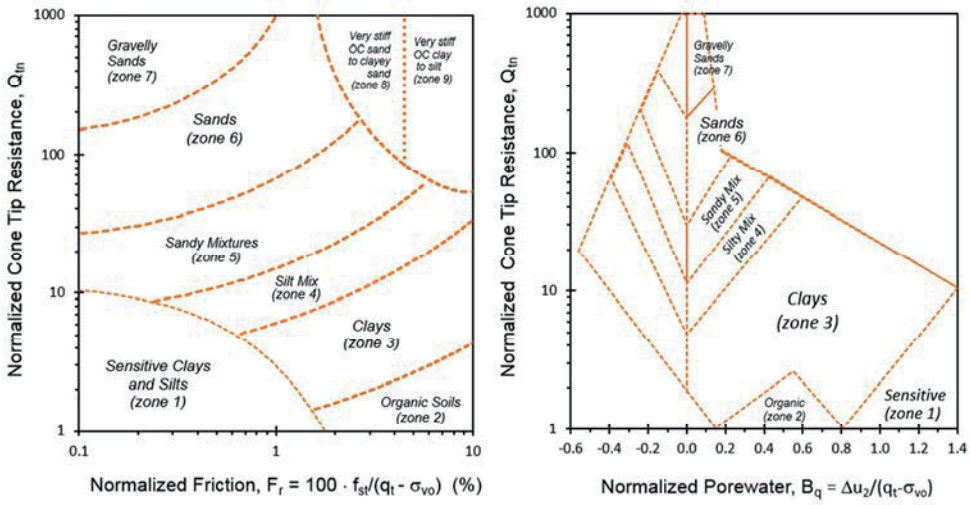

Figure 3.9. Normalized SBT chart (Robertson 1990).

Jeffries and Davies (1993) identified that the boundaries in the SBT chart can be assimilated to concentric circles. Therefore, they introduced an SBT index (I_c) by combining Q_t and F_r, which represents the radius of these circles. The introduction of I_c allows for an easier representation of the soil type, which can be defined based on a single parameter. Robertson and Wride (1998) modified the definition of I_c to apply to the Q_t–F_r chart proposed by Robertson (1990), thus obtaining the following equation.

$$I_c = \sqrt{[(3.47 - \log Q_t)^2 + (\log F_r + 1.22)^2]} \tag{3.7}$$

As shown in Fig. 3.10, small values of I_c indicate that the soil behaves as coarse-grained soil, whereas clayey soils are characterized by higher values of I_c. The transition between sands and clays is generally set by I_c = 2.60. Moreover, Jeffries and Davies (1993) pointed out that I_c is primarily controlled by soil compressibility, which can be linked to the soil plasticity; highly compressible plastic clays are characterized by I_c > 2.60.

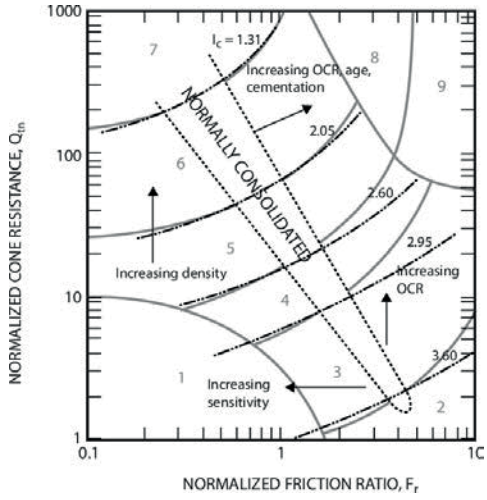

Figure 3.10. Contours of I_c on a normalized soil behavior type (SBTn) chart (Robertson 1990).

The proposed normalization is observed to work fairly well in clays, whereas it is not suitable in coarse-grained soils. As an example, in clean sands, the q_c tends to increase non-linearly with the increasing overburden pressure. Therefore, Robertson and Wride (1998) and the update by Zhang et al. (2002) suggested a normalized cone parameter with a variable stress exponent (n), defined as follows.

$$Q_{tn} = \left[\frac{(q_t - \sigma_{v0})}{p_a}\right]\left(\frac{p_a}{\sigma'_{v0}}\right)^n \tag{3.8}$$

Here, p_a is the atmospheric pressure expressed in the same unit as q_t and σ_{v0}. This normalized chart is indicated hereinafter as SBTn. Note that for $n = 1$, $Q_{tn} = Q_t$.

Robertson (2009) proposed a methodology to estimate the stress exponent based on the I_c and effective overburden stress, defining the stress exponent as follows:

$$n = 0.38(I_c) + 0.05\left(\frac{\sigma'_{v0}}{p_a}\right) - 0.15, \tag{3.9}$$

where $n \leq 1.0$. The proposed updated contours are shown in Fig. 3.11. As discussed, the stress exponent ranges between 0.5 and 0.9 for most coarse-grained soils, whereas it is equal to 1.0 in the clay region.

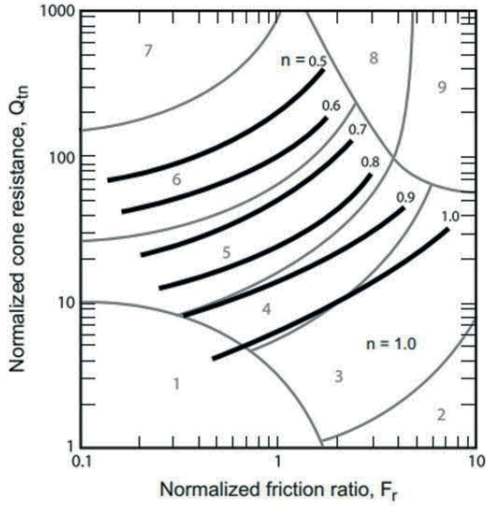

Figure 3.11. Contours of the stress exponent (n) on normalized SBTn chart (Robertson 2009).

3.3 Undisturbed sampling

Geotechnical sampling aims to obtain soil specimens for the geotechnical characterization of the investigated soil. The main objective of the laboratory tests is to define the properties of the tested geomaterials for modeling geotechnical engineering problems. The development of advanced testing techniques in terms of equipment and data interpretation has increased the confidence level of laboratory testing. However, limitations owing to the sample quality can be encountered in particular geological contexts. The role of sample quality in geotechnical investigation depends on the laboratory test class. In particular, class 1 includes characterization tests aiming to evaluate the physical and chemical soil composition (e.g., particle size distribution and XRD analysis). Class 2 tests aim to determine soil state variables such as porosity, degree of saturation, and soil fabric. Finally, laboratory tests performed to evaluate the soil mechanical properties such as strength, stiffness, compressibility, and permeability belong to class 3. To obtain representative soil parameters from laboratory tests, the retrieved samples must preserve the in situ conditions. In particular, higher sample quality is needed for laboratory tests belonging to class 3.

The issues related to undisturbed sampling have been extensively investigated for many years. Several studies have pointed out the difficulties encountered in retrieving

high-quality samples from soft clay deposits and the resulting implications in terms of quality and reliability of laboratory test data (e.g., Hvorslev 1949; Lunne et al. 2006; Karlsrud and Hernandez-Martinez 2013; Karlsson et al. 2016; Mataic 2016; Di Buò et al. 2019b). It is well recognized that all key design parameters such as compressibility, yield stress, and undrained shear strength are influenced by the disturbance induced during sampling operations and laboratory testing. The term sample disturbance accounts for all the undesired processes that cause alterations from the sample in situ condition. Except for the inevitable stress release experienced by the sample from the in situ to laboratory stress state, other disturbance factors can be limited and, in some cases, avoided using proper equipment and correctly following the sampling procedures (Lunne et al. 2006; Di Buò et al. 2019b). Therefore, several undisturbed sampling techniques have been developed over the past decades to minimize sample disturbance.

In this section, the causes of sample disturbance and their impact on laboratory test results are discussed. Moreover, details on the sampling program conducted at the investigated sites, including sampling apparatus, testing procedures, and sample storage are presented.

3.3.1 Causes of disturbance of soft sensitive clays

The sampling process includes several stages that contribute to the disturbance induced in the obtained sample. Hight (2003) summarized the factors associated with soil disturbance as (i) changes in the soil stress state, (ii) mechanical deformation, (iii) moisture content redistribution, (iv) chemical reactions, and (v) mixing and segregation of soil components. Similarly, Ladd and DeGroot (2003) illustrate the potential sources of sample disturbance by means of a hypothetical stress path experienced by the soil during tube sampling and specimen preparation (Fig. 3.12). During borehole drilling (path 1–2), the soil at the bottom of the hole is subjected to a significant stress relief owing to the total vertical stress (σ_v) reduction. The stress path passes through a particular stress state defined as "perfect sampling effective stress" (σ'_{ps}) that is characterized by deviator stress equal to zero. The path 2–3–4–5 illustrates the stress changes during tube sampling. Baligh et al. (1987) showed that the centerline soil initially experiences shear in compression (path 2–3), followed by shear in extension as it enters the tube (path 3–4) and compression once inside the tube (path 4–5). Path 5–6 refers to tube extraction, which causes significant disturbance to the soil located at the top and bottom of the sample. Path 6–7

represents the stress experienced by the soil during transportation and storage. In particular, during transportation, the soil can be subjected to severe disturbance owing to vibrations and temperature changes. During the storage, pore pressure dissipation in the distorted zones located in the external zone of the sample can occur, leading to a decrease in the overall effective stress. The sample extraction (path 7–8) causes additional disturbance owing to the bonding developed in the interface between the soil and the tube. Finally, during specimen preparation (path 8–9), the soil experiences a further decrease in effective stress owing to trimming and handling, thus reaching the final stress state (point 9, σ'_s). Ladd and Lambe (1963) showed that the total decrease in the sample effective stress can be well above 80% of the in situ stress. Despite further reconsolidation at the in situ stress, the disturbance induced by the sampling process may cause significant volumetric changes and soil destructuration, thus resulting in unrepresentative stress-strain behavior shown during laboratory tests.

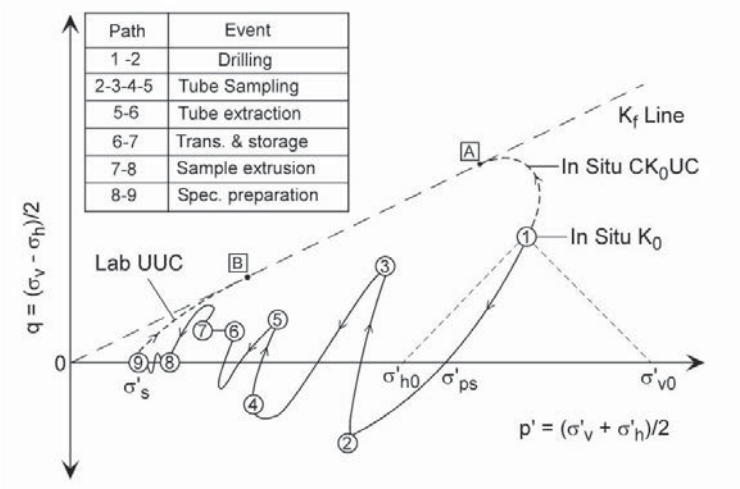

Figure 3.12. Hypothetical stress-path followed by a soil specimen during sampling (Ladd and DeGroot 2003).

Among all these factors, particular attention has been given to understand the effect of stress relief in a sample (Kirkpatrick and Khan 1984; Graham et al. 1987; Amudsen et al. 2017). In situ, the soil is subjected to an anisotropic stress state (σ'_{v0}, σ'_{h0}), which is reduced to zero prior to laboratory testing. The total stress relief has two different components: (i) the removal of deviatoric stress and (ii) the reduction of the mean total stress to zero. These processes cannot be avoided and may

considerably affect the achieved sample quality. In particular, the reduction of the total stress leads to the development of a negative pore pressure (u_r) in the sample, which is equal to the residual mean effective stress (p'_r). The typical stress path and pore-pressure response with time induced by sampling has been investigated by Amundsen et al. (2017) and shown in Fig. 3.13. The path (a)–(b)–(c) represents a theoretical response characterized by an initial reduction of the deviatoric stress ($q = \sigma_v - \sigma_h$) to zero, followed by a reduction of the mean effective stress [$p' = (\sigma'_v + 2\sigma'_h)/3$]. In this case, the theoretical maximum negative pore pressure ($-u_{ps}$) in a perfectly undisturbed sample is reached. However, stress relief is more likely to occur along the path (a)–(d)–(c), characterized by the simultaneous reduction of both the q and p' and the development of a lower negative pore pressure ($-u_r$).

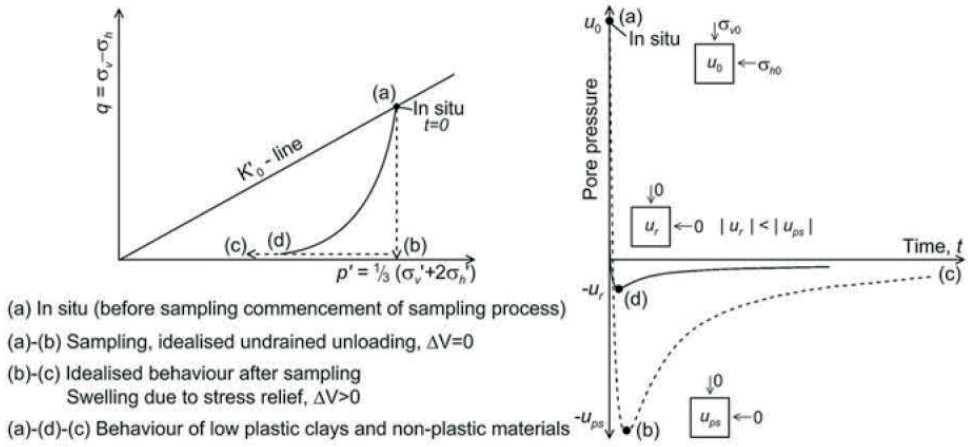

Figure 3.13. Stress path and pore pressure response of soil during sampling (Amundsen et al. 2017).

The mechanical stresses induced during the sampling stages as well as the stress relief are considered the main contributors to the disturbance of a soil sample. However, several processes occur during the storage time, which may negatively affect the sample quality. In geotechnical practice, the influence of storage has a key role when the samples have to be stored for a long time before testing. As an example, Bjerrum (1973) observed up to 10%–20% decrease in the measured undrained shear strength after three days of storage. Similar conclusions were made by La Rochelle et al. (1976) by investigating the long-term storage effect on the strength properties of low-plastic clays. In addition to the stress relief, water content and chemical changes are expected during the storage time. Leroueil (1991) concluded that in fully saturated clays, changes in water content are mostly related to long-term effects.

Moreover, the soil sample can experience migration of pore water from the remolded external zones to the intact central core (La Rochelle et al. 1981). Furthermore, the storage conditions may induce the activation of chemical processes (e.g., change in pH and electrolysis), resulting in pore-water chemistry modifications. In particular, severe changes can occur if the soil sample is stored in a steel, copper, brass, or zinc tube for a long time. However, the susceptibility for these changes largely depends upon the storage methods and soil properties. For example, the presence of swelling mineral or small lenses of silty layers within the sample may enhance changes in water content.

All the aforementioned factors can be somehow limited using suitable sampling apparatuses and adopting the correct procedure. However, sample disturbance is always present in laboratory samples, even though its severity depends on the soil properties. As an example, it has been shown that highly structured and low plastic overconsolidated clays are more susceptible to sample disturbance (Lunne et al. 2006; Di Buò et al. 2019b). In this section, a general overview of traditional samplers is presented and their performance in Finnish clays is discussed in detail.

3.3.2 Sampling equipment

To avoid or limit the disturbance induced during the sampling process, several techniques have been developed over the past decades. The types of equipment adopted worldwide depend on sampling traditions, economic issues, project requirements, and soil types. Borehole samplers can be classified as drive, rotary, and block samplers. Drive samplers are pushed into the soil without rotation, whereas rotary samplers are rotated and pushed downward into the soil, thus cutting and grinding the soil beneath it. In contrast, block samplers (e.g., Sherbrooke and mini-block) use water pressure to core out an annulus around a block of the soil to be sampled. Although high-quality samples can be obtained using borehole samplers, their use has been limited owing to the perceived high costs, practical difficulties, and time required. In the following, details on the devices and procedures adopted to retrieve samples from the investigated sites are presented. The performances of these samplers in Finnish clays have been extensively investigated by Di Buò et al. (2019b).

3.3.2.1 ST:1 50 stationary piston sampler

The ST:1 50 is a piston drive sampler developed by the Swedish Geotechnical Institute in 1961 to retrieve undisturbed samples in soft clays, silts, or fine sands. Details on the equipment and procedures can be found in the Report 1:99, 1996 (Swedish Geotechnical Society). The sampler has been widely used in Finland and Sweden, and it is characterized by a relatively easy and effective sampling procedure. The sampler comprises a piston, a locking system, extension tubes, and removable sample liners into which the soil is pushed during sampling. The piston is fixed and connected to the inner rods while the sampler body is connected by means of the extension tubes. The inner diameter is 49.5 mm and the outer diameter is 53.8 mm, giving an area ratio of 17%. The cutting edge angle is 9.7°. The total sampling length is 510 mm, and it is given by three 170-mm plastic cylinders located inside the sampler body. The sampler apparatus is shown in Fig. 3.14.

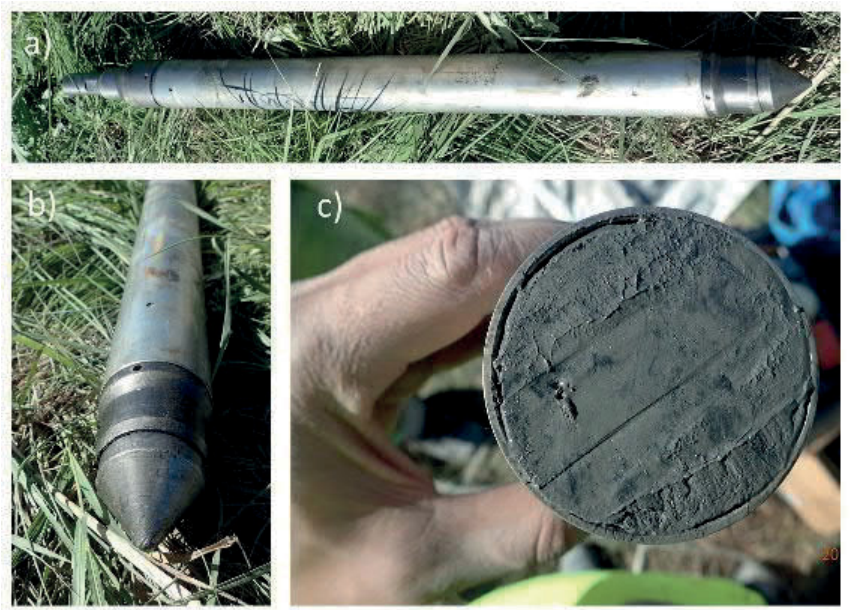

Figure 3.14. ST:1 50 piston sampler. a) ST:1 50 apparatus; b) details of the sampler tip; c) details of the soil sample.

The sampling procedure consists of three phases: insertion of the sampler, sampling, and withdrawal of the apparatus. The entire apparatus is initially pushed into the soil, with the piston locked be means of a threaded spindle, thus preventing the entrance

of the material into the sampler body. Once the sampling depth is reached, the piston is kept locked. The locking system ensures that the further downward movement is transmitted only to the sampling cylinder. The sampling is performed at approximately 1–2 cm/s to minimize the disturbance induced to the sampled soil. After reaching the final sampling depth, before the withdrawal of the apparatus, the standard procedure requires a waiting time of 5 min to ensure good adhesion between the soil and cylinder. However, in quick clays, longer time is recommended. For this stage, several standard procedures have been defined. As an example, the Swedish Geotechnical Society (Report 1:96, 1996) as well as the Norwegian Geotechnical Society (NGF 2013) suggests to recover the apparatus by pulling the entire system up at a very low speed. In contrast, in Finnish Geotechnical practice, the sampled soil is cut off from the deposit by rotating the sampler 20 times. Both procedures have been adopted at the investigated sites and their influence on the achieved sample quality is discussed by Di Buò et al. (2019b).

3.3.2.2 Aalto 86 piston sampler

The Aalto 86-mm piston sampler (Fig. 3.15), also referred to as the NGI 86-mm sampler (Mataic 2016), is a scaled version of the traditional NGI 54 (Hvroslev 1949; Andresen and Kolstad 1979). The sampler was employed in previous studies conducted at Tampere University to retrieve undisturbed samples from the Perniö site (Mansikkamäki 2015; Lehtonen 2015). Compared with the NGI 54, the Aalto 86 is modified in terms of the sampling cylinder and sampler body dimensions to allow the retrieval of larger samples. Moreover, the Aalto 86 sampler is equipped with a thin-walled self-cutting steel tube on which the sample is kept stored and extruded prior to the laboratory testing. The sampling cylinder has an external diameter of 88.94 mm and an average inner diameter of 85.88 mm, thus giving an area ratio of 6.8%. The tube length is 650 mm, even though the total sampling length is 450 mm. The cutting edge angle is 12°, and the cylinder has no inside clearance.

Compared with the ST:1 50, the sampling operation of the Aalto 86-mm piston sampler is slightly different. In particular, once the desired depth is reached, the piston is released and withdrawn upward by turning the inner rod, enabling the soil entrance into the sampling cylinder. Then, the sampling is performed by pushing the apparatus into the soil at a low speed (≈1 cm/s). Finally, the apparatus is recovered by pulling the entire system upward without using any rotation.

Figure 3.15. Aalto 86-mm sampler. a) Aalto University version, b) sampling cylinder and outdrawn piston position, and c) sampling cylinder and withdrawn piston position (Mataic 2016).

3.3.2.3 Mini-block sampler

The mini-block sampler (Emdal et al. 2016) has been developed at the Norwegian University of Science and Technology (NTNU) to overcome the difficulties encountered by the Sherbrooke block sampler (Lefebvre and Poulin 1979). In particular, the mini-block sampler has a smaller outer diameter than Sherbrooke (from 410 to 230 mm) to allow more efficient rigging and sampling operations. The sampler has been employed only at the Perniö site and its performance compared with the other sampling methods has been discussed by Di Buò et al. (2019b).

The sampler is shown in Fig. 3.16. It comprises a metallic cage made of stainless steel and is capable of sampling 300-mm-height and 160-mm-diameter specimens using horizontal cutters and a set of three blades located at the bottom of the sampler (Fig. 3.16b). These blades provide support to the block specimen during sampler retrieval. The sampling operations are illustrated in Fig. 3.17. Before starting the sampling operations, a 400-mm borehole above the sampling depth is needed. In general, the stability of the borehole is ensured by water or mud, although sometimes casing can be required. Afterward, the sampler is inserted into the borehole with the bottom blades in open configuration. Once the desired depth is reached, the sampling is performed using a water jet flowing from orifices located at the bottom ends of the three hollow arms (Fig. 3.17b) while the sampler rotates at low angular speed (5 rpm). After carving a cylindrical specimen, the locking system of the bottom blades is activated by dropping a weight from the ground surface (Fig. 3.17b), which hits the retaining pins located at the top of the sampler (Fig. 3.17c). The entire

apparatus with the sampled soil is then recovered, and the specimen is wrapped with a plastic film to avoid moisture losses and placed inside a plastic box filled up with foam chips (Fig. 3.17f) to provide lateral confinement during sample transportation and storage.

Figure 3.16. Mini-block sampler: a) sampler device, b) bottom holes and blades details, and c) details of the retaining pins.

Figure 3.17. Mini-block sampling operations: a) sampler insertion into the borehole, b) details of the drop weight, c) apparatus withdrawn, d) sampled soil details, e) wrapping of the sampled soil with plastic foil, and f) details of the PVC tube with styrofoam spheres.

3.3.2.4 TUT 132 tube sampler

TUT developed a new 132-mm open-drive tube sampler (TUT 132), inspired by the Laval sampler (La Rochelle et al. 1981). In general, the tube sampling process is more expensive, time-consuming, and delicate compared with traditional piston samplers. However, in sensitive clays, its use is justified by the sample quality achieved, which can be comparable to block sampling techniques. The sampler consists of a thin-walled sampling tube; its head is equipped with a screw-type valve, which can be opened by rotating the inner rod. Moreover, a 5° inclination cutting edge is mounted at the bottom of the sampling tube to ensure soil cutting during sampler penetration. The sampling tube has a thickness of 4 mm, an outer diameter of 139.7 mm, and an inner diameter is 131.7 mm, giving an area ratio of 12%. The total length of the sampling tube is 500 mm. In addition, 750-mm long tubes have been used at Paimio and Sipoo sites.

The operations of the TUT 132 tube sampler are shown in Fig. 3.18. Similar to the Sherbrooke sampler, a borehole is needed to reach the sampling depth. The apparatus is lowered to the hole with the valve opened (Fig.3.18b) to ensure that the mud flows upward. Once the bottom of the borehole is reached, the sampling process starts by pushing the apparatus into the soil at a very low speed (0.5 cm/s) till the final depth. Then, a resting time of 20 min is planned to ensure pore pressure dissipation and therefore better adhesion between the soil and tube. Finally, the head valve is closed by turning the inner rod to ensure an effective vacuum above the sample during withdrawal. The sample is cut from the surrounding soil by means of a cutting wire (Fig. 3.18d) pulled from the ground surface. This procedure was first introduced by Larsson (2011) to replace the sampler rotation adopted by the Laval method to shear the soil at its base, thus dividing the sample from the deposit. Before retrieving the entire apparatus, air is injected from the ground surface into the pipe to create an air flow on the cutting plane, therefore avoiding suction while lifting the sampler. Finally, the tube is disassembled from the apparatus, sealed using a plastic film and caps at the bottom ends, and transported to the laboratory. Unlike the traditional Laval sampler, the TUT 132 allows the sample to be stored into the tube and extruded only prior to the laboratory testing. The storage method along with the use of the cutting wire is considered beneficial in terms of the achieved sample quality because the stress relief is partially reduced and the torsion induced by the sampler rotation is avoided.

Figure 3.18. TUT 132 sampler: a) apparatus; b) details of the screw cap, open valve configuration; c) details of the cutting edge; d) cutting wire and pipe details; e) lower end of the sampler.

3.4 Constant rate of strain (CRS) oedometer test

CRS oedometer tests are performed on undisturbed specimens of 45-mm diameter and 15-mm initial thickness at a constant strain rate of 0.001 mm/min (0.4%/h), which is the commonly used strain rate in Finland when testing soft clay samples. The automated CRS testing apparatus was designed by Tampere University (Kolisoja et al. 1987). The equipment (Fig. 3.19) consists of an oedometer cell, a loading frame, an electric stepping motor, a control unit, a data logger, and a microcomputer.

The tested specimen is obtained by pushing a thin-walled steel oedometer ring into the natural sample prior extruded from the tube (TUT 132 or Aalto 86) or plastic liner (ST:1 50) or cut out from the block sample (mini-block). The inner area of the ring is covered with silicon oil to reduce the friction between the soil and steel wall. Once the ring is completely filled with soil, the excess material is removed using a steel wire saw and spatula. Then, saturated filter papers are placed on both sides of the specimen and the ring is locked on the oedometer cell previously filled with water. Finally, the oedometer cell is mounted on the CRS frame. The different CRS sample preparation stages are illustrated in Fig. 3.20.

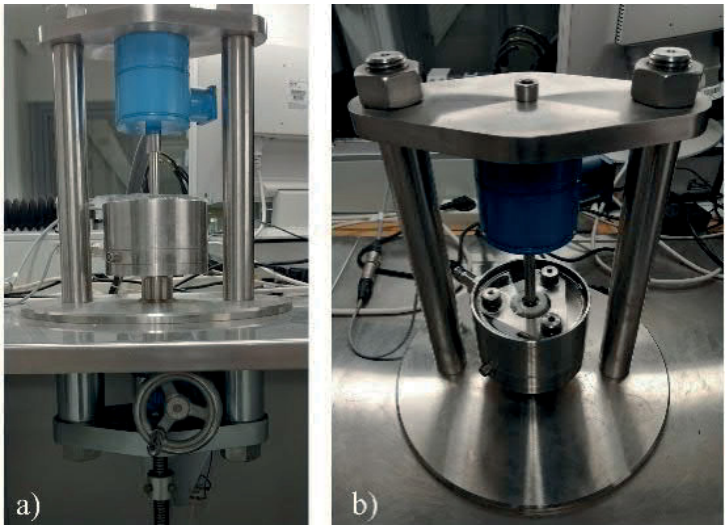

Figure 3.19. CRS oedometer testing apparatus: a) loading frame; b) oedometer cell details.

Figure 3.20. CRS oedometer test sample preparation: a) extruded sample; b) sample trimming; c) insertion of the ring; d) details of the specimen inside the ring; e) saturation of the oedometer cell; f) oedometer frame details.

Vertical deformation is applied to the tested sample using a stepping motor and mitre gear, thus transferring the motor rotation to a vertical motion. The rotary speed is controlled via a control unit by a microcomputer on the basis of previous measurements, whereas the sample vertical deformation is calculated from the total number of steps of the stepping motor. The sample basement is impervious, but it contains porous stone connected to a pore pressure transducer. During the test, vertical load and pore pressure are measured at short intervals (5–10 min) using electronic strain gauge transducers and transferred to the microcomputer unit for storage.

4 EXPERIMENTAL PROGRAM RESULTS

4.1 Introduction

This section presents the results of the experimental program, including CPTu soundings, index tests, CRS consolidation tests, and sample quality evaluation. The investigated sites are located in the southern region of Finland, along the railway tracks connecting the cities of Turku, Helsinki, and Tampere (Fig. 4.1). Despite local differences in terms of natural water content, plasticity, and sensitivity, these sites are characterized by similar geological origin which is connected to the Baltic Sea formation as discussed in chapter 2.

All the tests are conducted in accordance with the ISO standards (ISO 22476-1:2012 for piezocone testing, ISO/TS 17892-12:2004 for laboratory testing, and CEN ISO/TS 17892-5:2004 for oedometer testing). The CPTu soundings are shown for each site in terms of the corrected cone tip resistance (q_t), sleeve friction (f_s), pore-water pressure (u_2), normalized friction ratio (F_r), pore-pressure ratio (B_q), and additional measurements performed using the seismic and resistivity modules. Moreover, the SBTn chart proposed by Robertson (2009) is presented.

The laboratory testing program comprises soil classification tests, index tests and CRS consolidation tests. All the tests have been conducted in the laboratory on samples retrieved from the investigated sites. In particular, for the Atterberg limits evaluation, the fall cone (FC) test is used for evaluating w_L and S_t while w_P is measured by means of the rolling test. Finally, the clay fraction is determined based on the hydrometer analysis.

The collected data is used to establish a database, which is exploited to assess the validity of existing correlations and develop new methods to derive the soil geotechnical parameters from CPTu data. Therefore, particular emphasis is given to the test quality evaluation. In particular, the quality of the CPTu soundings are assessed based on the procedures discussed earlier in the thesis (e.g., repeatability, zero load readings, and porous stone saturation), while the sample quality is classified based on the Lunne et al. (1997) criteria.

Figure 4.1. Location of the "FINCONE" test sites.

4.2 Perniö test site

4.2.1 Index properties

The Perniö test site worked as a benchmark site for several research studies conducted at Tampere University. As an example, a full-scale railway embankment failure test was conducted in 2009 with the aim of collecting data to improve the reliability of the existing stability calculation methods (Lehtonen et al. 2015; Di Buò et al. 2019a). Moreover, an extensive experimental program has been conducted by Mataic (2016) to evaluate the mechanical behavior and rate dependence of Perniö clay. The test site is located on the southwestern coast of Finland, about 140 km west of the city of Helsinki. The lithostratigraphic condition of the deposit includes a 1–1.5-m-thick dry crust underlain by 8–9-m-thick soft clay layer; silt and stiff sandy

layers can be found at a greater depth. The groundwater table is located at 1-m depth. The geotechnical properties of the site are shown in Fig. 4.2 and Table 4.1. Among all the investigated sites, the Perniö site has clay that is characterized by natural w ranging between 80% and 100%. The PI value varies between 20% and 40%, with the lowest values observed at around 5-m depth. The FC test indicates S_t values between 40 and 60 over the entire deposit. The undrained shear strength (s_u) ranges between 10 and 15 kPa, whereas s_u^{re} is nearly constant with depth, with values between 0.20 and 0.30 kPa. Finally, the hydrometer test revealed clay content varying between 50% and 90%, with the highest values observed below 6-m depth, and organic content of less than 2%.

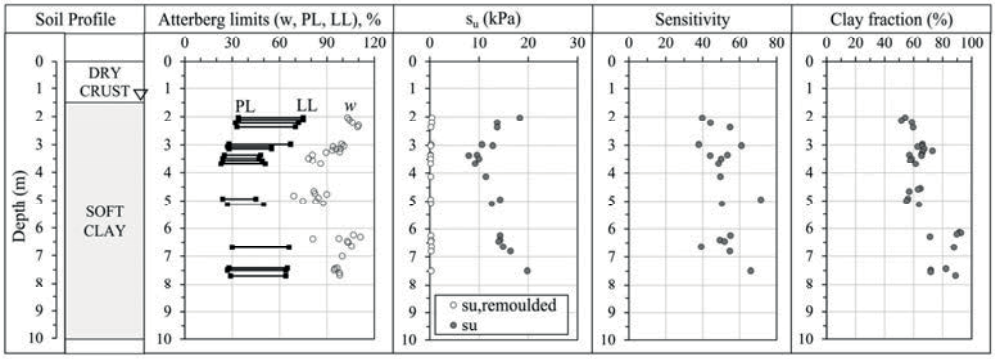

Figure 4.2. Stratigraphy and index properties of the Perniö site.

Table 4.1. Geotechnical properties of the Perniö clay.

Site	Depth (m)	w (%)	PI (%)	S_t	Clay fraction (%)
Perniö	2–3	100–110	40	40–60	50–60
	3–4	70–100	30	40–50	50–70
	4–6	70–90	30	50–70	50–70
	6–8	90–110	40	40–70	70–90

4.2.2 CPTu soundings

The CPTu results from the Perniö site are shown in Fig. 4.3. A total of four piezocone soundings are performed, one of which (T1) was performed with the high-capacity cone. Measurements scatter is observed in the dry crust layer and below 9-m depth owing to small lenses of silts. The soil stratigraphy presents a

homogeneous soft clay layer between 3 and 9 m depth, characterized by q_t increasing from 200 to 350 kPa and u_2 from 120 to 270 kPa. The f_s value is characterized by lack of accuracy owing to the sensor resolution (≈2 kPa) as shown in Fig. 4.3b. As previously discussed (section 3.2.1), this leads to high scatter in the measured data, resulting in high uncertainties when using these parameters for soil interpretation. As an example, the soil classification based on the SBTn chart (Fig. 4.3h and 4.3i) reveals that most of the data points fall far from the sensitive clay region both in the Q_{tn}–F_r and Q_{tn}–B_q. This is probably due to the inaccuracy of the sleeve sensor in measuring small values of f_s as discussed by Di Buò et al. (2020). Tests with additional modules are also performed. In particular, v_s is measured at 1-m depth intervals, from 2 to 8 m depth, indicating values between 50 and 100 m/s. The soil conductivity, measured using the resistivity modules, increases from 50 to 100 mS/s in the upper layer and is approximately constant and equal to 100 mS/s from 5 to 9 m depth.

Overall, the repeatability between the different soundings is very good, and the pore-pressure response indicates that the saturation of the porous stone is ensured for all soundings. The decrease in the u_2 value observed from the T3 vertical sounding is related to the dissipation test performed at 5.5-m depth. The application class of each CPTu sounding is evaluated according to the EN-ISO 22476-1, as discussed in section 3.2.6. The zero shift loads and maximum error calculated for q_t, f_s, and u_2 are summarized in Table 4.2. The T1 sounding is characterized by the lowest quality (class 3) in terms of the q_c, while all the other CPTu verticals belong to the highest class (class 1).

Table 4.2. CPTu quality, Perniö.

CPTu sounding	q_c (kPa)			f_s (kPa)			u_2 (kPa)		
	Zero shift	Maximum error	Class	Zero shift	Maximum error	Class	Zero shift	Maximum error	Class
T1	−2.3	102.3	3	−0.1	3.1	1	−1.5	6.5	1
T2	6.8	21.8	1	0.6	2.6	1	−4.3	9.3	1
T3	6.2	21.2	1	1	3	1	−1.0	6.0	1
T4	15.1	30.1	1	−0.2	2.2	1	−4.7	9.7	1

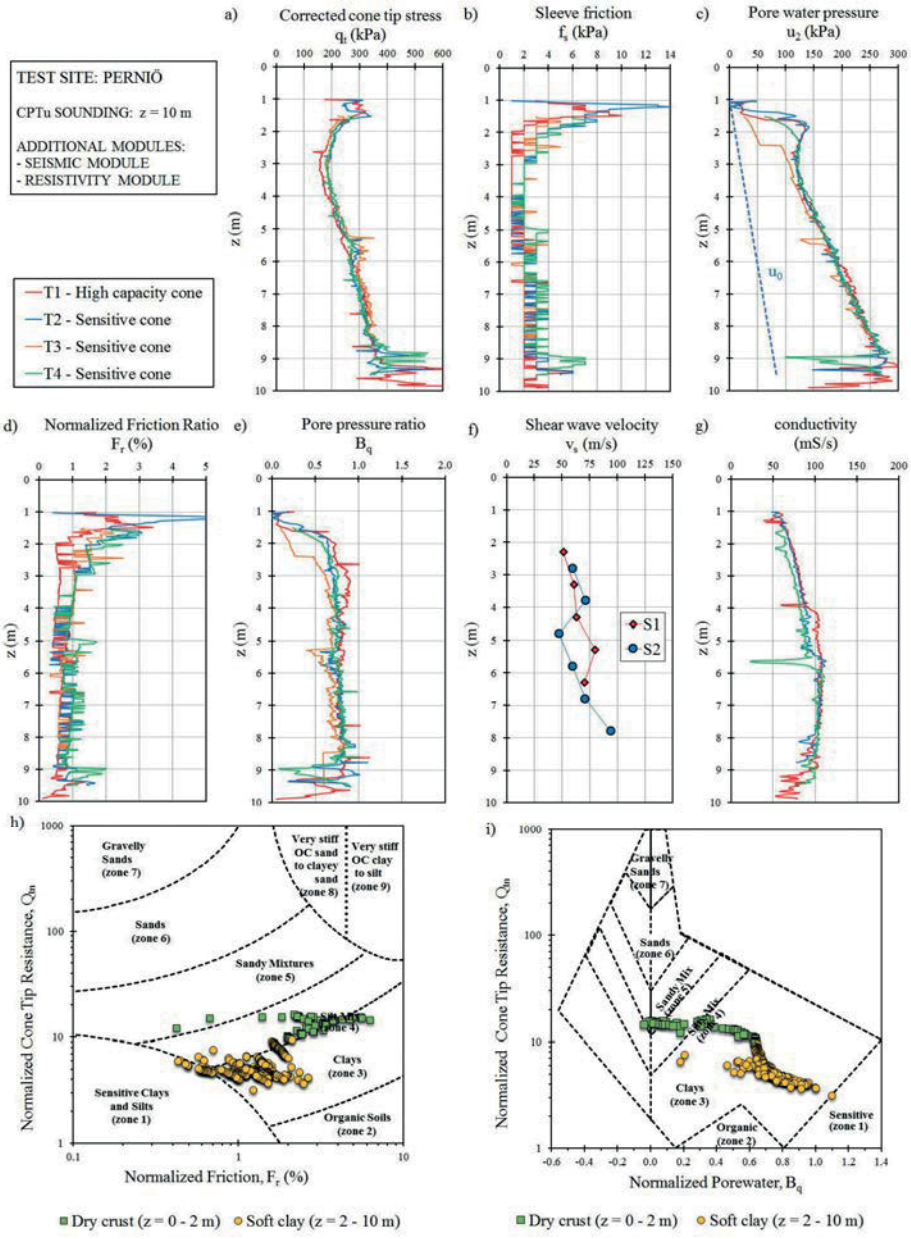

Figure 4.3. CPTu soundings result, Perniö; a) corrected cone tip resistance, q_t; b) sleeve friction, f_s; c) pore-water pressure, u_2; d) normalized friction ratio, F_r; e) pore-pressure ratio, B_q; f) shear wave velocity, v_s; g) conductivity; h) normalized soil behavior type (SBTn) chart based on Q_{tn}–F_r; i) normalized soil behavior type (SBTn) chart based on Q_{tn}–B_q.

4.2.3 CRS consolidation tests

The CRS consolidation tests are performed on undisturbed samples obtained using the four different samplers described in section 3.3. A total of 46 tests are available for the Perniö site and the results are summarized (Appendix 1). Fig. 4.4 shows few CRS test results in terms of σ'_v versus ε_a and M versus σ'_v.

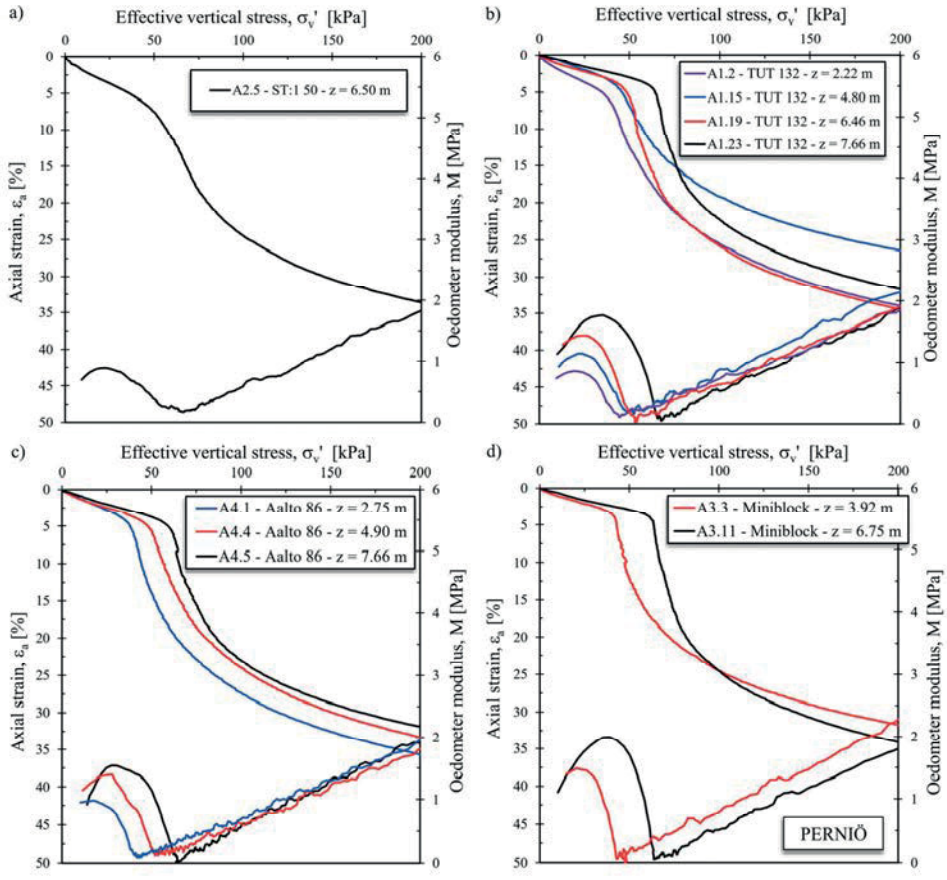

Figure 4.4. CRS consolidation test results of specimens retrieved with different sampling methods from Perniö: a) ST:1 50 piston; b) TUT 132; c) Aalto 86; d) Mini-block.

The observed stress-strain behavior is the typical behavior of marine sensitive clays. It is worth observing that the soil behavior is clearly influenced by the sampling method. As an example, samples obtained by the mini-block sampler are characterized by a stiffer response in the OC region and a more evident drop beyond

σ'_p compared with the only ST:1 50 piston sample available. Most of the ST:1 50 piston samples are completely disturbed and could not be used for interpretation. These aspects will be discussed in section 4.7. The behavior in the NC region is similar for all the tested samples, characterized by an initial drop of the effective vertical stress and a nonlinear stress-strain behavior shown in the σ'_v versus ε_a chart while *M* increases linearly with increasing stress. However, the compressibility of the tested samples appears to be influenced by the water content. These aspects will be discussed later in the thesis.

4.3 Lempäälä test site

4.3.1 Index properties

The Lempäälä test site is located near the city of Tampere, along the railway track to Helsinki. The soil stratigraphy consists of a 1–1.5-m-thick dry crust layer, followed by 1–1.5 m of organic soil underlain by a soft sensitive low-plastic clay layer. The groundwater table is located at 0.60-m depth. The index properties of Lempäälä clay are shown in Fig. 4.5 and Table 4.3. The investigation conducted at the site revealed that the shallow layer is composed of fill material placed in situ during the embankment work construction. This layer is characterized by high water content, high plasticity, and lower sensitivity compared with the soft clay layer. The natural soil layer shows varying value of w between 70% and 80%. The w_L value is lower than the natural water content over the entire deposit, which is commonly observed in Finnish clays. The PI is approximately 25%–30%, even though smaller values can be noticed between depths of 4 and 5 m. The FC test indicates a significant variability of S_t, which may suggest the presence of thin layers of different properties within the deposit. Moreover, the s_u measured by the FC test ranges between 6 and 15 kPa, whereas s_u^{re} is lower than 0.50 kPa over the entire deposit. The clay content is slightly higher than 60% in the soft clay layer, while lower values can be noticed at shallow depth. Finally, Lempäälä clay shows low organic content (<1%) even though higher values (≈5%) are encountered in the dry crust layer.

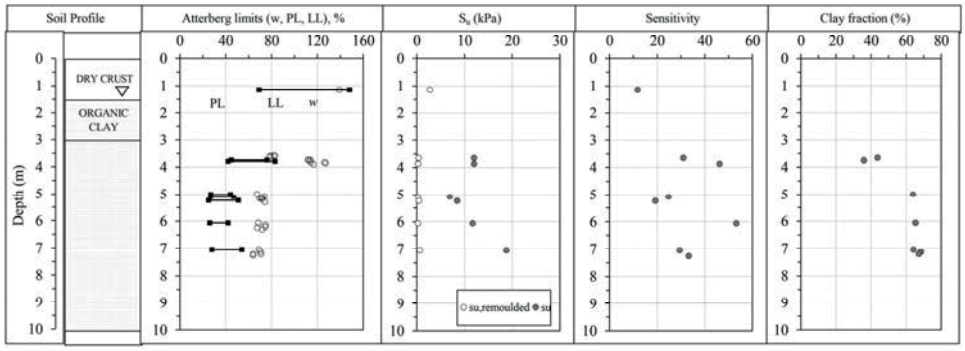

Figure 4.5. Stratigraphy and index properties of the Lempäälä site.

Table 4.3. Geotechnical properties of Lempäälä clay.

Site	Depth (m)	w (%)	PI (%)	S_t	Clay fraction (%)
Lempäälä	1–2	130	60	10	–
	3–4	100–130	40	30–50	35–45
	5–7	60–80	30	20–50	60–70

4.3.2 CPTu soundings

The field investigation includes five CPTu soundings, one performed using the high capacity cone (T1) and four with the sensitive cone. Piezocone sounding results are presented in Fig. 4.6. As shown by the laboratory test results, the uppermost part of the deposit is composed of a dry crust layer (0–1 m), followed by a 2-m-thick layer of organic material (1–3 m) and a soft clay deposit between 3 and 10 m depth. The corrected cone tip resistance (q_t) appears to be constant between 3 and 5 m depth ($q_t \approx 180$ kPa), increasing up to 300 kPa at 8-m depth. The excess pore-water pressure (u_2) measurements are consistent among all the soundings, with values from 90 kPa at 3-m depth to 250 kPa at 8-m depth. Below, scatter of data is observed in terms of both q_t and u_2, probably due to the presence of silty layers. As observed at Perniö site, scatter of f_s measurement is observed due to the low accuracy of the sleeve sensor. The F_r value varies between 1% and 2%, while B_q is lower than 1.0. The v_s value ranges between 40 and 100 m/s in the soft clay layer. The conductivity of the soil is approximately constant with depth with an average value of 60 mS/s. The soil classification provided by the SBTn charts indicates data points from the

upper layer falling into the silt region, while the soil from the bottom layer can be classified as clay. However, data points are quite scattered in the chart.

The test quality is summarized in Table 4.4. All the soundings are characterized by high quality (class 1) except for the q_c data from the T1 sounding, which belongs to class 3. Overall, good repeatability between the different test verticals is observed.

Table 4.4. CPTu quality, Lempäälä.

CPTu sounding	q_c (kPa)			f_s (kPa)			u_2 (kPa)		
	Zero shift	Maximum error	Class	Zero shift	Maximum error	Class	Zero shift	Maximum error	Class
T1	0.5	100.5	3	0.3	3.3	1	−0.6	5.6	1
T2	7.7	22.7	1	−0.2	2.2	1	1.6	6.6	1
T3	10.4	25.4	1	0.2	2.2	1	−1.3	6.3	1
T4	−4.4	19.4	1	1.1	3.1	1	−1.7	6.7	1
T5	−0.1	15.1	1	1.6	3.6	1	3.8	8.8	1

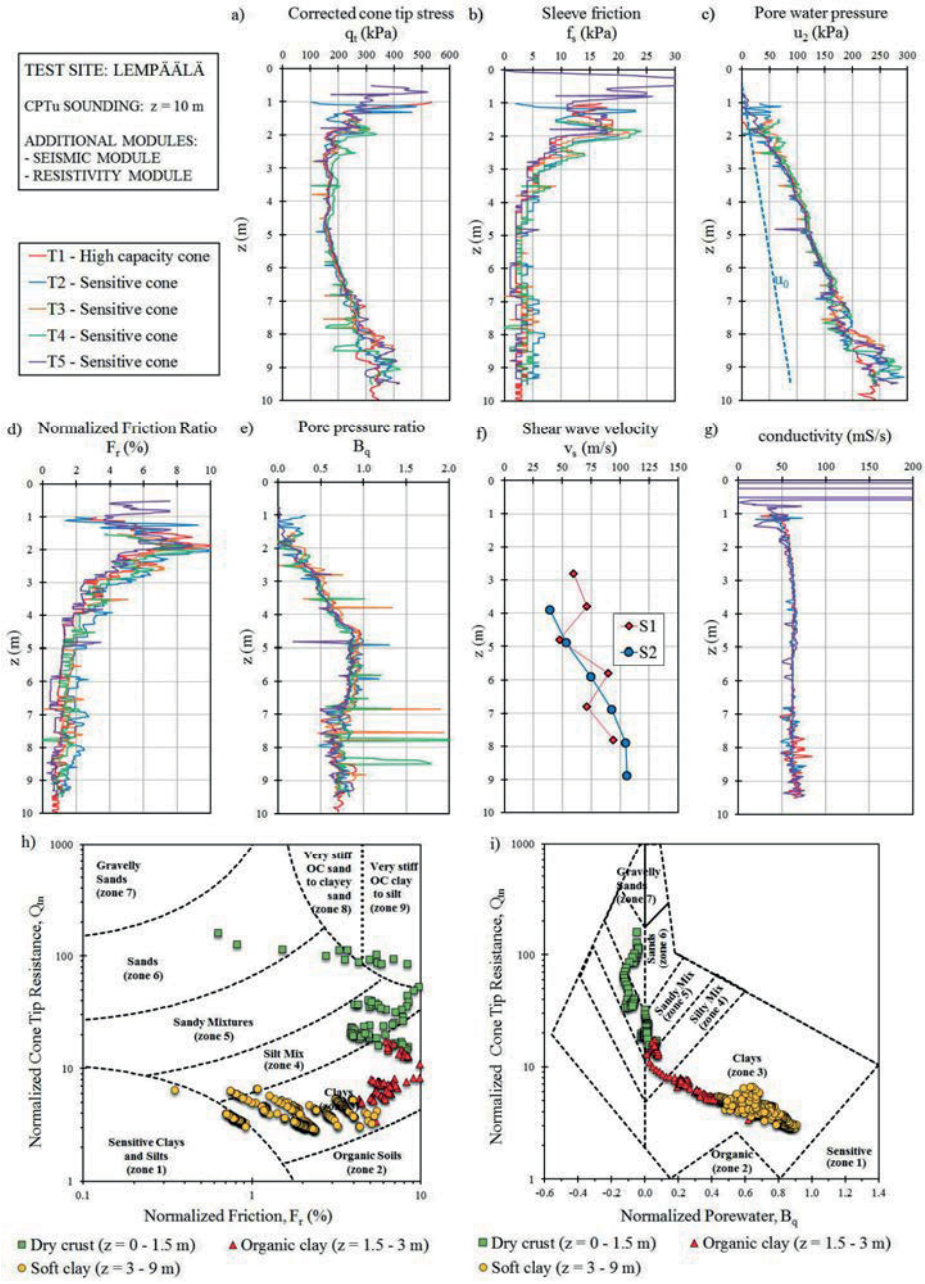

Figure 4.6. CPTu soundings result, Lempäälä; a) corrected cone tip resistance, q_t; b) sleeve friction, f_s; c) pore-water pressure, u_2; d) normalized friction ratio, F_r; e) pore pressure ratio, B_q; f) shear wave velocity, v_s; g) conductivity; h) normalized soil behavior type (SBTn) chart based on Q_{tn}–F_r; i) SBTn chart based on Q_{tn}–B_q.

4.3.3 CRS consolidation tests

Results from CRS consolidation tests from Lempäälä clay are summarized in Appendix 2. Samples were taken from 3 to 7 m depth using the ST:1 50 piston and TUT 132 tube samplers. A total of 21 samples were tested and some results are shown in Fig. 4.7. Compared with the other investigated sites, the achieved sample quality at the Lempäälä site is the lowest. From Appendix 2, it can be noted that several samples appear to be totally disturbed and therefore could not be used for data interpretation. The reasons of the low quality samples are discussed in detail in section 4.7.

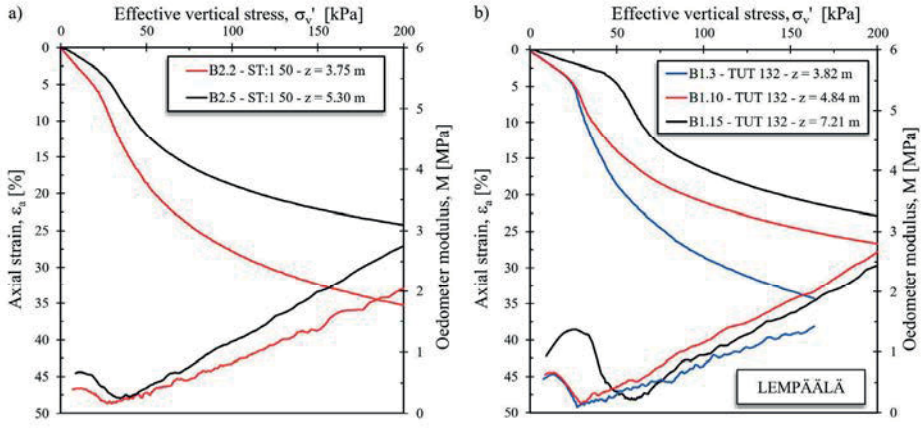

Figure 4.7. CRS consolidation test results of specimens from Lempäälä, retrieved with a) ST:1 50 piston and b) TUT 132.

4.4 Masku test site

4.4.1 Index properties

The Masku test site is located at the southwestern coast of Finland, near the city of Turku. The soil stratigraphy includes a 1.5-m-thick weathered clay crust, followed by an 8-m-thick soft clay layer. The groundwater table is located at 1.20 m depth. At this site, samples were taken only at 3, 5, and 8 m depth. The water content is about 80% at 3 and 8 m depth, even though values up to 120% are encountered in the intermediate layer. The PI is about 60% at 5-m depth while lower values can be noticed at the other depths. Compared with the other sites, Masku is one of the least sensitive, with values ranging between 15 and 20. In particular, s_u, evaluated by the FC test, varies between 15 and 20 kPa, whereas s_u^{re} is slightly higher than 0.50 kPa. The clay content is particularly high, with values increasing from 60% at 3-m depth to 90% at greater depths. Finally, the organic content is lower than 2% over the entire deposit. The geotechnical properties of Masku clay are shown in Fig. 4.8 and Table 4.5.

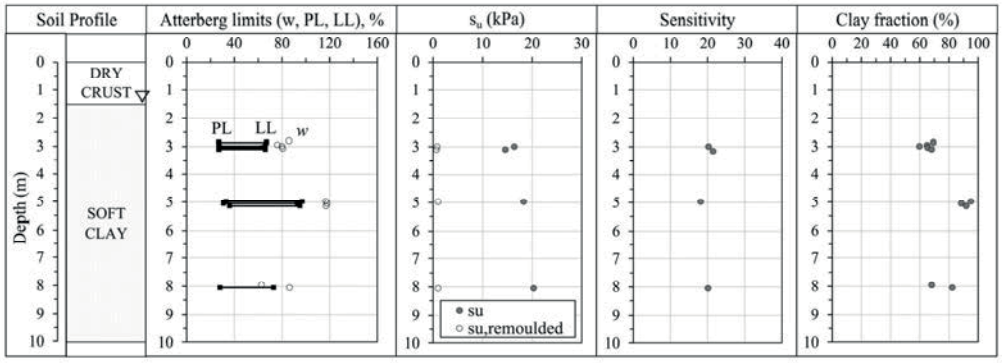

Figure 4.8. Stratigraphy and index properties of the Masku site.

Table 4.5. Geotechnical properties of Masku clay.

Site	Depth (m)	w (%)	PI (%)	S_t	Clay fraction (%)
Masku	3	80	40	20	60–70
	5	120	70	20	90–100
	7	60–80	50	20	70–80

4.4.2 CPTu soundings

As for the other sites, the CPTu soundings, shown in Fig. 4.9, are performed using both the high-capacity cone (T1) and sensitive cones (T2–T5). To avoid cone desaturation when penetrating the dry crust, an initial pre-drilling in the upper layer is made. Overall, the different tests show good repeatability even though T1 provides slightly higher f_s. Moreover, T4 sounding is clearly affected by pore pressure issues, probably due to inaccurate initial saturation of the porous stone. The q_t and u_2 increase linearly with depth. The F_r value is lower than 2% while B_q ranges between 0.5 and 0.8. The v_s value measured using the seismic module ranges between 75 and 100 m/s. The conductivity increases till 4-m depth, thus remaining constant till 10-m depth (≈250 mS/s). Finally, the SBTn charts indicate a quite homogeneous clay layer, even though few data points fall in the silt mix region, as observed in the Q_{tn}–F_r chart.

The CPTu data quality is summarized in Table 4.6. Except the T1 sounding, all the CPTu tests are characterized by high quality (class 1). However, as discussed earlier, the pore pressure response from T4 is clearly affected by desaturation. This aspect is not revealed by the zero shift measurement.

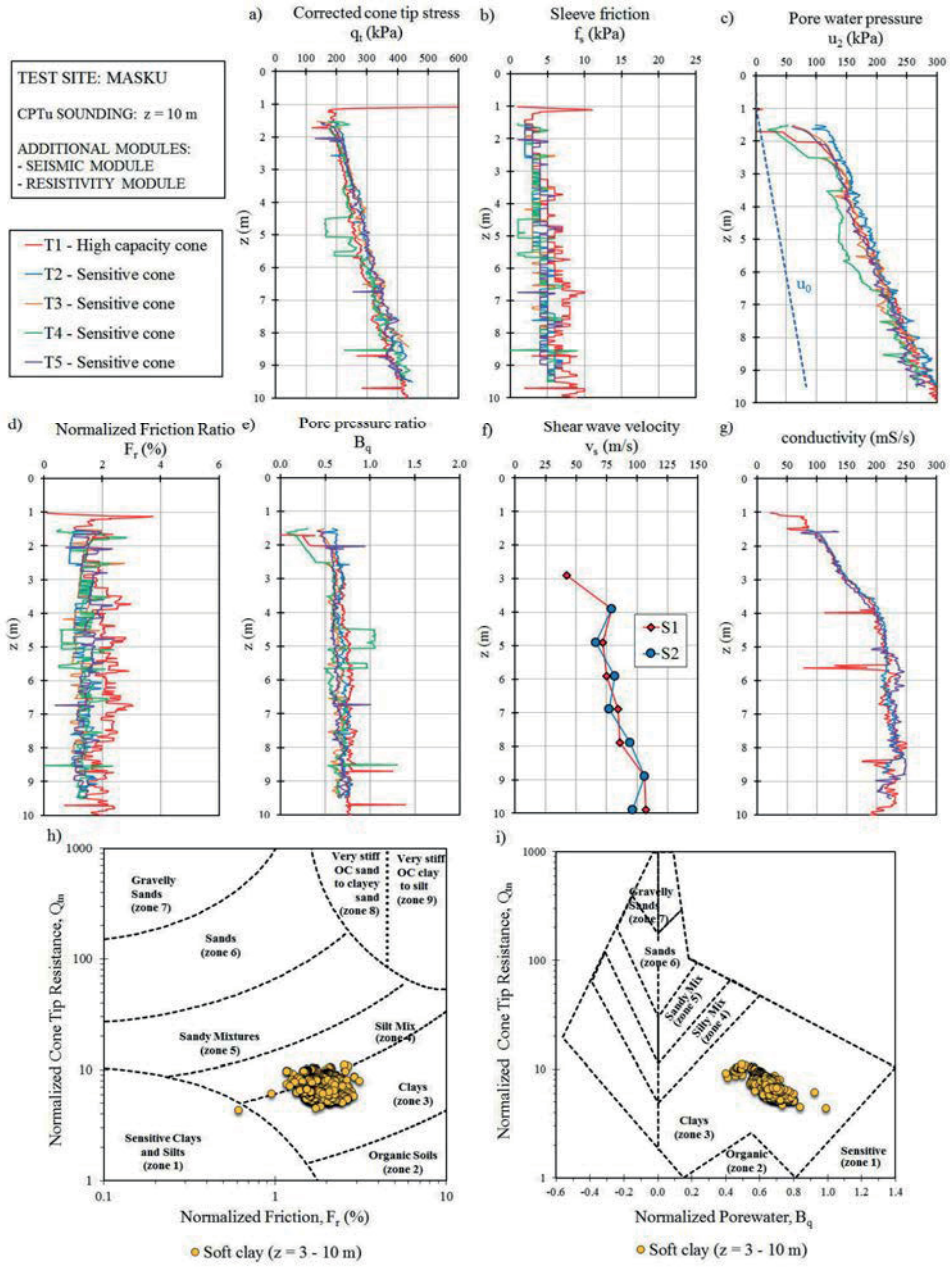

Figure 4.9. CPTu soundings result, Masku; a) corrected cone tip resistance, q_t; b) sleeve friction, f_s; c) pore-water pressure, u_2; d) normalized friction ratio, F_r; e) pore pressure ratio, B_q; f) shear wave velocity, v_s; g) conductivity; h) normalized soil behavior type (SBTn) chart based on Q_{tn}–F_r; i) SBTn chart based on Q_{tn}–B_q.

Table 4.6. CPTu quality, Masku.

CPTu sounding	q_c (kPa)			f_s (kPa)			u_2 (kPa)		
	Zero shift	Maximum error	Class	Zero shift	Maximum error	Class	Zero shift	Maximum error	Class
T1	6.5	106.5	3	0.4	3.4	1	−4.0	9.0	1
T2	7.5	22.5	1	0.8	2.8	1	−3.5	8.5	1
T3	−0.8	15.8	1	1.3	3.3	1	−2.2	7.2	1
T4	1.1	16.1	1	1.5	3.5	1	−5.1	10.1	1
T5	−6.1	21.1	1	1.6	3.6	1	−3.7	8.7	1

4.4.3 CRS consolidation tests

Undisturbed samples from the Masku site were obtained using only the TUT 132 tube sampler. Therefore, for this site, a direct comparison between the different sampling techniques is not possible. The sampling was performed at three different depth levels (3, 5, and 8 m). Results are summarized in Appendix 3; Fig. 4.10 shows the results of three different CRS consolidation tests. The stress-strain behavior of Masku clay is similar to that of the other investigated clays. However, the sample retrieved from 5-m depth shows a more brittle behavior when passing σ'_p.

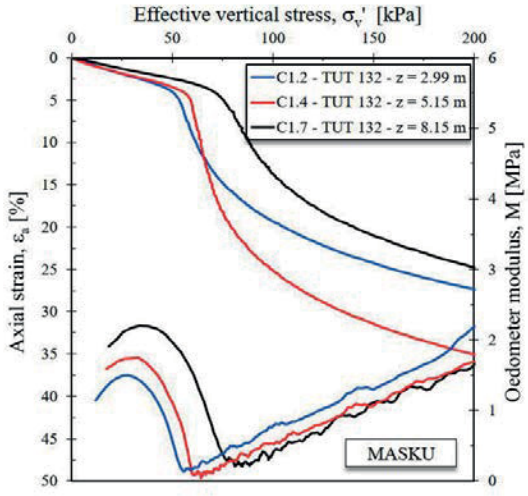

Figure 4.10. CRS consolidation test results of specimens retrieved from Masku with TUT 132.

4.5 Paimio test site

4.5.1 Index properties

Paimio is located about 25 km from the city of Turku, in the southwestern region of Finland. The stratigraphy consists of a 2-m-thick clay crust overlaying an 8-m-thick soft clay layer. The groundwater table is located at 0.80-m depth. The index properties of Paimio clay (Fig. 4.11) reveal the presence of a leaner upper clay layer above 6.5-m depth and a more plastic clay layer below. The shallow layer is characterized by w of 50%–80% and PI of 15%–20%, whereas higher w (90%–110%) and PI (30%) can be noticed at greater depths. Paimio clay is characterized by high S_t, with values varying between 60 and 90. In addition, the FC test revealed s_u between 13 and 17 kPa, whereas s_u^{re} was lower than 0.3 kPa over the entire deposit. The clay content increases with depth, from 40% at shallow depth to values of about 100% between 6 and 7 m depth, whereas the organic content is less than 1%. The geotechnical properties of Paimio clay are summarized in Table 4.7.

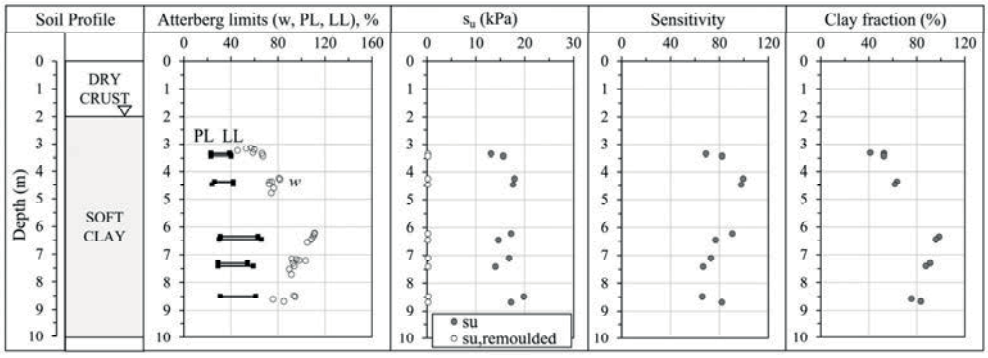

Figure 4.11. Stratigraphy and index properties of the Paimio site.

Table 4.7. Geotechnical properties of Paimio clay.

Site	Depth (m)	w (%)	PI (%)	S_t	Clay fraction (%)
Paimio	3–5	40–80	20	60–100	40–60
	6–7	90–110	40	80–90	95
	7–9	70–90	40	60–80	80–90

4.5.2 CPTu soundings

The CPTu soundings from the Paimio site are illustrated in Fig. 4.12. As observed for the other sites, the q_t and u_2 values increase linearly with depth in the soft clay layer, while f_s is constantly below 5 kPa. The F_r value is lower than 2% over the entire clay layer, while B_q is approximately constant and equal to 0.6–0.7. Two S-CPTu verticals are performed, showing v_s values ranging between 50 and 100 m/s. Moreover, the R-CPTu verticals indicate constant conductivity throughout the soft clay layer, approximately equal to 60 mS/s. Finally, the classification of the soil type indicates the presence of sensitive clays, in agreement with the results from the FC test.

The quality of each CPTu sounding is shown in Table 4.8 in terms of zero shift load measurements and maximum error. In particular, tests T1 and T2 are affected by low accuracy in terms of q_t and u_2, whereas all the other tests are characterized by the highest quality class.

Table 4.8. CPTu quality, Paimio.

CPTu sounding	q_c (kPa)			f_s (kPa)			u_2 (kPa)		
	Zero shift	Maximum error	Class	Zero shift	Maximum error	Class	Zero shift	Maximum error	Class
T1	17.3	117.3	3	0.9	3.9	1	−7.7	12.7	2
T2	−1.6	16.6	1	0.3	2.3	1	−5.4	10.4	2
T3	0.3	15.3	1	1.1	3.1	1	−4.4	9.4	1
T4	−6	21	1	0.7	2.7	1	−3.9	8.9	1
T5	−1.8	16.8	1	1.7	3.7	1	−4.9	9.9	1

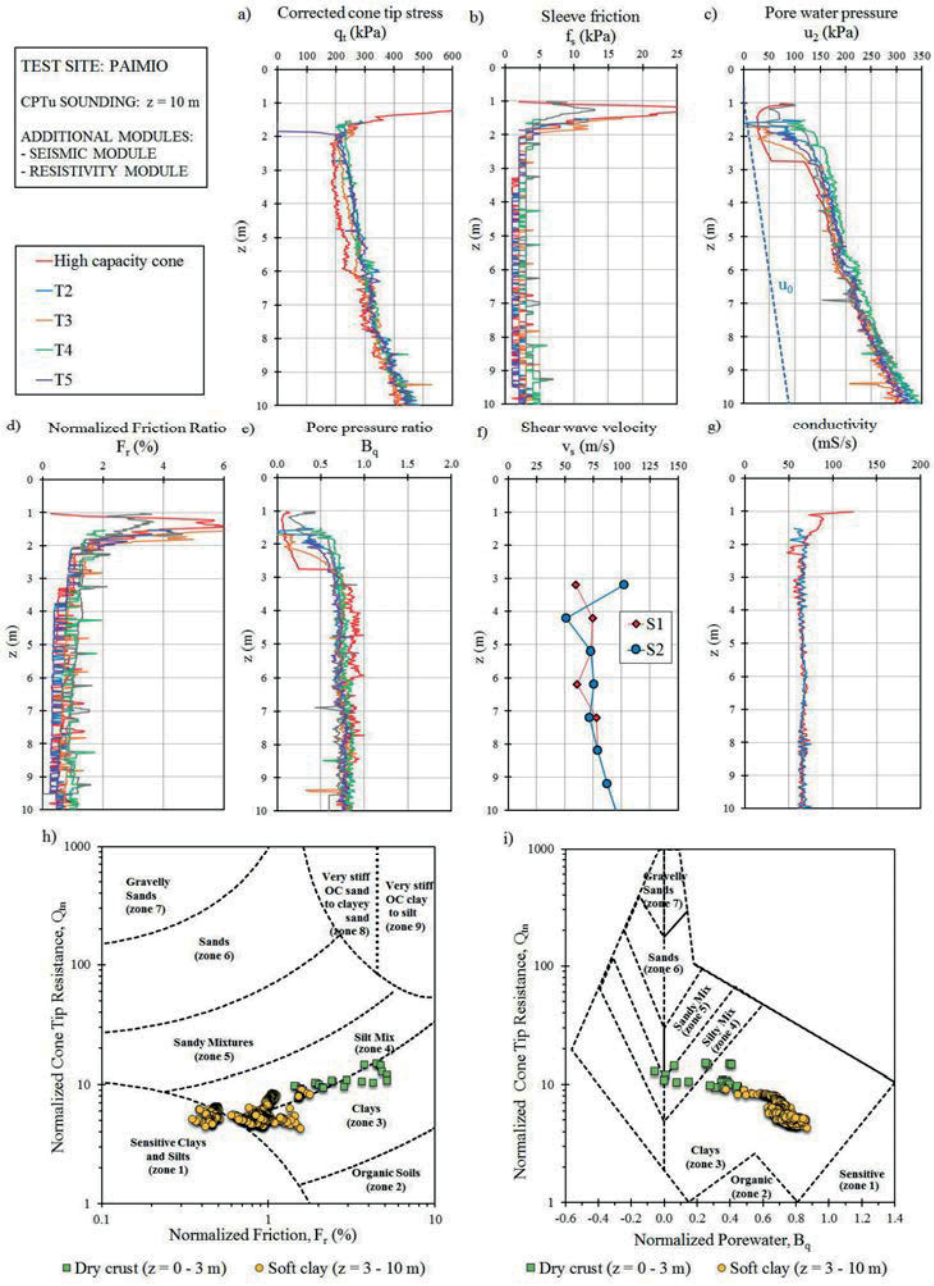

Figure 4.12. CPTu soundings result, Paimio; a) corrected cone tip resistance, q_t; b) sleeve friction, f_s; c) pore-water pressure, u_2; d) normalized friction ratio, F_r; e) pore pressure ratio, B_q; f) shear wave velocity, v_s; g) conductivity; h) normalized soil behavior type (SBTn) chart based on Q_{tn}–F_r; i) SBTn chart based on Q_{tn}–B_q.

4.5.3 CRS consolidation tests

The laboratory investigation conducted on Paimio clay includes a total of 22 CRS consolidation tests on ST:1 50 and TUT 132 samples. Results are summarized in Appendix 4 and shown in Fig. 4.13. It is worth observing that the compressibility in the NC region is considerably lower in the upper layer (z = 3–5 m), where the water content is lower ($w \approx 40\%–80\%$) than the bottom layer (z = 5–9 m), which is characterized by higher water content ($w \approx 80\%–110\%$). Overall, the samples show rather good quality. The sample quality achieved at the site is discussed in section 4.7.

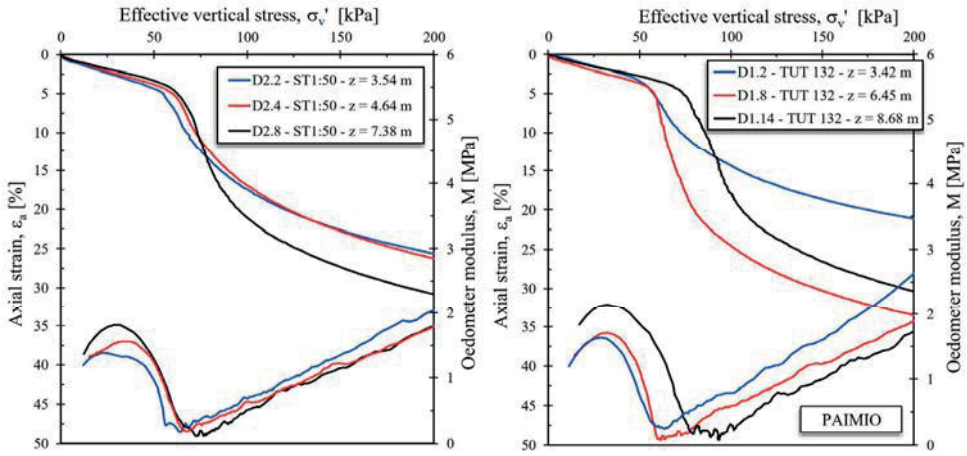

Figure 4.13. CRS consolidation test results of specimens retrieved from Paimio with (a) ST:1 50 piston and (b) TUT 132.

4.6 Sipoo test site

4.6.1 Index properties

The Sipoo site is situated 30 km north of the city of Helsinki. The deposit consists of a homogeneous soft clay layer between 2 and 9 m depth and a 2-m-thick dry crust layer. The groundwater table is located at 1-m depth. Compared with the clays at the other investigated sites, Sipoo clay is characterized by the highest plasticity and lowest sensitivity. The PI reaches values of 60% between 5 and 6 m depth. Also, the

measured water content of samples retrieved from the site is considerably high, with values up to 120% at 6-m depth. The S_t value, evaluated by the FC test, ranges between 20 and 30. The s_u value is about 15 kPa while s_u^{re} varies between 0.50 and 1 kPa. The clay content increases from 60% at 3-m depth to 90% at greater depths. As observed for the other sites, the organic content is lower than 2% throughout the deposit; therefore, Sipoo clay can be classified as inorganic clay. The geotechnical properties of the Sipoo site are shown in Fig. 4.14 and Table 4.9.

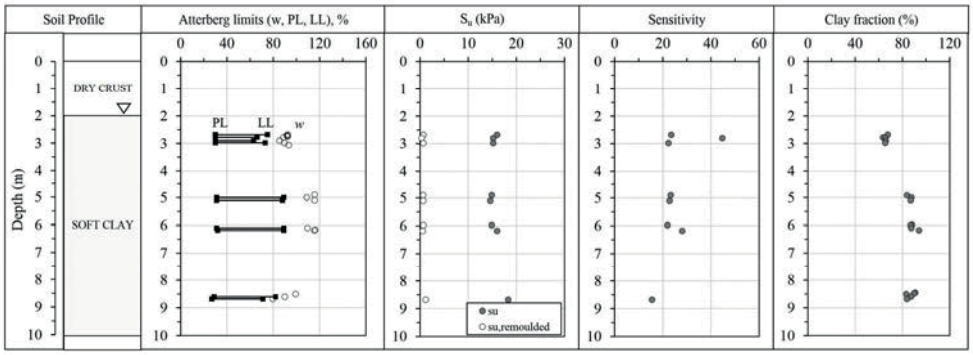

Figure 4.14. Stratigraphy and index properties of Sipoo site.

Table 4.9. Geotechnical properties of Sipoo clay.

Site	Depth (m)	w (%)	PI (%)	S_t	Clay fraction (%)
Sipoo	2–3	80–100	50	20–40	60
	5–7	90–110	60	20–30	90
	8–9	80–100	50	15	80–90

4.6.2 CPTu soundings

A total of six CPTu soundings are performed at the site, including one high-capacity cone test. Results are shown in Fig. 4.15, indicating the presence of a dry crust layer underlain by a soft clay layer. In particular, q_t appears to be nearly constant and equal to 200 kPa between 2 and 4 m depth; this value increases to 400 kPa at 9-m depth. Similarly, u_2 increases from 100 to 300 kPa between 2 and 9 m depth. Despite inaccuracy affecting the f_s measurements, F_r appears to be quite low, with values varying between 1% and 3% over the entire soft clay layer. The B_q value ranges between 0.6 and 0.7. Additional measurements are performed with seismic and

resistivity modules. The shear wave velocity is quite low in the upper part, with values lower than 50 m/s and increases to 100 m/s at 9-m depth. The conductivity is constant and approximately equal to 60 mS/s.

Overall, the quality of the CPTu measurements is fairly good. However, both T1 and T2 are characterized by poor quality, as shown by Table 4.10. Therefore, these tests are not taken into account in the data interpretation.

Table 4.10. CPTu quality, Sipoo.

CPTu sounding	q_c (kPa)			f_s (kPa)			u_2 (kPa)		
	Zero shift	Maximum error	Class	Zero shift	Maximum error	Class	Zero shift	Maximum error	Class
T1	−14.4	114.4	3	4.5	7.5	2	−143.2	148.2	4
T2	59.4	74.4	2	−4.5	6.5	2	9.8	14.8	2
T3	−2.4	17.4	1	1	3	1	−0.2	5.2	1
T4	4.8	19.8	1	0.5	2.5	1	−1.8	6.8	1
T5	10.8	25.8	1	0.5	2.5	1	−5.6	10.6	2
T6	2.2	17.2	1	0.6	2.6	1	−2.3	7.3	1

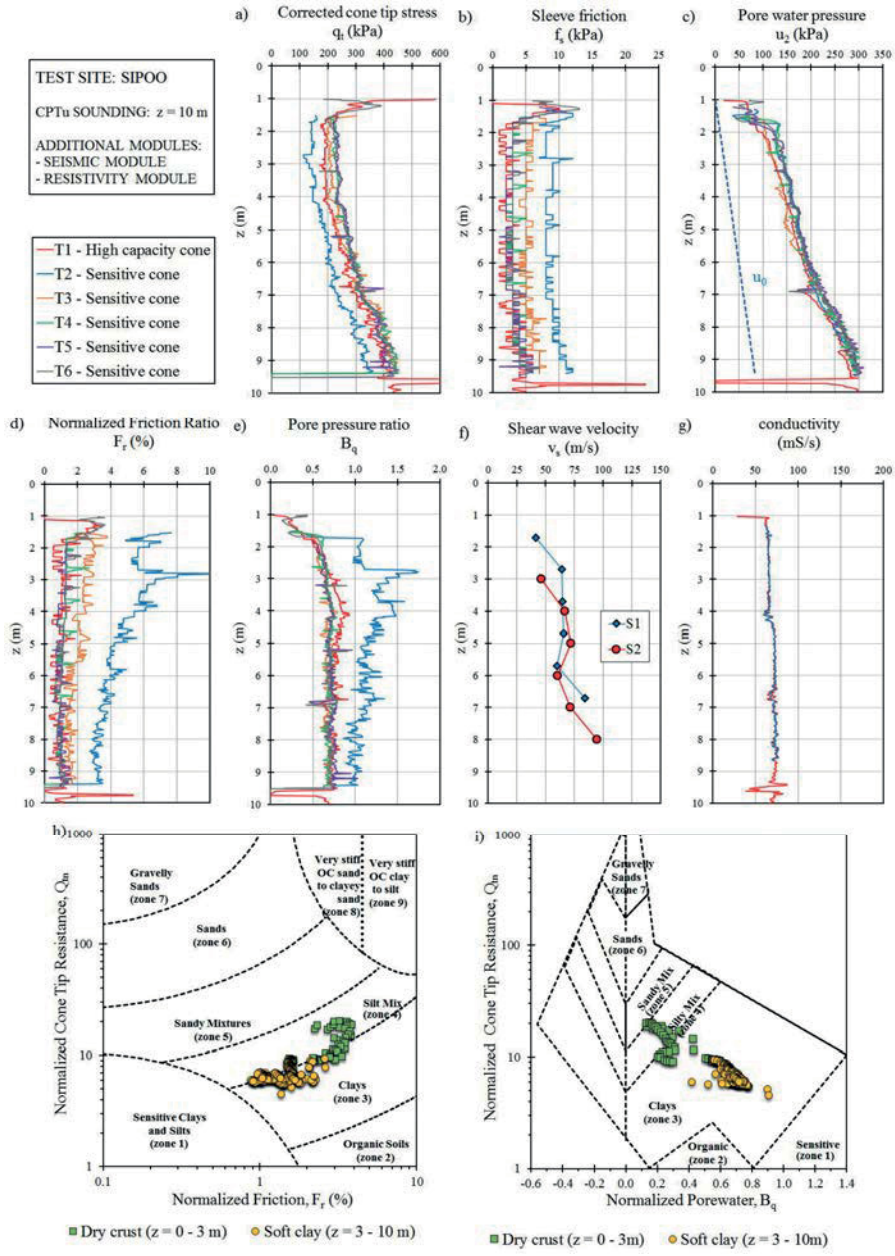

Figure 4.15. CPTu soundings result, Sipoo; a) corrected cone tip resistance, q_t; b) sleeve friction, f_s; c) pore-water pressure, u_2; d) normalized friction ratio, F_r; e) pore pressure ratio, B_q; f) shear wave velocity, v_s; g) conductivity; h) normalized soil behavior type (SBTn) chart based on Q_{tn}–F_r; i) SBTn chart based on Q_{tn}–B_q.

4.6.3 CRS consolidation tests

The CRS consolidation tests are carried out on 19 undisturbed samples taken from 2.7 to 9 m depth using both the ST:1 50 piston and TUT 132 tube samplers. A summary of the test results is presented in Appendix 5 and Fig. 4.16. As previously observed, the stress-strain behavior is characterized by a significant strain increase when passing the σ'_p with highly nonlinear behavior in the NC region. The interpretation of the soil parameters, including stress history and deformation properties, is discussed later in the thesis. Moreover, the achieved sample quality is discussed in detail in section 4.7.

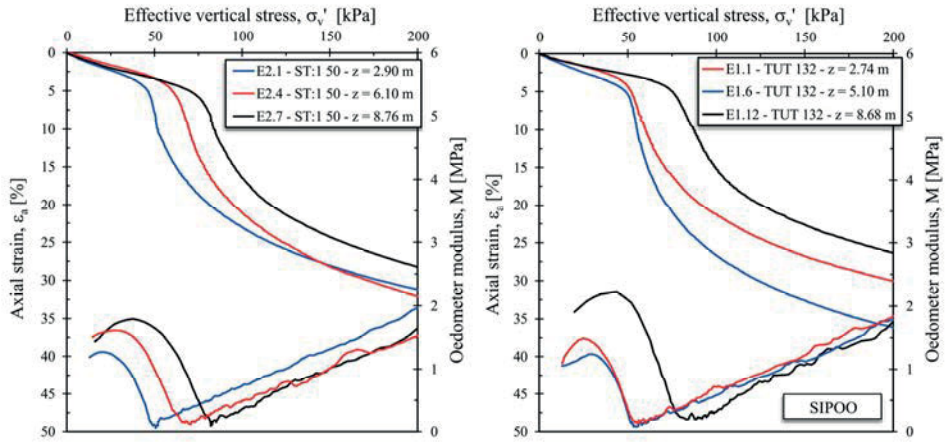

Figure 4.16. CRS consolidation test results of specimens retrieved from Sipoo with (a) ST:1 50 piston and (b) TUT 132.

4.7 Evaluation of soil properties from CRS consolidation tests

This section presents the methodology adopted to derive the stress history and deformation properties based on the CRS consolidation test results. In particular, three methods are examined: the compression index method, Janbu's method, and Sällfors' method. The theoretical formulation and applicability of these methods are discussed in section 2.3.3. In the following, the experimental results are analyzed and the suitability of each method in soil settlement prediction is assessed.

4.7.1 Preconsolidation stress evaluation

The evaluation of σ'_p is a key factor when performing soil settlement calculation. This parameter represents the threshold value, which defines the transition between the OC and NC region. In section 2.4, the processes causing the development of σ'_p are analyzed in detail. In particular, the clays included in this study are not mechanically overconsolidated, but they have been subjected to secondary consolidation and chemical processes, referred to as "aging." Therefore, the threshold value is generally named "yield stress" or "apparent σ'_p."

In conventional geotechnical practice, σ'_p is evaluated from oedometer tests performed on undisturbed samples. The oedometer test result is then analyzed based on various methods such as those proposed by Casagrande (1936), Janbu (1969), Pacheco Silva (1970), Butterfield (1979), Becker et al. (1987), Burland (1990), Karlsrud (1991), Jacobsen (1992), Onitsuka et al. (1995), and Boone (2010). These methods define the standard methodologies for the interpretation of σ'_p using graphical constructions applied to the stress-strain curve. Note that the assumption of an interpretation method is necessary when dealing with low-quality samples. Indeed, in the previous section, it has been observed that sample disturbance results in higher curvature being observed in the stress-strain plot, resulting in a less distinct transition between the OC and NC region. In this scenario, the evaluation of σ'_p may be affected by the operator's personal judgment. These problems are avoided in high-quality samples because the determination of σ'_p can be easily performed by analyzing the soil stress-strain response.

In this study, the interpretation of σ'_p is performed based on a curve-fitting procedure applied to the Sällfors' interpretation method and analyzing the pore pressure response. In particular, the drop observed in the effective stress and the increase of the pore water pressure once reached the yielding stress clearly indicate the transition between the OC and NC region, providing a reliable value of σ'_p, as shown in Fig. 4.17 and 4.18. It is worth observing that this procedure can be easily adopted with respect to high-quality sample while uncertainties are encountered in low-quality samples.

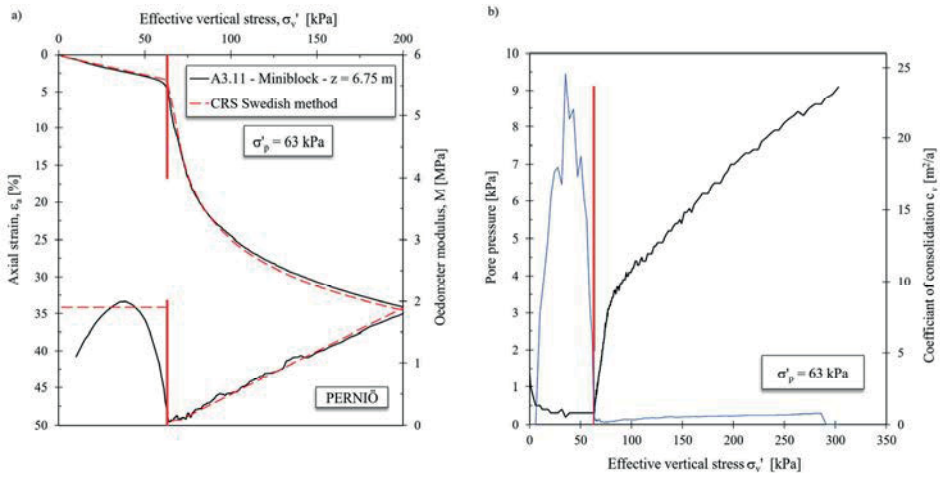

Figure 4.17. Evaluation of the preconsolidation stress from a high-quality sample from Perniö site: a) curve-fitting applied to the Sällfors method; b) pore-pressure response.

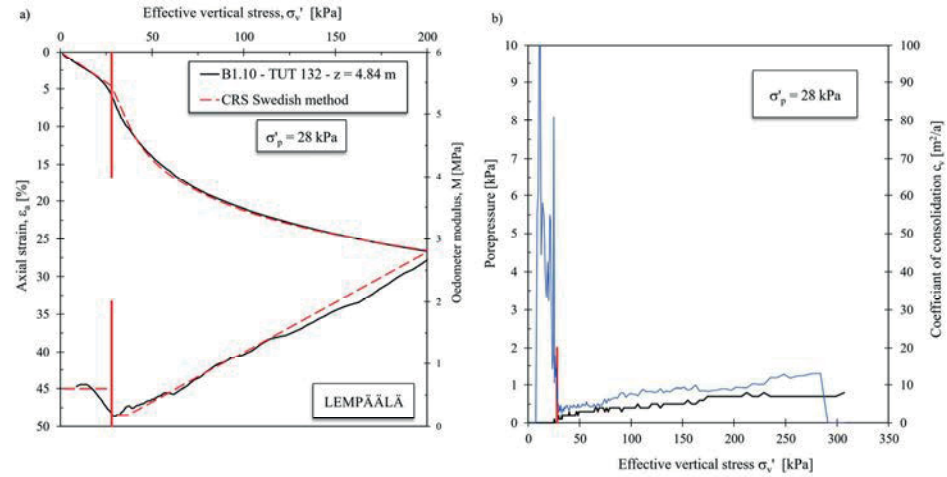

Figure 4.18. Evaluation of the preconsolidation stress from a low-quality sample from Lempäälä site: a) curve-fitting applied to the Sällfors method; b) pore-pressure response.

The in situ and preconsolidation stress profiles of each site are plotted in Fig. 4.19. All the deposits are slightly overconsolidated with the lowest values observed at Lempäälä site (OCR ≈ 1.20) while the other sites are characterized by 1.50 < OCR < 2.50, with the highest values observed mainly at shallow depths.

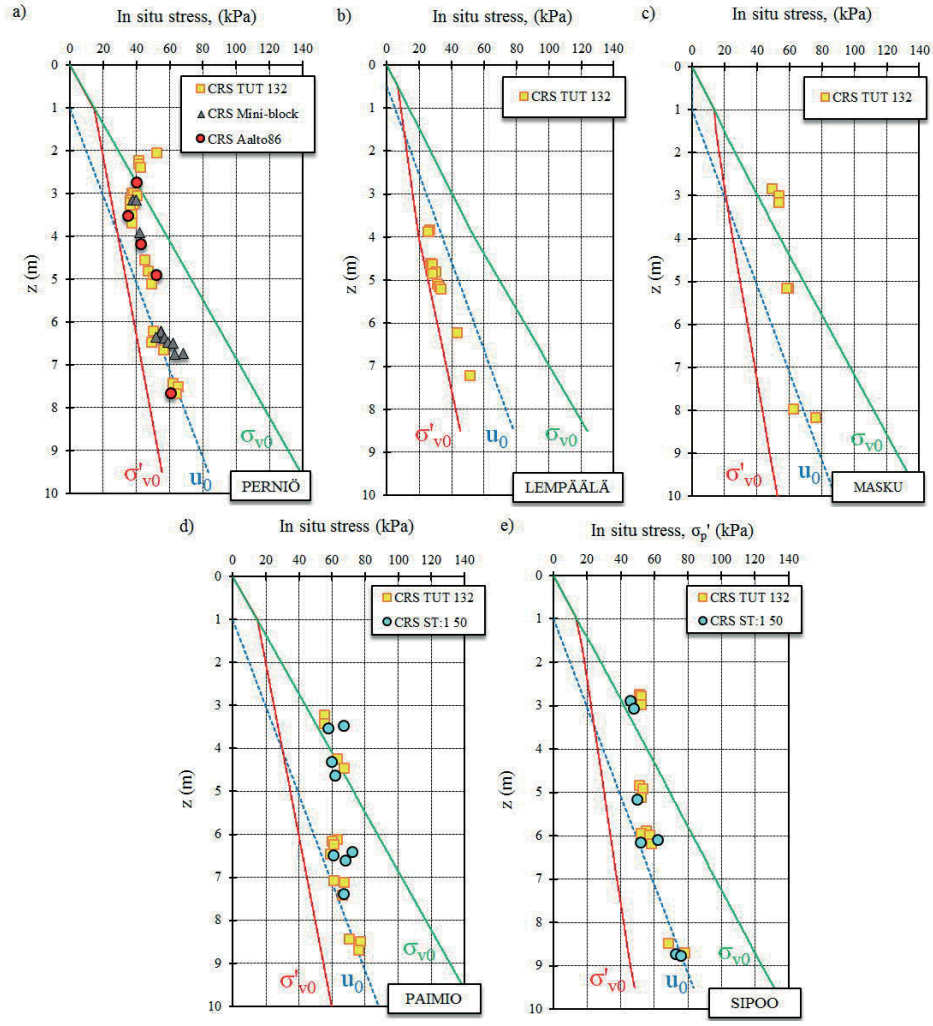

Figure 4.19. In situ stress profiles: a) Perniö; b) Lempäälä; c) Masku; d) Paimio; e) Sipoo.

4.7.2 Evaluation of deformation properties

As previously discussed (section 2.3.3), several methods are proposed in the literature to perform soil settlement analyses. The applicability of the compression index method is considerably low in sensitive clays because the assumption of a constant C_c value is valid only for a small stress range. In contrast, Janbu's method and Sällfors' method appear to be more suitable for settlement prediction in such

soils. In this section, the applicability of these methods is assessed based on the experimental results from CRS consolidation tests. In addition, the deformation parameters used in these methods are derived.

Figures 4.20 – 4.24 show the comparison between the soil stress-strain behavior from CRS consolidation tests and the model prediction. The deformation parameters are calibrated to obtain the best curve-fitting with the experimental data. Overall, both Janbu's and Sällfors' methods provide a rather good representation of soil compressibility. However, at large deformation, the prediction by Janbu's method is less accurate. In particular, effective vertical stress Janbu's model is based on an exponential equation; therefore, it results in a misleading representation of the soil behavior because M increases linearly with the effective vertical stress. Moreover, to model the structure breakdown when passing σ'_p, a negative value of the stress exponent β is assumed. In contrast, for Norwegian clays, the stress exponent is assumed equal to zero (Länsivaara 1999), resulting in a linear increase of the stiffness with stress.

The soil deformation parameters are evaluated for each CRS consolidation test and the results are summarized in Appendix 1–5. In the OC region, Janbu's method is characterized by stress exponent $\beta = 1$ and modulus number $m = M/100$. However, in the NC region, the variability of m is wider, with values ranging from 3 to 12 while β varies between -0.5 and -2. In particular, highly structured clays (e.g., Perniö) are characterized by an evident drop when passing the σ'_p, resulting in lower values of m and β (e.g., test A3.11: $m = 4$; $\beta = -2$). In contrast, Lempäälä clay shows softer response in the NC region, with higher values of m and β (e.g., test A1.10: $m = 11.2$; $\beta = -0.6$). The Sällfors' method appears to be more suitable for the settlement calculation of sensitive clays. Note that the curve-fitting between the model prediction and experimental data is generally very good when proper parameters are selected. In particular, the constrained modulus in the OC region (M_0) varies between 1.5 and 2 MPa even though Lempäälä clay shows values lower than 1 MPa. However, this value is prone to be affected by sample disturbance, as discussed in section 4.7. The lowest value of the constrained modulus (M_L) ranges between 100 and 300 kPa. The stress limit (σ'_L) is generally reached from 5 to 15 kPa beyond σ'_p. Then, the modulus increases with the stress, with the ratio M' varying between 12 and 15.

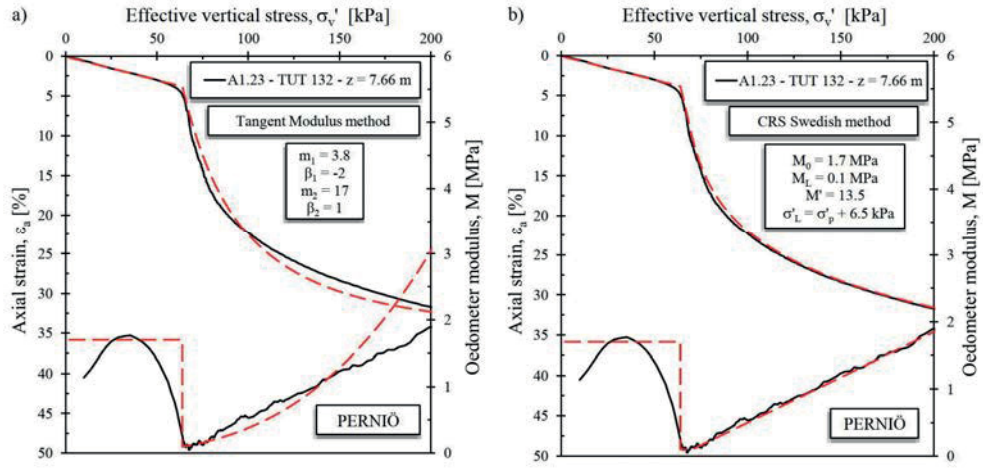

Figure 4.20. Application of the settlement calculation methods to CRS consolidation testing at Perniö: a) tangent modulus method; b) CRS Swedish method.

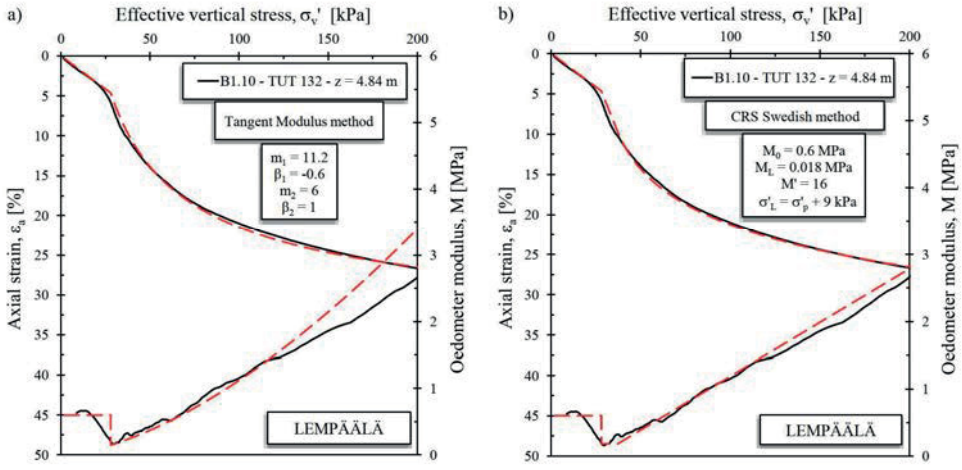

Figure 4.21. Application of the settlement calculation methods to CRS consolidation testing at Lempäälä: a) tangent modulus method; b) CRS Swedish method.

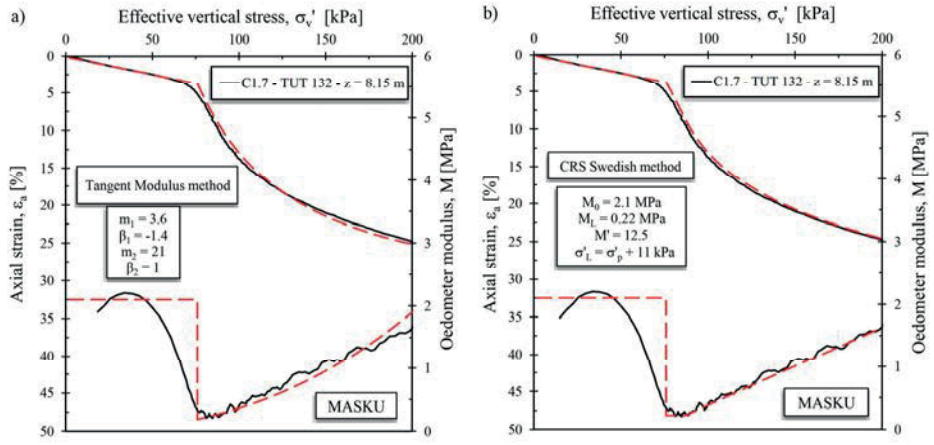

Figure 4.22. Application of the settlement calculation methods to CRS consolidation testing at Masku: a) tangent modulus method; b) CRS Swedish method.

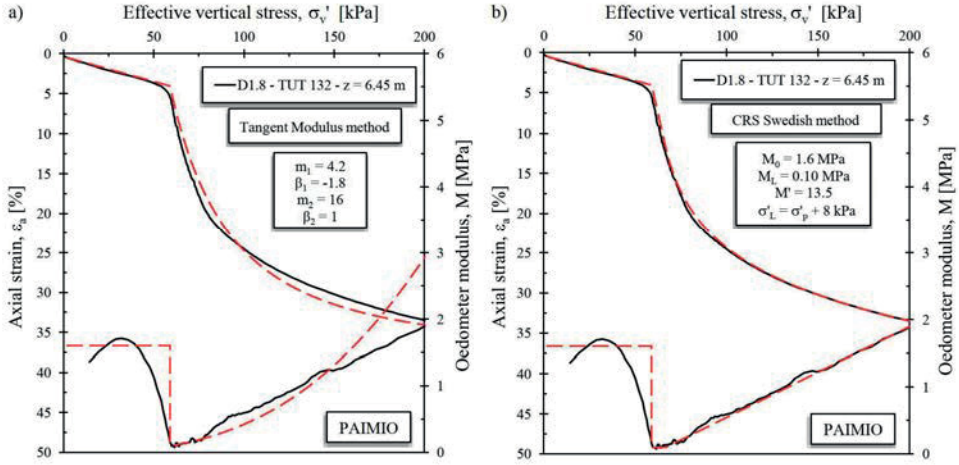

Figure 4.23. Application of the settlement calculation methods to CRS consolidation testing at Paimio: a) tangent modulus method; b) CRS Swedish method.

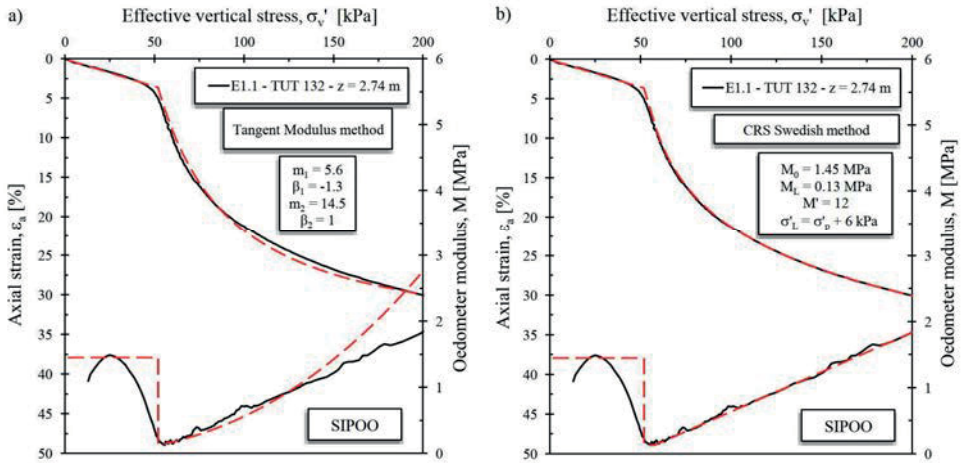

Figure 4.24. Application of the settlement calculation methods to CRS consolidation testing at Sipoo: a) tangent modulus method; b) CRS Swedish method.

4.8 Sample quality evaluation

The impact of sample quality on the evaluation of reliable geotechnical properties from laboratory testing has been discussed earlier in the thesis. Many authors have highlighted the difficulties encountered in obtaining high-quality samples from soft sensitive clay deposits using standard sampling methods such as stationary piston samplers (Lunne et al. 2006; Karlsrud and Hernandez–Martinez 2013; Karlsson et al. 2016; Di Buò et al. 2019b). Considering these aspects, particular effort has been given to the sampling program within this study. This is fundamental for establishing a database of high-quality laboratory data to be exploited to validate the existing correlations and develop new analytical methods valid for Finnish clays. In this section, the performance of the samplers employed at the investigated sites is evaluated based on the experimental results obtained from CRS consolidation tests and using existing methods for the evaluation of the sample quality. These aspects have been discussed by Di Buò et al. (2019b).

In the literature, a number of methods have been proposed to quantify the disturbance experienced by the tested sample during the entire sampling process. Among them, the standard methodology proposed by Lunne et al. (1997), hereinafter referred to as "NGI criterion," is widely used to assess the sample quality. This method is based on the recompression volume of the sample during reconsolidation to the in situ effective vertical stress (σ'_{v0}) in terms of normalized

change in void ratio ($\Delta e/e_0$). The principle idea of this criterion is that disturbance induces higher volumetric deformation when reconsolidating the sample back to in situ stress. Therefore, the sample quality is classified as "very good to excellent", "good to fair", "poor", and "very poor" according to the value of $\Delta e/e_0$ given in Table 4.11.

Table 4.11. NGI criterion for the evaluation of sample quality.

	$\Delta e/e_0$			
OCR	**Very good to excellent**	**Good to fair**	**Poor**	**Very poor**
1 – 2	< 0.04	0.04 – 0.07	0.07 – 0.14	> 0.14
2 – 4	< 0.03	0.03 – 0.05	0.05 – 0.10	> 0.10

In this study, the NGI criterion is applied to the CRS consolidation test results of undisturbed samples retrieved using the different apparatuses. Unfortunately, the comparison between all the sampling methods is possible only at the Perniö site, where all the apparatuses have been employed at the same time.

The NGI criterion is applied to a total of 115 CRS consolidation tests performed on the undisturbed samples retrieved using the different samplers. Results are presented in Fig. 4.25 and Fig. 4.26 by means of two different plots: (i) vertical deformation at reconsolidation to the in situ stress (ε_{v0}) versus w; (ii) $\Delta e/e_0$ versus depth. The NGI criterion based on the $\varepsilon_{v0} - w$ was introduced by Mansikkamäki (2015) based on the assumption of fully saturation (S_r = 100%) which can be considered representative for the analyzed samples.

Note that the majority of the samples are characterized by very good to excellent quality, without any clear influence of the water content and sampling depth on the achieved quality.

However, few TUT 132 and ST:1 50 samples from Perniö show good to fair quality, whereas most of the samples retrieved from Lempäälä are characterized by very poor quality. In particular, several ST:1 50 piston samples from both Perniö and Lempäälä appear to be completely disturbed and σ'_p cannot be determined from the stress-strain behavior (Fig. 4.27). In contrast, the ST:1 50 piston samples from Paimio and Sipoo are characterized by very good quality, comparable to those obtained using the TUT 132 tube sampler.

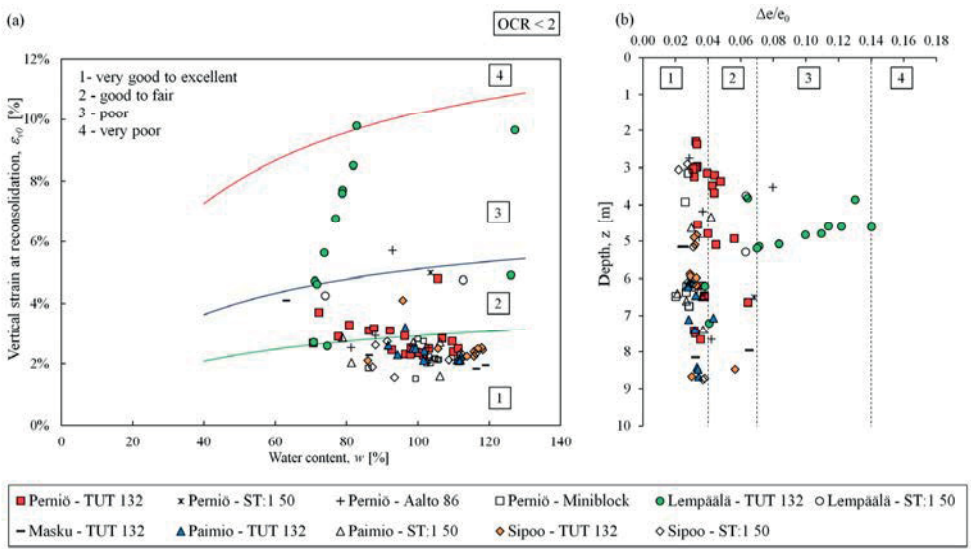

Figure 4.25. Sample quality according to Lunne et al. (1997) for OCR < 2: a) vertical deformation at reconsolidation versus water content; b) change of normalized void ratio at reconsolidation versus depth.

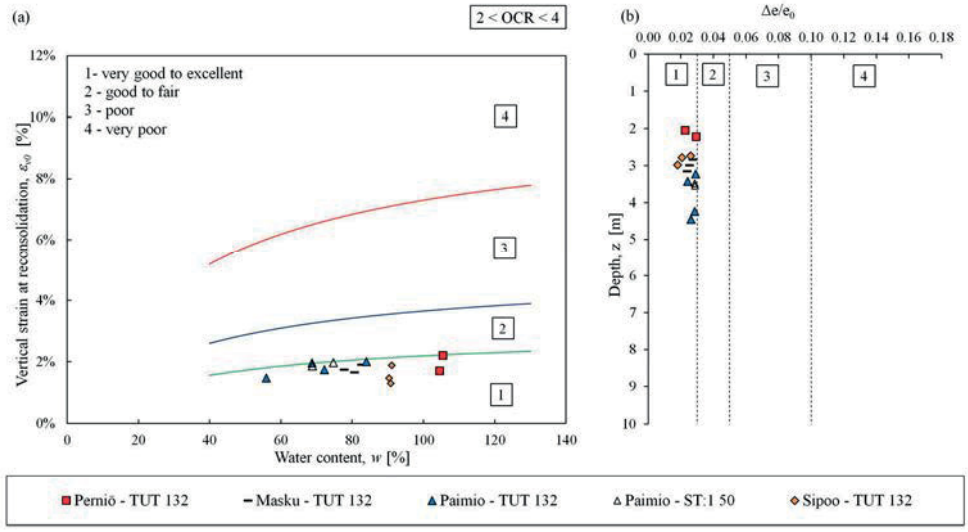

Figure 4.26. Sample quality according to Lunne et al. (1997) for 2 < OCR < 4: a) vertical deformation at reconsolidation versus water content; b) change of normalized void ratio at reconsolidation versus depth.

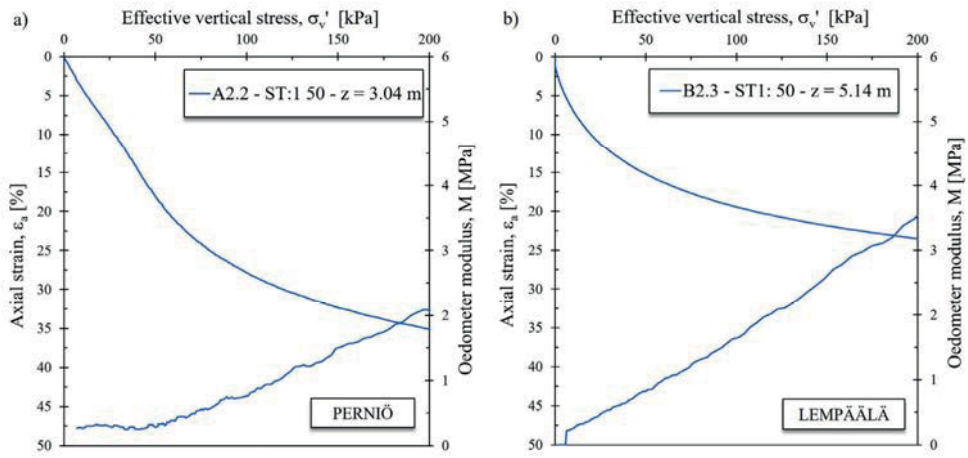

Figure 4.27. CRS consolidation test results of completely disturbed samples.

4.8.1 Performance of the different sampling methods in Finnish clays

The adopted sampling method plays a crucial role in the achieved sample quality. During the sampling stage, the soil is subjected to a stress level that may induce severe disturbance, which may lead to total destructuration, as observed from the CRS consolidation test results of Perniö and Lempäälä clays. Previous research studies (Lunne et al. 2006; Amudsen et al. 2017) revealed that highly sensitive and low-plastic clays (e.g., Norwegian clays) are more prone to sample disturbance. Moreover, disturbances occurring after sampling (e.g., transportation, storage, and sample preparation) should be taken into account; they can be limited by using proper precautions. As shown, the performance of the different samplers has been assessed based on the NGI criterion, which shows that most of the samples retrieved are characterized by very good quality. However, several issues are observed at the Lempäälä and Perniö sites and possible explanations are given later in this section.

The sample quality evaluation according to the NGI criteria, presented in Fig. 4.25 and Fig. 4.26, clearly proves that the sampling method may considerably affect the achieved quality. For example, by comparing the results obtained from Perniö site (Fig. 4.28), it is clear that the mini-block samples are characterized by the highest quality. However, very good quality is also achieved using both TUT 132 and Aalto 86 samplers. In contrast, as pointed out earlier, the majority of the samples retrieved using the ST:1 50 appear to be highly disturbed or completely destructured. The only ST:1 50 test available (A2.5) is characterized by rather poor quality, particularly

evident when compared to CRS consolidation tests conducted on TUT 132 and mini-block samples (Fig. 4.28a). The same behavior is observed at the Lempäälä site, where both TUT 132 and ST:1 50 samplers provide rather poor quality. The experimental results observed at these two sites may suggest that the ST:1 50 piston sampler is not suitable for high-quality sampling in low-plastic sensitive clays. A similar conclusion was made by Lunne et al. (1997), who pointed out the difficulties encountered in obtaining undisturbed samples in Norwegian clays using 75- and 95-mm stationary piston samplers.

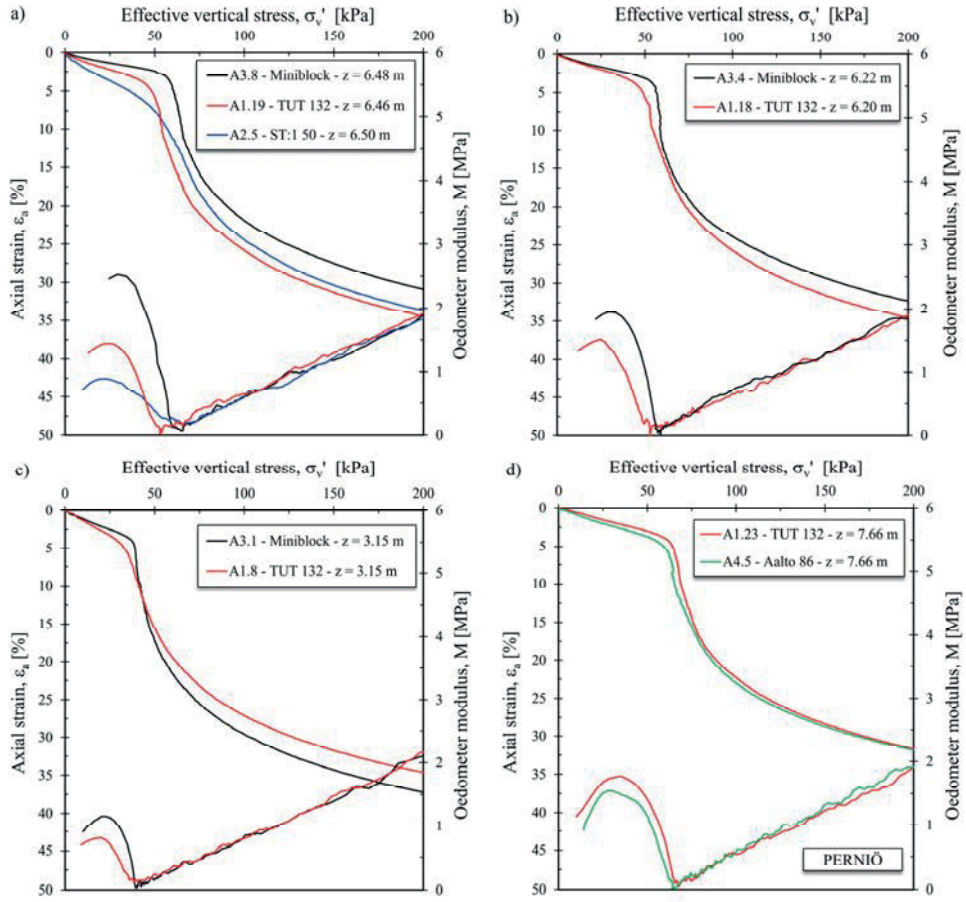

Figure 4.28. Comparison of CRS consolidation test results of Perniö clay.

CRS consolidation test results of Paimio and Sipoo clays prove that very good quality can be achieved using the ST:1 50 piston sampler. It may be observed that Sipoo clay is characterized by high PI, thus suggesting that the soil is less susceptible to sample disturbance. However, despite Paimio clay showing similar soil properties as Lempäälä and Perniö clays in terms of PI and S_t, the quality of samples obtained using the ST:1 50 piston sampler is considerably high but still lower than those obtained using the TUT 132 sampler (Fig. 4.29). Possible reasons that may justify these results can be found in the different sampling procedure adopted at these sites. In particular, at the Perniö and Lempäälä sites, no rotation was applied when using the ST:1 50 piston sampler to cut off the sampled soil from the deposit, as suggested by the Norwegian guidelines for sampling (NGF 2013). In addition, the apparatus used at these two sites suffered from lack of maintenance in terms of sharpness of the cutting edge (Fig. 4.30). Therefore, at the Paimio and Sipoo sites, a brand new ST:1 50 sampler was used along with a different sampling procedure that involved sampler rotation (20 times) before withdrawal, as indicated by the Finnish geotechnical guidelines. Clearly, the use of a new apparatus, together with the different procedure, played a fundamental role in the enhanced quality achieved at the Paimio and Sipoo sites. However, at this stage, it is not possible to discern if sampler rotation induces less sample disturbance than sampler lifting because both procedures have not been tested at the same site. By comparing the CRS consolidation tests results of different samples, it was possible to observe that sample quality is reflected in a stiffer response in the OC region, leading to a higher constrained modulus (M_0). Moreover, σ'_p is systematically higher and it is reached at lower strain level ($\varepsilon_a \approx 4\%$). That said, it is reasonable to assume that sample quality can be evaluated based on the deformation at the reconsolidation stress, thus confirming the effectiveness of the NGI criterion.

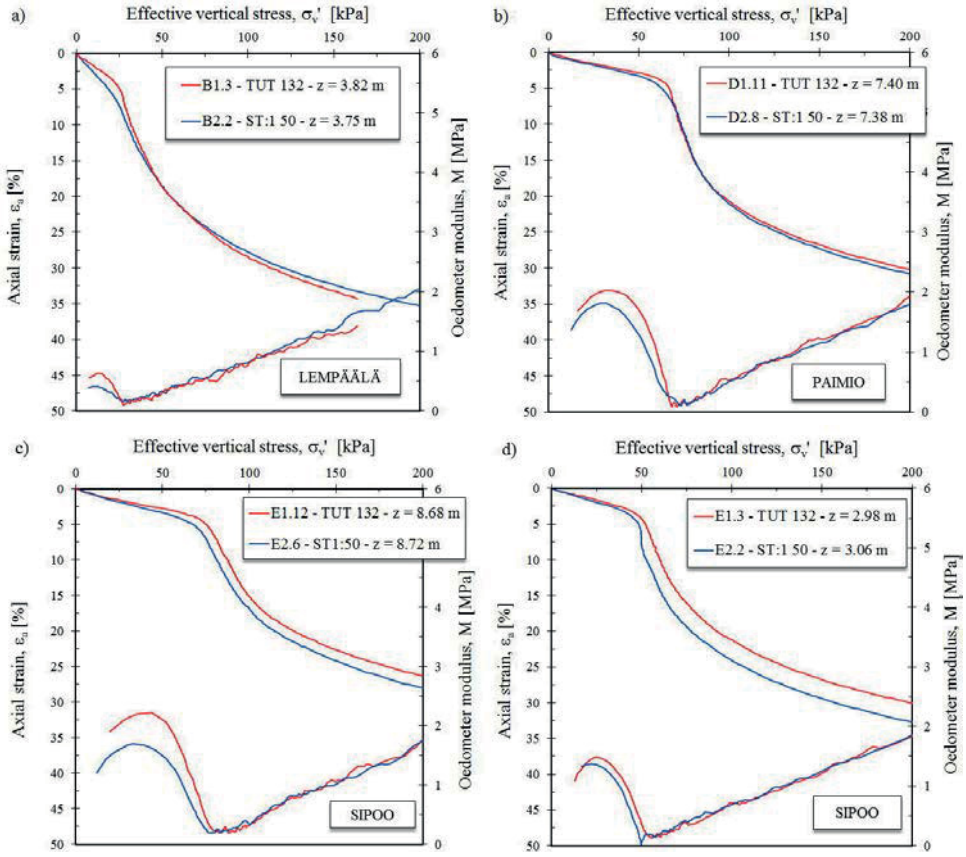

Figure 4.29. Comparison of CRS consolidation tests carried out on specimens obtained using different sampling methods.

Figure 4.30. Details of the ST:1 50 cutting edge employed at the Perniö and Lempäälä sites.

4.8.2 Storage influence on sample quality

Most of the consolidation tests were carried out immediately after the sampling stage, within three months. However, the need for collecting a large amount of data to fill the dataset led to tests being performed at different time intervals, up to three years after the sampling. In this scenario, the influence of storage time on sample quality cannot be neglected. As discussed earlier, several processes may occur during this time interval, including inadequate sealing, stress relief, migration of water, and chemical changes, resulting in additional disturbance factors. These aspects have been taken into account in the design of the TUT 132 tube sampler. In particular, the soil sample was kept stored into the tube with the bottom ends sealed using plastic films and caps to avoid loss of natural water content and oxidation. The soil was extruded only prior to laboratory testing which has a positive effect on preserving the sample quality as stress relief and water content variation are somehow limited. Fig. 4.31 presents the comparison of CRS consolidation test results on TUT 132 samples carried out at different time intervals. Comparison of the stress-strain behavior shows that the sample seems to preserve its good quality for up to three months of storage even though a small reduction of σ'_p and M_0 is observed. This reduction is particularly evident only after two years of storage (e.g., D1.12, E1.1), indicating that stress relief should be taken into account when testing tube samples after such a long time interval. However, the confinement provided by the tube during the sample storage has a beneficial effect in terms of sample quality. Moreover, the water content does not seem to be subjected to sensible variation, thus proving that adequate sealing is ensured.

Similarly, the influence of storage time on the mini-block samples is investigated. However, owing to the lack of tests, the comparison at different time intervals is made only between two tests carried out 3 and 250 days after sampling. Results shown in Fig. 4.32 reveal that stress relief may be an important aspect to be considered when testing mini-block samples after long storage time owing to the lack of proper confinement. However, further investigation should be made before drawing any conclusion. These aspects are discussed in detail by Amudsen (2018), who conducted extensive research to investigate the influence of storage on mini-block samples obtained from Norwegian clay deposits.

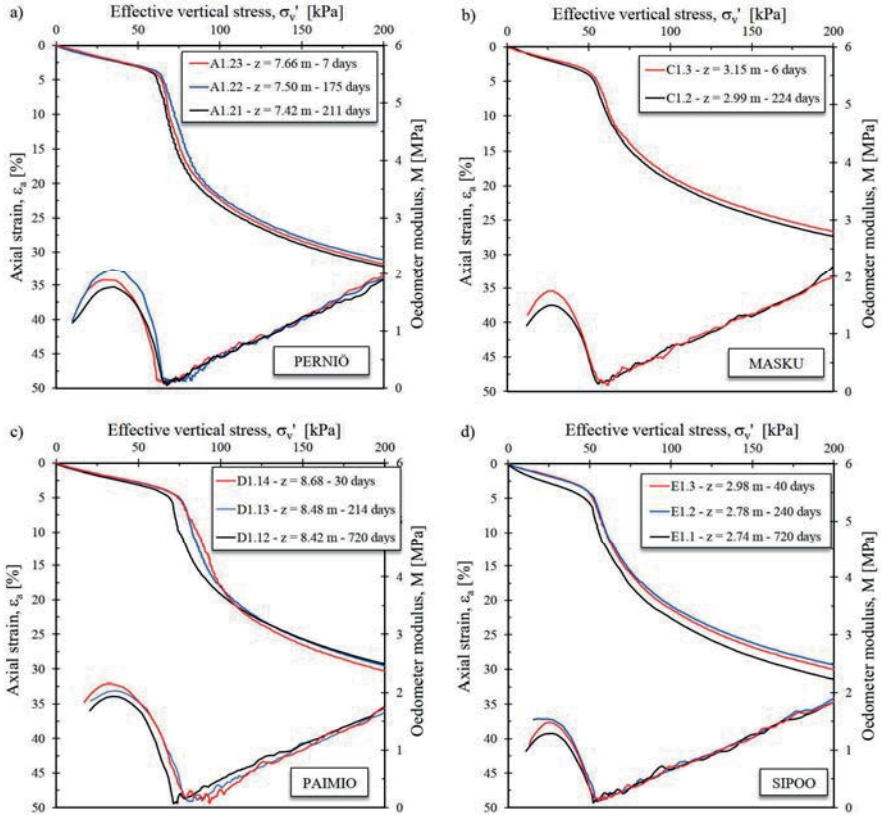

Figure 4.31. Storage influence on TUT 132 sample quality. CRS consolidation test results from (a) Perniö, (b) Masku, (c) Paimio, and (d) Sipoo.

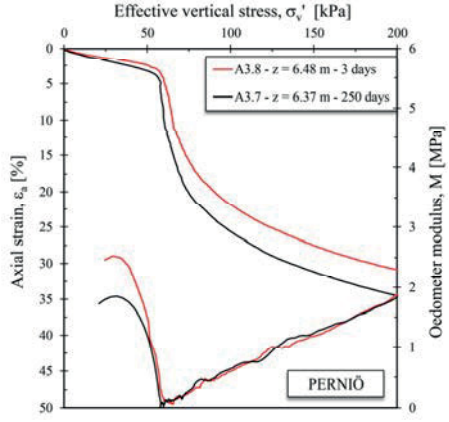

Figure 4.32. Storage influence on mini-block sample quality from Perniö clay.

4.9 Conclusions

The present chapter outlined the experimental program results. Several aspects of the soil behavior have been investigated, with particular emphasis on the stress history and deformation characteristics. The possibility of establishing a database of field and laboratory data plays a crucial role due to the lack of well-documented test sites or relevant research studies on the applicability of CPTu testing on Finnish clays. Therefore, particular effort has been given in collecting high-quality data from the investigated sites.

The obtained results reveal that CPTu testing performs generally well in the investigated sites, providing accurate and repeatable measurements. However, the main issue is represented by the significant data scatter in terms of f_s observed at the sites. Therefore, in soft soils, it would be necessary to rely on piezocones characterized by high accurate sleeve sensor (< 1 kPa) for the correct evaluation of f_s. These aspects are discussed by Di Buò et al. (2020).

The laboratory testing were conducted on undisturbed samples retrieved using different sampling methods. As previously discussed, the sample quality is a key aspect in soft sensitive soils as it may lead to erroneous evaluation of the geotechnical parameters (e.g., σ'_p and M_0). In this study, several issues related to the sampling equipment, procedures, and storage effect are addressed. Overall, the TUT 132 and mini-block samplers provided the highest sample quality while the ST:1 50 piston sampler encountered several problems related to apparatus maintenance and sampling operations especially in low plastic clays. However, high-quality ST:1 samples are obtained from Paimio and Sipoo using a brand-new apparatus and adopting different sampling procedure. Clearly, further studies are required for a better understanding of these issues.

The CRS consolidation test results have been analyzed to derive the σ'_p, M_0, and the deformation characteristics based on the Janbu's Tangent Modulus and CRS Swedish methods. It has been observed that the evaluation of σ'_p on high-quality samples is generally straightforward and it does not require the assumption of complex graphical methods. Moreover, the CRS Swedish method provides more suitable curve fitting with the experimental results compared to the Tangent Modulus method.

5 EVALUATION OF THE PRECONSOLIDATION STRESS OF FINNISH CLAYS FROM CPTu DATA

5.1 Introduction

The aspects related to depositional and post-depositional processes as well as the development of a quasi-preconsolidation stress in natural clay deposits have been extensively discussed in section 2.4. In particular, it has been shown as the overconsolidation of a soil deposit is the result of several processes, including changes in total stress and pore-water pressure as well as geo-environmental factors. Overconsolidation induced by reduction of total stress is attributable to erosion, glaciation, and excavation. Examples of overconsolidation caused by pore-water pressure changes are groundwater table fluctuations, pore-water changes owing to artesian flow, and desiccation. Among the geo-environmental factors, aging and chemical alterations are the most common processes observed in natural clays, which induce the development of a quasi-preconsolidation state. The aforementioned processes may occur simultaneously, thus leading to a rather difficult stress history profile evaluation. In such cases, the use of σ'_{vy} and yield stress ratio (YSR = $\sigma'_{vy}/\sigma'_{v0}$) is considered more appropriate when referring to the stress history of these soils. Nevertheless, the terms σ'_p and OCR are used herein owing to their commonplace recognition.

Many aspects of soil behavior are influenced by their stress history, including volume change during consolidation, stress dilatancy, induced pore pressure, peak strength, and time-dependent behavior during shearing (Chen and Mayne 1994). Traditionally, the σ'_p and OCR profiles are determined from 1D consolidation tests (CRS and/or incremental loading tests) performed on undisturbed samples. Although the utilization of such testing procedures has proliferated owing to its simplicity, it is worth pointing out that oedometer testing is characterized by several issues. First, the stress state of natural clays is not a 1D phenomenon, but it is controlled by a four-dimensional condition, involving three effective stress variables in the X, Y and Z directions (σ'_x, σ'_y, σ'_z) and time (t). Consequently, the stress history would be best represented by a three-dimensional, time-dependent yield envelope. Second, as observed in sections 3.3 and 4.8, sample disturbance may

negatively affect the interpretation of test results. Finally, laboratory testing provides discrete information depending on the sampling depth, and it requires a relatively long testing time, thus making it rather expensive.

The interpretation of stress history from field data is attractive because several issues related to laboratory testing are avoided. To this end, the piezocone test offers a relatively quick and cost-effective testing method. However, a proper investigation plan should always combine both laboratory and field tests. In particular, consolidation tests are fundamental for the interpretation of piezocone data, which can be then used to extrapolate information to other depths.

This section discusses the capability of piezocone testing for evaluating σ'_p of Finnish clays. In relation to this, empirical and analytical methods are reviewed with particular emphasis on the model proposed by Mayne (1991) and Chen and Mayne (1994), which is based on cavity expansion (Vesic 1972; Vesic 1977) and modified Cam clay (MCC) (Wroth 1984; Wroth and Houlsby 1985) theories. This method is implemented on piezocone data obtained from the investigated sites to evaluate the stress history profiles in terms of σ'_p and OCR. The effectiveness of the model is assessed by comparing the model prediction and CRS consolidation tests. Finally, simplified CPTu-based correlations valid for Finnish clays are derived.

5.2 Methods for evaluating the stress history of clays from CPTu data

Several interpretative empirical and analytical approaches have been proposed over the past decades for evaluating the stress history of clays based on piezocone measurements. Empirical correlations are commonly used in geotechnical practice to derive preliminary geotechnical parameters. In general, these correlations work fairly well only in limited geological contexts; therefore, they need to be validated when applied to different soils. In contrast, analytical methods are derived from well-established theories, including elasticity, plasticity, and cavity expansion, and they can be calibrated to match the local conditions. However, one of the major issues related to analytical methods lies in the determination of advanced soil input parameters that may not be available in low to medium risk projects.

This section reviews, in chronological order, existing interpretation methods proposed in the literature. These approaches are generally based on q_t, u_2, and normalized CPTu parameters (Q and B_q). In this study, f_s has been considered only

for soil classification (SBT) because the low accuracy of the measuring system does not allow reliable correlations to be established.

5.2.1 Empirical models

One of the earliest interpretation methods to evaluate the OCR using CPT data was proposed by Schmertmann (1978). It involved approximating the increase of q_c with depth as a straight line to extrapolate the original ground elevation, thus obtaining the σ'_p profile with depth. The applicability of the method is limited to clays where the OCR is caused only by the mechanical removal of the overburden, and the method does not account for other processes such as desiccation, groundwater fluctuations, and secondary compression.

The introduction of the pore-pressure measurement contributed to improve the reliability of the empirical correlations. Several authors suggested the use of $\Delta u_m/q_c$ for indexing the OCR profile with depth, where Δu_m is the excess pore water pressure measured at the tip (u_1) or behind the shoulder (u_2), depending on the position of the porous filter element.

Campanella et al. (1982) suggested that, for normally consolidated clays, a constant ratio of $\Delta u_2/q_c$ equal to 0.7 can be assumed. In contrast, for overconsolidated clays, Tumay et al. (1982) observed that $\Delta u_m/q_c$ decreases with increasing OCR.

Smits (1982) investigated the influence of the pore-pressure ratio $(u_m - u_0)/(q_c - u_0)$ on the OCR. The piezocones used were equipped with filter elements located behind the tip (u_2 position) and in a truncated cone tip (u_1). Results indicate a decrease in the pore-pressure ratio with increasing OCR. The same trend is observed with reference to the filter elements at both locations.

The modern pushing equipment allows the piezocone test to be performed at great depths, which is particularly common in offshore applications. In such cases, it is necessary to refer to normalized CPTu parameters to take into account the effect of the overburden pressure on the measured data. Senneset et al. (1982) and Jefferies and Funegard (1983) introduced a dynamic pore-pressure ratio, $B_q = (u_m - u_0)/(q_c - \sigma_{v0})$, which was later modified by replacing q_c with q_t (Wroth 1984). In addition, the normalized cone resistance $Q_t = (q_t - \sigma_v)/\sigma'_v$, the normalized effective cone resistance $Q_{eff} = = (q_t - u_2)/\sigma'_v$. Exploiting data from the Onsøy site, Wroth (1984) obtained a good site-specific correlation between B_q and OCR. However, difficulties arise when investigating the relationship between B_q and OCR for different sites.

Studies conducted by several authors (Jamiolkowski et al. 1985; Lunne et al. 1985; Keaveny and Mitchell 1986; Robertson et al. 1986), after examining piezocone data from different clay sites, indicate that a simple B_q – OCR relationship cannot be established. For example, the results from the North Sea clays (Lunne et al. 1985) are characterized by an evident data scatter. Based on this, it may be concluded that the correlation between OCR and B_q in indeed very site specific (Jamiolkowski et al. 1985; Konrad et Law 1987).

Sully et al. (1988) proposed a different pore-pressure-based correlation for deriving the OCRs in clays. In particular, three different parameters were defined: PPR1 = u_1/u_2; PPR = $(u_1 - u_0)/(u_2 - u_0)$, and PPD = $(u_1 - u_2)/u_0$. Exploiting data from several different sites, they suggested OCR = 0.66 + 1.43 PPD valid for 1 < OCR < 10. Although good data fitting can be achieved, this method is not easily implemented because it requires a dual-element piezocone, which is not commonly used in geotechnical practice.

Over the past decades, a number of empirical correlations to derive the σ'_p and OCR from CPTu parameters have been proposed in the geotechnical literature. In particular, Chen and Mayne (1996) conducted simple and multiple regression analyses to evaluate correlative trends compiling a database of 205 clay sites around the world. More recently, D'Ignazio et al. (2019) proposed "best-fit" CPTu-based correlations from linear regression analyses based on a large database of 249 high-quality data points covering onshore and offshore clays worldwide, including Finnish clay sites. This study indicates linear relationship between Q_t and OCR in slightly OC clays, with coefficient ranging between 0.15 and 0.5. In contrast, for OCR>5, an exponential trend is observed.

The most relevant and used empirical correlations in the common practice are summarized in Table 5.1. As previously noted, most of these correlations are derived in particular geological contexts and their applicability in different soil conditions should always be assessed. Furthermore, it has been observed that the correlations based on normalized CPTu parameters are generally more reliable, particularly when deep measurements are performed.

Table 5.1. Summary of empirical methods for evaluating the stress history of clays.

Parameter	Correlation	Reference
σ'_p	$\sigma'_p = f(q_c)$	Mayne (1986)
	$\sigma'_p = f(q_c - \sigma_{v0})$	Tavenas and Leroueil (1987)
	$\sigma'_p = 0.305\ (q_t - \sigma_{v0}) = 0.305\ q_{net}$	Chen and Mayne (1996)
	$\sigma'_p = 0.53\ (u_2 - u_0) = 0.53\ \Delta u_2$	Chen and Mayne (1996)
	$\sigma'_p = 0.50\ (q_t - u_2) = 0.50\ q_{eff}$	Chen and Mayne (1996)
	$\sigma'_p = [f(q_t - \sigma_{v0})]; [f(u_2 - u_0)]; [f(q_t - \sigma'_{v0})]$	D'Ignazio et al. (2019)
OCR	$OCR = f(q_c - \sigma_{v0})/\sigma'_{v0}$	Schmertmann (1978)
	$OCR = f(u_1/q_c)$	Baligh and Levadoux (1986)
	$OCR = 0.317\ Q_t$	Chen and Mayne (1996)
	$OCR = (Q_t/3)^{1.2}$	Karlsrud et al. (2005)
	$OCR = 0.314\ [(u_2 - u_0)/\sigma'_v]^{1.35}$	Mayne and Holtz (1988)
	$OCR = f[(u_1 - u_2)/\sigma'_{v0}]; f[(q_t - \sigma_{v0})/\sigma'_{v0}]$	Larsson and Mulabdic (1991)
	$OCR = 0.545\ Q_{eff}^{0.969}$	Chen and Mayne (1996)
	$OCR = 1.026\ B_q^{-1.077}$	Chen and Mayne (1996)
	$OCR = 0.63\ B_q^{-1.286}$	Schroeder et al. (2006)

5.2.2 Analytical models

A number of analytical models to assess the stress history of clays have been proposed in the literature. Most of these are formulated on the basis of well-established theories involving elasticity, plasticity, limit equilibrium, and cavity expansion. Most notably, many formulations combining the SCE and CSSM theories (Wroth 1984; Mayne 1991) have been developed and implemented, providing a rather good estimation of σ'_p and OCR. This section presents an overview of the existing theories and solutions developed over the past decades.

Konrad and Law (1987) derived an analytical solution by studying the stress path and pore pressures induced in a soil element beneath the cone during penetration. The vertical yield stress mobilized during penetration (σ'_{yc}) is expressed as follows.

$$\sigma'_{yc} = \frac{q_t - \alpha u_2}{1 + \delta \tan\Phi' \cot\theta} \tag{5.1}$$

Based on equation (5.1), the vertical effective yield stress is derived as the difference between the induced total vertical stress and the total pore pressure. The total vertical stress is expressed as the cone tip resistance, assuming that the unit shear stress at the cone–soil interface is computed using effective stress parameters combined with the measured pore pressures generated during penetration. The model requires the assumption of a corrective factor $\alpha = u_1/u_2$, which is used to determine the pore pressure induced in the failure zone, a friction factor between the soil and cone

surface (δ), the apex angle (2θ), and the effective friction angle (ϕ'). For sensitive Canadian clays, a factor $\alpha = 1.0–1.1$ is suggested while $\delta = 0.50–0.75$ for smooth steel and $\delta = 1.0$ for normal roughness can be assumed. As an example, by assuming $\alpha = 1.0$, $\delta = 1.0$, $\phi' = 30°$, and $\theta = 30°$, OCR can be expressed as follows.

$$OCR = 0.5\left(\frac{q_t - u_2}{\sigma'_{v0}}\right) \tag{5.2}$$

Sandven et al. (1988) and Senneset et al. (1989) proposed an effective stress analytical approach to estimate the in situ preconsolidation stress based on the effective cone tip resistance ($q_{eff} = q_t - u_2$), attraction ($a' = c'/\tan\phi'$), and bearing capacity coefficient as a function of ϕ' and B_q, defined as follows:

$$\sigma'_p = \frac{q_{eff} + a'}{N_c} - a'. \tag{5.3}$$

Similarly, Sandven (1990) suggested a total stress approach based on classical bearing capacity concepts ($q_t - \sigma_{v0} = N_c s_u$) and assuming s_u as a function of σ'_p ($s_u = \alpha'(\sigma'_p + a)$), resulting in the following expression:

$$\sigma'_p = \frac{q_t - \sigma_{v0}}{N_c \alpha'} - a, \tag{5.4}$$

where $\alpha' = \sin\phi'/2$ and N_c is the cone bearing factor.

Several analytical models have been derived using cylindrical and spherical cavity expansion theories with the MCC theory (Wroth 1984; Mayne and Holtz 1988; Mayne 1991; Mayne and Chen 1994). These models were later improved to account for the different behaviors characterizing sensitive and structured clays (Agaiby and Mayne 2018). Section 5.4 describes in detail the theoretical framework, development, and application of such models.

5.3 Applicability of existing empirical correlation for evaluating the stress history of Finnish clays

In the previous sections, several existing correlations and analytical models for evaluating the stress history of natural clay deposits have been presented. As pointed out, most of these are derived for limited geological context and soil types while others are based on large database (e.g., Chen and Mayne 1996; D'Ignazio et al. 2019). However, their applicability in particular soils, as soft sensitive clays, should always be verified to avoid misleading prediction of geotechnical parameters. As an example, Di Buò et al. (2018) and Selänpää et al. (2018) investigated the applicability of proposed empirical correlations for deriving the strength and deformation properties of Finnish clays, pointing out that a proper calibration of such correlations is needed to fit the experimental data.

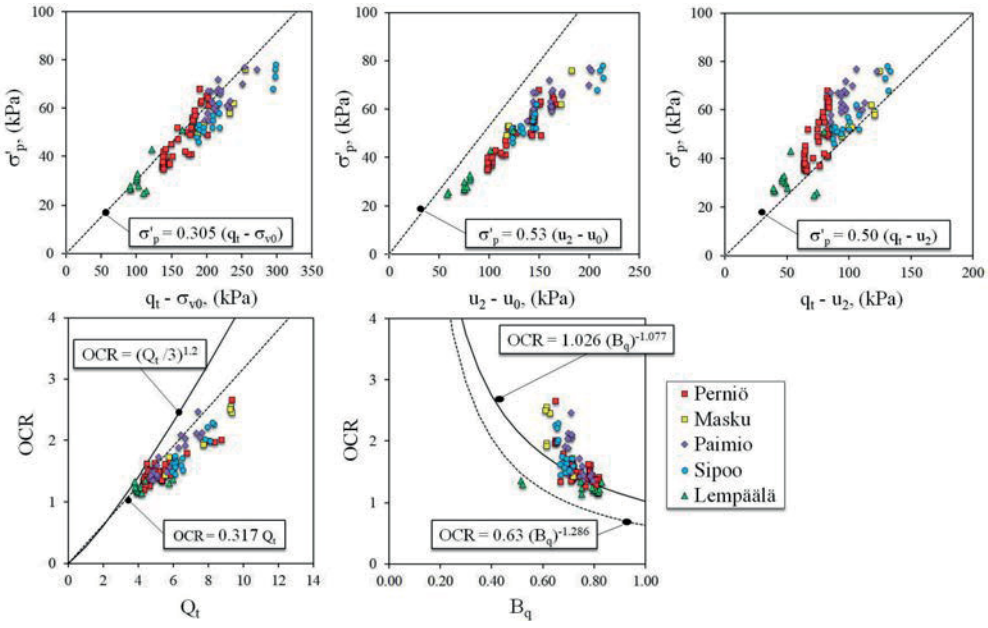

Figure 5.1. Validity of the empirical CPTu-based correlations in Finnish clays.

This section examines the applicability of some of existing CPTu-based correlations in Finnish clays based on the experimental results obtained in this study. The plots illustrated in Fig. 5.1 indicate fair trend between σ'_p and OCR with the CPTu parameters q_{net}, Δu_2, q_{eff}, and the normalized parameter Q_t. In contrast, as previously mentioned, higher data scatter is observed when the parameter B_q is adopted. It is

worth to point out that the proposed empirical factors do not always fit the experimental data. In particular, the correlation proposed by Chen and Mayne (1996) based on Δu_2 provides higher values compared to the experimental data while the one based on q_{eff} slightly underestimates σ'_p. Similarly, the OCR vs Q_t and OCR vs B_q correlations appear to not fully match the experimental data. These observations clearly prove that a proper validation and calibration of these empirical factors is needed to improve the reliability of the geotechnical parameters estimation. These aspects will be analyzed in detail in the following sections.

5.4 Evaluation of the stress history of clays based on the spherical cavity expansion (SCE) and critical state soil mechanics (CSSM) theories

5.4.1 Introduction

Several methods for evaluating the stress history of clays are presented in the previous section. As observed, most of the empirical methods are developed based on a limited database; therefore, their applicability in different geological contexts should always be investigated. In contrast, analytical methods appear to be more reliable, although they often require the assumption of advanced geotechnical parameters. Several authors have pointed out that a proper methodology should be based on physical reasoning, a well-established theoretical framework, and normalized engineering parameters. In addition, these methods should be implemented to a variety of soil conditions to investigate their applicability and limitations (Wroth 1988; Chen and Mayne 1994).

This section presents a hybrid analytical model proposed by Mayne (1991) and Chen and Mayne (1994), which is based on the SCE and CSSM theories to derive the soil stress history from piezocone data. A modified SCE-CSSM solution has been recently proposed by Agaiby (2018), which is more suitable in highly sensitive and structured clays. Both approaches are presented and used for assessing the σ'_p and OCR profiles for the sites investigated in this study.

5.4.2 Original SCE-CSSM solution

The evaluation of the commonly known "point resistance" is fundamental in many geotechnical applications involving the bearing capacity of deep foundations, breakout resistance of anchors, and piezocone data interpretation. Based on the conventional plastic theories, q_t can be expressed in terms of s_u as follows:

$$q_t = N_{kt} s_u + \sigma_{v0}, \tag{5.5}$$

where N_{kt} is the cone bearing factor, which depends on the specific theory employed. Konrad and Law (1987) provide a summary of 13 different expressions for determining N_{kt}. By investigating the theoretical problem of the expansion of cavities in infinite soil mass, Vesic (1972) proposed the following formulation:

$$N_{kt} = \frac{4}{3}(\ln I_R + 1) + \frac{\pi}{2} + 1, \tag{5.6}$$

where I_R is the rigidity index, defined as the ratio of the shear stiffness modulus (G) and s_u. Combining equations (5.5) and (5.6), an expression to derive q_{net} can be obtained as follows.

$$q_{net} = q_t - \sigma_{v0} = \left[\frac{4}{3}(\ln I_R + 1) + \frac{\pi}{2} + 1\right] s_u \tag{5.7}$$

Keaveny and Mitchell (1986) showed that during cone penetration, the soil beneath the cone tip follows a stress path corresponding to the one followed during a triaxial compression test. The cavity expansion theory proposed by Vesic (1977) provides a suitable representation of the cone tip resistance (q_t) when the value of s_u is determined from the CK_0UC triaxial test. Therefore, the value of s_u can be derived from the MCC theory in terms of effective stresses and stress history effects (Wroth and Houlsby 1985) as follows:

$$s_u = \frac{M}{2}\left(\frac{OCR}{2}\right)^{\Lambda} \sigma'_{vo}, \tag{5.8}$$

where $M = 6\sin\phi'/(3 - \sin\phi')$ is the slope of the frictional envelope for triaxial compression in q/p' space, ϕ' is the effective stress friction angle, and Λ is the plastic volumetric strain potential [$\Lambda = 1 - (C_r/C_c)$], where C_r is the swelling index and C_c is the virgin compression index in 1D compression). The value of Λ can be assumed

as constant for natural clays, varying from 0.80 for insensitive clays to 0.9–1 for structured and/or sensitive clays. Because the MCC model specifically applies to isotropically consolidated soils, equation (5.8) provides an approximate expression for evaluating the soil strength (Mayne 1991).

By combining the SCE and MCC solutions, the net cone tip resistance can be expressed as follows.

$$q_t - \sigma_{v0} = \left[\frac{4}{3}(\ln I_R + 1) + \frac{\pi}{2} + 1\right]\frac{M}{2}\left(\frac{OCR}{2}\right)^{\Lambda}\sigma_{v0}' \tag{5.9}$$

Therefore, the soil stress history can be derived by rearranging equation (5.9) to obtain the following.

$$OCR = 2\left[\frac{\left(\frac{2}{M}\right)(q_t - \sigma_{v0})/\sigma_{v0}'}{\frac{4}{3}(\ln I_R + 1) + \frac{\pi}{2} + 1}\right]^{(1/\Lambda)} \tag{5.10}$$

Similarly, the excess pore water pressure ($\Delta u_2 = u_2 - u_0$) induced by advancing the probe can be expressed in terms of the SCE and CSSM theories, as detailed by Mayne and Bachus (1988). In particular, Δu_2 can be divided into two main contributors:

$$\Delta u_2 = \Delta u_{oct} + \Delta u_{shear}, \tag{5.11}$$

where Δu_{oct} is the change in the octahedral stresses and Δu_{shear} is the change in the shear stresses. Using the strain path method, Levadoux et al. (1986) showed that when using the piezocone with the filter element located at the cone tip (type 1), Δu_1 is mostly controlled by Δu_{oct}, whereas Δu_{shear} is generally less than 20% of the total measured excess pore pressure. Therefore, Δu_{shear} can be neglected ($\Delta u_2 \approx \Delta u_{oct}$). In contrast, when the pore pressure is measured behind the tip (type 2), higher shear-induced pore water pressure is generated and the assumption $\Delta u_2 \approx \Delta u_{oct}$ cannot be considered valid.

By implementing the SCE theory, Δu_{oct} can be expressed as follows.

$$\Delta u_{oct} = \frac{4}{3} s_u \ln(I_R) \tag{5.12}$$

Mayne and Bachus (1988) proposed an equation to derive the shear-induced component of the excess pore pressure by assuming a constant stress path P, thus obtaining the following equation:

$$\Delta u_{shear} = \sigma'_{v0}\left[1 - \left(\frac{OCR}{2}\right)^{\Lambda}\right]. \quad (5.13)$$

Combining equations (5.11), (5.12), and (5.13), Δu_2 can be expressed as follows.

$$\Delta u_2 = \frac{4}{3} s_u \ln(I_R) + \sigma'_{v0}\left[1 - \left(\frac{OCR}{2}\right)^{\Lambda}\right] \quad (5.14)$$

Using the MCC model, the value of s_u can be expressed in terms of M and OCR (eq. 5.8), and the Δu_2 can be defined as follows.

$$\Delta u_2 = \frac{2}{3} M \left(\frac{OCR}{2}\right)^{\Lambda} \sigma'_{vo} \ln(I_R) + \sigma'_{v0}\left[1 - \left(\frac{OCR}{2}\right)^{\Lambda}\right] \quad (5.15)$$

Equation (5.15) can be rearranged to provide a direct expression for OCR.

$$OCR = 2\left[\frac{\left(\frac{\Delta u_2}{\sigma'_{v0}}\right) - 1}{\frac{2}{3} M \ln(I_R) - 1}\right]^{(1/\Lambda)} \quad (5.16)$$

Equation (5.16) takes into account the contribution of both Δu_{oct} and Δu_{shear}. However, for soft to firm clays, the shear component of pore water pressure is small (<20% of the total measured pore water pressure). Considering low overconsolidated clays (OCRs < 3), this portion can essentially be neglected, which reduces equation (5.16) to the following.

$$OCR = 2\left[\frac{\left(\frac{\Delta u_2}{\sigma'_{v0}}\right)}{\frac{2}{3} M \ln(I_R)}\right]^{(1/\Lambda)} \quad (5.17)$$

Finally, the OCR can be expressed in terms of the effective cone tip resistance ($q_{eff} = q_t - u_2$) by subtracting equation (5.14) from equation (5.7) to obtain

$$q_t - \sigma_{v0} - u_2 + u_0 = \sigma_{v0}'\left[(1.95M + 1)\left(\frac{OCR}{2}\right)^{\Lambda} - 1\right], \quad (5.18)$$

which can be rearranged as follows.

$$OCR = 2\left[\frac{1}{1.95M+1}\left(\frac{q_t - u_2}{\sigma_{v0}'}\right)\right]^{(1/\Lambda)} \quad (5.19)$$

Equations (5.10), (5.17), and (5.19) provide three different formulations to estimate OCR from the piezocone data and additional soil parameters, including the plastic volumetric strain potential (Λ), rigidity index (I_R), and friction angle (ϕ') is needed.

Based on this theoretical framework, Mayne (2005) derived simplified expressions for evaluating the stress history of inorganic, low overconsolidated (OCR < 2), and low sensitive clays. To this end, characteristic values of $\Lambda = 1$, $I_R = 100$, and $M = 1.2$ (corresponding to $\phi' = 30°$) are adopted, resulting in the following.

$$\sigma'_p = 0.33(q_t - \sigma_{v0}) \tag{5.20}$$

$$\sigma'_p = 0.54(u_2 - u_0) \tag{5.21}$$

$$\sigma'_p = 0.60(q_t - u_2) \tag{5.22}$$

The simplified equations fairly agree with the experimental test results from 22 Canadian clay sites investigated by Demers and Leroueil (2002). However, the coefficients (0.33; 0.54; 0.60) should be calibrated to fit with local geological soil conditions.

Mayne et al. (2009) showed that equation (5.20) provides a rather good estimation of σ'_p when compared with the experimental results from a large database of natural clays while fissured clays do not fit in the same trend, thus requiring different calibration factors (Fig. 5.2).

The application of this method to "well-behaved" clays appears to be rather effective, as shown for soft Brisbane clay in eastern Australia, soft Bothkennar clay in the UK, soft offshore clays at Troll East in the North Sea (Mayne 2008), and soft Burswood clay in western Australia (Mayne et al. 2010). However, the SCE-CSSM solution provides misleading results when applied to organic, sensitive, and structured clays. As an example, Fig. 5.3 illustrates the application of the SCE-CSSM model to Haney sensitive clay, resulting in an evident prediction disagreement. Experimental evidence shows that the hybrid SCE-CSSM framework developed by Mayne (1991) and Chen and Mayne (1994) suffers from inaccuracy when implemented in sensitive and structured clays, resulting in three different profiles characterized by $0.6(q_t - u_2) < 0.33(q_t - \sigma_{v0}) < 0.53(u_2 - u_0)$.

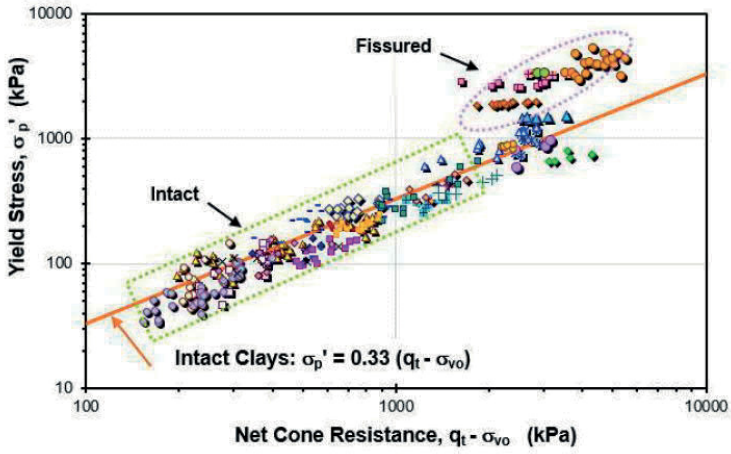

Figure 5.2. Relationship between the σ'_p and net cone resistance (q_{net}) in intact and fissured clays (after Mayne et al. 2009).

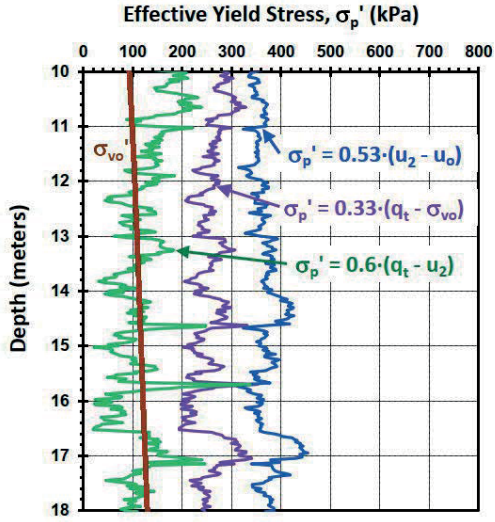

Figure 5.3. SCE-CSSM method applied to the CPTu data of Haney sensitive clay (Mayne et al. 2018).

Similar results are observed for Leda sensitive clay at the Gloucester site (Fig. 5.4), where the SCE-CSSM model is characterized by the inconsistent prediction of the soil stress history.

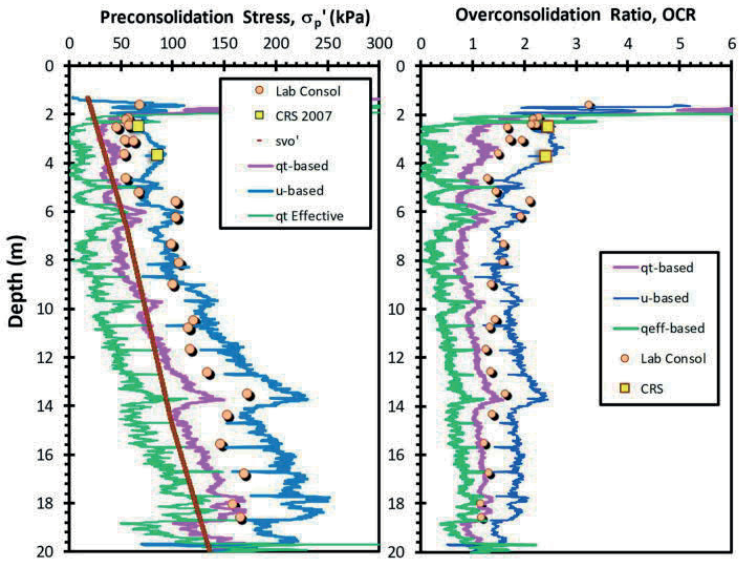

Figure 5.4. Stress history profiles evaluated from the SCE-CSSM framework for the Gloucester site (Agaiby 2018).

5.4.3 Modified SCE-CSSM solution

To overcome the issues related to the implementation of the SCE-CSSM, Agaiby (2018) developed a modified SCE-CSSM method to address the stress history of sensitive clays. The main reason for the inaccuracy of the analytical method is the strain incompatibility between the deviatoric stress ($q = \sigma_1 - \sigma_3$) and u_2 observed from triaxial compression testing. In particular, CICU triaxial data from the Perniö clay (Fig. 5.5) shows that when the deviatoric stress reaches a peak at a strain of about 1%, the pore water pressure is still developing and reaches its peak at a larger strain (>10%). This stress-strain incompatibility is well-documented in the literature for various structured geomaterials (e.g., Leroueil and Hight 2003).

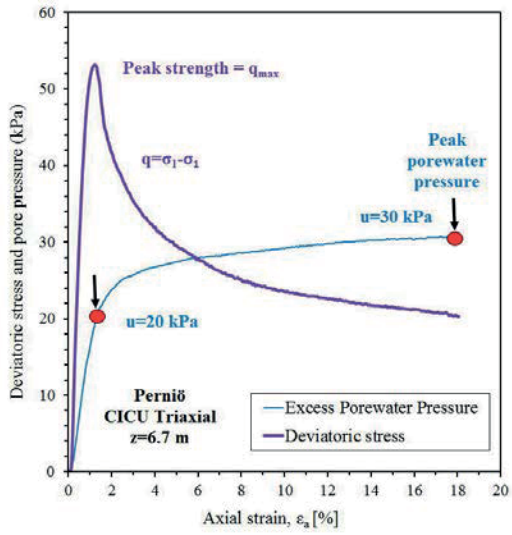

Figure 5.5. Strain incompatibility between the deviatoric stress (q) and excess pore water pressure (u_2) for Perniö clay.

The modified SCE-CSSM solution developed by Agaiby (2018) is based on two "operational" effective frictional parameters: (a) M_{c1} corresponding to the friction angle at maximum deviatoric stress (ϕ'_{PEAK}) and related to the cone tip resistance (q_t); (b) M_{c2} corresponding to the friction angle at maximum obliquity (ϕ'_{MO}) related to the measured u_2. Therefore, with these assumptions, equations (5.9) and (5.15) can be rearranged as follows.

$$q_t - \sigma_{v0} = \left[\frac{4}{3}(\ln I_R + 1) + \frac{\pi}{2} + 1\right]\frac{M_{c1}}{2}\left(\frac{OCR}{2}\right)^{\Lambda}\sigma_{v0}' \tag{5.23}$$

$$\Delta u_2 = \frac{2}{3}M_{c2}\left(\frac{OCR}{2}\right)^{\Lambda}\sigma'_{vo}\ln(I_R) + \sigma'_{v0}\left[1 - \left(\frac{OCR}{2}\right)^{\Lambda}\right] \tag{5.24}$$

On the basis of these modified derivations, OCR can be expressed by three different formulations as follows.

$$OCR = 2\left[\frac{Q/M_{c1}}{[0.667\ln(I_R)+1.95]}\right]^{(1/\Lambda)} \tag{5.25}$$

$$OCR = 2\left[\frac{U^*-1}{0.667M_{c2}\ln(I_R)-1}\right]^{(1/\Lambda)} \tag{5.26}$$

$$OCR = 2\left[\frac{Q-\left(\frac{M_{c1}}{M_{c2}}\right)(U^*-1)}{1.95M_{c1}+\frac{M_{c1}}{M_{c2}}}\right]^{(1/\Lambda)} \quad (5.27)$$

Here, $Q = (q_t - \sigma_{v0})/\sigma'_{v0}$ is the normalized tip resistance, U^* is an alternative normalized pore water pressure [$U^* = (u_2 - u_0)/\sigma'_{v0}$], as detailed by Schneider et al. (2008), M_{c1} and M_{c2} are the CSSM frictional parameters in the q/p' space taken at maximum peak strength and maximum obliquity, defined respectively as follows:

$$M_{c1} = \frac{6\sin\phi'_{PEAK}}{3-\sin\phi'_{PEAK}} \quad (5.28)$$

$$M_{c2} = \frac{6\sin\phi'_{MO}}{3-\sin\phi'_{MO}}. \quad (5.29)$$

In the case of advanced geotechnical analysis, a more sophisticated and versatile solution can be developed that includes an effective cohesion intercept (c'), two rigidity indices, and two plastic strain terms. For the purpose of this study, the original and modified SCE-CSSM approaches are implemented for the stress history evaluation of the investigated sites presented. However, in this study, both solutions are implemented with the careful evaluation of the soil parameters used in the models.

5.4.4 Evaluation of SCE-CSSM soil parameters

As previously detailed, the modified SCE-CSSM formulation requires the assumption of two friction angles (ϕ'_{PEAK} and ϕ'_{MO}), I_R, and Λ. This section discusses the procedures adopted for evaluating these parameters for the investigated clays.

The effective friction angles are determined using three different approaches: (a) exploiting the available triaxial test results from each investigated site; (b) based on the NTH solution; (c) as "operational" values that provide the best fitting between the model prediction and experimental data. The experimental program conducted within the present thesis does not include triaxial compression tests. However, results from studies conducted by Mansikkamäki (2015), Lehtonen (2015), and Selänpää (2020) are exploited to determine the value of ϕ'_{PEAK} and ϕ'_{MO}. Moreover, the NTH solution, proposed by the Norwegian Institute of Technology, offers a methodology for evaluating the effective friction angle (ϕ') based on the normalized parameters Q and B_q. The method has been extensively discussed by Janbu and Senneset (1974), Senneset and Janbu (1985), Senneset et al. (1989), Sandven (1990),

and Sandven and Watn (1995). Based on the original NTH framework, Mayne (2007) derived an approximate solution as follows:

$$\Phi' = 29.5\, B_q^{0.121}\left[0.256 + 0.336\, B_q + \log Q\right]. \tag{5.30}$$

The validity of equation (5.30) is limited to OCR < 2.5, $20° \leq \phi' \leq 45°$, and $0.1 \leq B_q \leq 1.0$. Finally, the values of M_{c1} and M_{c2} are obtained by calibrating the SCE-CSSM model to fit the CRS consolidation test results and are compared with those provided by the abovementioned procedures.

The rigidity index ($I_R = G/s_u$) is a key parameter in many geotechnical applications and is incorporated in various theories and analytical solutions. However, the evaluation of I_R is not straightforward and requires careful analysis (Krage et al. 2014). In particular, owing to the dependency of the shear modulus (G) on the shear strain (γ), it is necessary to set a reference stress range when evaluating I_R. As an example, Konrad and Law (1987) and Schnaid et al. (1997) suggested to use the shear modulus corresponding to 50% of the total mobilized strength (G_{50}). In addition, it has been shown that I_R depends on soil sensitivity, OCR, PI, and organic content (Randolph et al., 1979). In the literature, several attempts have been made to correlate I_R based on the soil index properties (Keaveny 1985; Keaveny and Mitchell 1986; Mayne 2001). Clearly, these uncertainties related to the assumption of the correct value of I_R may result in misleading estimation. Therefore, the use of CPTu-based models for evaluating I_R is of great interest to avoid all issue related to laboratory testing. To this end, the SCE-CSSM framework offers the possibility to determine I_R in terms of the CPTu normalized parameters (Q and U^*) and soil friction angles. By combining equations (5.10) and (5.17), I_R can be expressed as follows:

$$I_R = \exp\left[\frac{1.5+2.925\, M\, a_q}{M(1-a_q)}\right], \tag{5.31}$$

where a_q is the slope parameter defined as

$$a_q = \frac{U^*-1}{Q} = \frac{u_2-\sigma_{vo}}{q_t-\sigma_{vo}}. \tag{5.32}$$

The parameter a_q can be then evaluated for any clay deposit as the slope parameter of the plot ($U^* - 1$) versus Q. Alternatively, a_q is found as the slope of ($u_2 - \sigma_{v0}$) versus ($q_t - \sigma_{v0}$).

Similarly, for highly sensitive clays, the expression for I_R can be derived using equations (5.25) and (5.26), thus obtaining the following.

$$I_R = \exp\left[\frac{1.5+2.925\, M_{c1}\, a_q}{M_{c2}-M_{c1}a_q}\right] \tag{5.33}$$

In the present study, both equations (5.31) and (5.33) are adopted to determine I_R for both the original and modified SCE-CSSM solutions.

Experimental results from laboratory strength data indicate that the value of Λ can be assumed as constant for natural clay. Mayne (1988) proposed values of 0.75, 0.80, and 0.85 for compression, simple shear, and extension modes, respectively. Chandler (1988) indicates that for low overconsolidated clays, $\Lambda = 1$ is a reasonable value.

5.5 Application of the SCE-CSSM model to Finnish clays

Recent studies conducted by Agaiby (2018) and Mayne et al. (2019) showed that the modified SCE-CSSM solutions generally provide reliable stress history prediction when applied to highly sensitive and structured clays. Di Buò et al. (2019d) investigated in detail the implementation of the SCE-CSSM models in Finnish clays, deriving simplified correlation valid in Finnish clays.

In this section, both the original and modified SCE-CSSM models have been adopted for deriving the σ'_p and OCR profiles of the investigated sites. In particular, the solutions have been implemented by considering one representative CPTu sounding for each site, which is selected based on the achieved test quality (section 3.2.5) and overall repeatability. The model prediction is then compared to the CRS laboratory test results to assess the validity of the prediction.

5.5.1 Perniö

As mentioned earlier, the Perniö site worked as a benchmark for a number of studies conducted at Tampere University and Aalto Universities (Mansikkamäki 2015; Lehtonen 2015; Mataic 2016; Di Buò et al. 2019a), which provided an extensive database of field and laboratory tests. The available data is exploited to determine the input parameters (I_R, ϕ', and Λ) necessary for implementing the SCE-CSSM solutions. The effective strength properties of Perniö clay have been investigated by

Mansikkamäki (2015) and Lehtonen (2015). In particular, Mansikkamäki (2015) suggested an effective peak friction angle ϕ'_{PEAK} = 25°–26° (assuming cohesion c' = 0) based on the interpretation of CAUC tests, while Lehtonen (2015) recommended a slightly higher value of ϕ'_{PEAK} = 27.8° with a cohesion c' = 3.4 kPa. Available CAUC and CIUC tests for Perniö clay are summarized in Table 5.2, while the effective stress paths are shown in Fig. 5.6. It is worth observing that the determination of the friction angles ϕ'_{MO} and ϕ'_{PEAK} from the TX test results is not straightforward. The applied fitting is not consistent for all the available tests. Possible reasons that justify this evidence may lie in the sample disturbance affecting the test results and in the assumption of c' = 0 of the SCE-CSSM method, which significantly influences the fitting procedure. However, as shown in Fig. 5.6, a line is fitted through the stress points at maximum q/p and maximum obliquity, giving values of ϕ'_{PEAK} = 28° and ϕ'_{MO} = 36°, respectively. Moreover, the NTH solution is used to estimate the friction angle based on the normalized parameters Q and B_q, shown in Fig. 5.7b and 5.7c, respectively. By assuming B_q = 0.80 and Q = 4.50, equation (5.30) gives a friction angle of ϕ' = 33.7°.

Both the original and modified SCE-CSSM solutions have been implemented by assuming the effective friction angles that provide the best fitting with the experimental data, regardless of the experimental results from TX testing. Therefore, the selected parameters should be considered as "operational" values adopted by the analytical models. The original solution has been implemented by assuming ϕ' = 28°, I_R=580 (eq. 5.31 with slope parameter a_q = 0.54), and Λ = 1. The modified solution, instead, provides the best fitting with the CRS consolidation test results with the following set of parameters: ϕ'_{PEAK} = 31°, ϕ'_{MO} = 33°, I_R = 191 (based on eq. 5.33), and Λ = 1. Results presented in Fig. 5.7 show that both solutions provide fairly good prediction of the preconsolidation stress. Note the original solution is characterized by slightly inconsistent prediction owing to the disagreement between the three equations, particularly evident below 5-m depth. However, such disagreement does not appear to be as significant as the one observed by Agaiby (2018) for Leda sensitive clay. In contrast, the modified solution is more suitable for Perniö clay. Therefore, the assumption of ϕ'_{PEAK} and ϕ'_{MO} overcomes the issues related to the strain incompatibility observed from the TX test results. However, the friction angles giving the best fitting between the model prediction and CRS consolidation test results are slightly different than those evaluated from the TX test results. Possible reasons justifying this observation will be discussed later in this section.

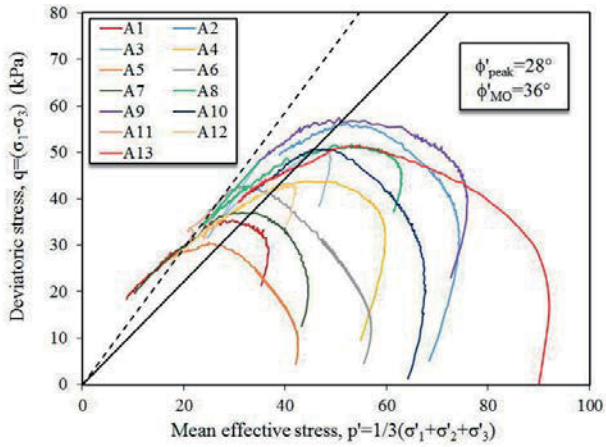

Figure 5.6. Effective stress paths of TX compression tests for Perniö clay, indicating mobilized friction angle at maximum stress q_{max} and maximum obliquity.

Table 5.2. Summary of triaxial test results, Perniö.

Test ID	Type	Depth (m)	In situ stress state			Consolidation state		
			σ'_{v0} (kPa)	σ'_{p} (kPa)	OCR	σ'_{1} (kPa)	σ'_{3} (kPa)	OCR (test)
A1	CAUC	2.65	22	36	1.60	51.4	30	1.00
A2	CAUC	3.2	25	40	1.60	71.8	66.7	1.00
A3	CAUC	3.2	25	40	1.60	72.4	33.8	1.00
A4	CAUC	3.4	26	41	1.60	61.2	51.7	1.00
A5	CAUC	3.85	28	40	1.40	46.5	41.5	1.00
A6	CAUC	3.85	28	40	1.40	60.5	55.5	1.00
A7	CAUC	4.05	29	41	1.40	52	40.5	1.00
A8	CAUC	4.2	31	45	1.45	86.2	48.9	1.00
A9	CAUC	4.4	33	46	1.40	87.9	65.0	1.00
A10	CIUC	4.4	33	46	1.40	65	63.7	1.00
A11	CAUC	4.4	33	46	1.40	44.8	13.5	1.00
A12	CAUC	4.4	33	46	1.40	63.2	28.7	1.00
A13	CIUC	6.1	50	55	1.10	90	90	1.00

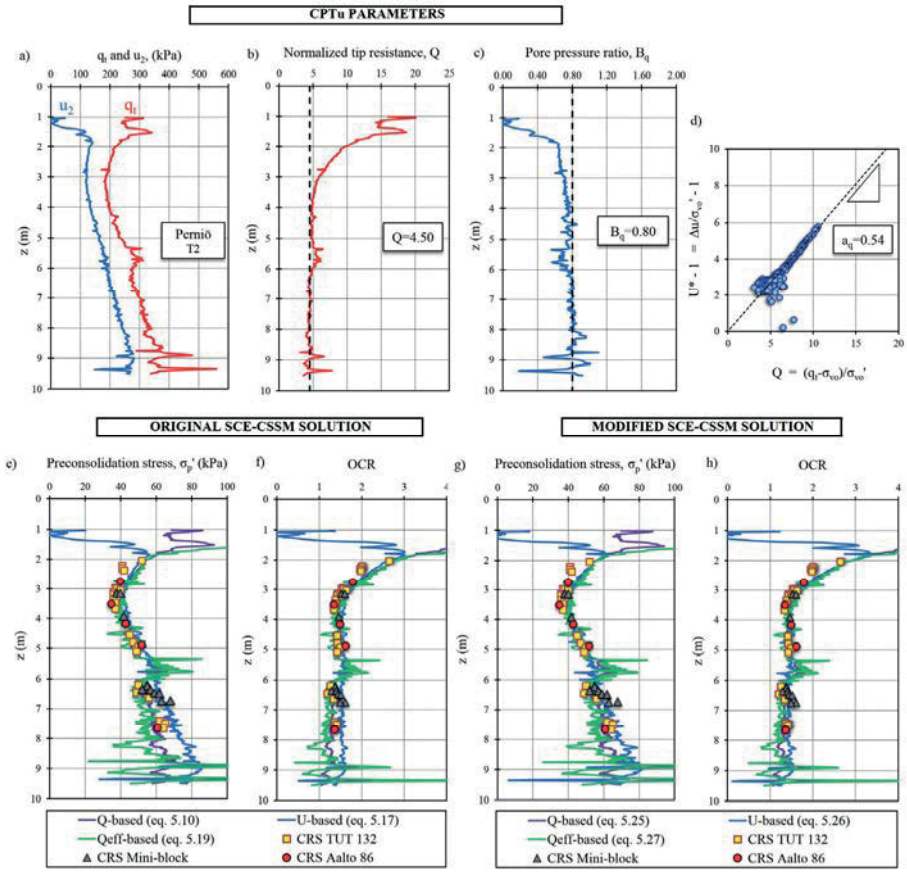

Figure 5.7. Implementation of the modified SCE-CSSM analytical solution on Perniö clay: a) CPTu soundings; b) normalized tip resistance (Q) versus depth; c) normalized pore pressure ratio (B_q) versus depth; d) evaluation of the slope parameter a_q; e) and f) implementation of the original SCE-CSSM for evaluating σ'_p and OCR, respectively; g) and h) implementation of the original SCE-CSSM for evaluating σ'_p and OCR, respectively.

5.5.2 Lempäälä

The investigation conducted at the Lempäälä site is characterized by the lowest sample quality among all the sites. Problems related to sampling and soil disturbance are discussed in section 4.8. To avoid misleading interpretation, the analysis is conducted considering only the TUT 132 samples, which show higher quality compared with the ST:1 50 piston samples. The triaxial compression tests of Lempäälä clay are not available; therefore, the friction angle is evaluated based on

the analytical approaches. Based on equation (5.30), the NTH solution gives a value of $\phi' = 30°$ by assuming $Q = 3.50$ and $B_q = 0.75$. The original SCE-CSSM solution provides the best fitting with the experimental data, assuming $\phi' = 30°$, $I_R = 142$ (eq. 5.31, $a_q = 0.47$), and $\Lambda = 1$. As observed for Perniö clay, the three equations show a slight disagreement among each other (Fig. 5.8e and 5.8f). In contrast, the modified solution has been applied assuming $\phi'_{PEAK} = 28°$ and $\phi'_{MO} = 30°$, $I_R = 88$ (eq. 5.33), and $\Lambda = 1$, proving more consistent prediction among the three equations (Fig. 5.8g and 5.9h). Note that the upper 4-m layer, which constitutes organic fill material, is characterized by evident disagreement among the three profiles. Clearly, the applicability of the SCE-CSSM models in such soils needs further investigation.

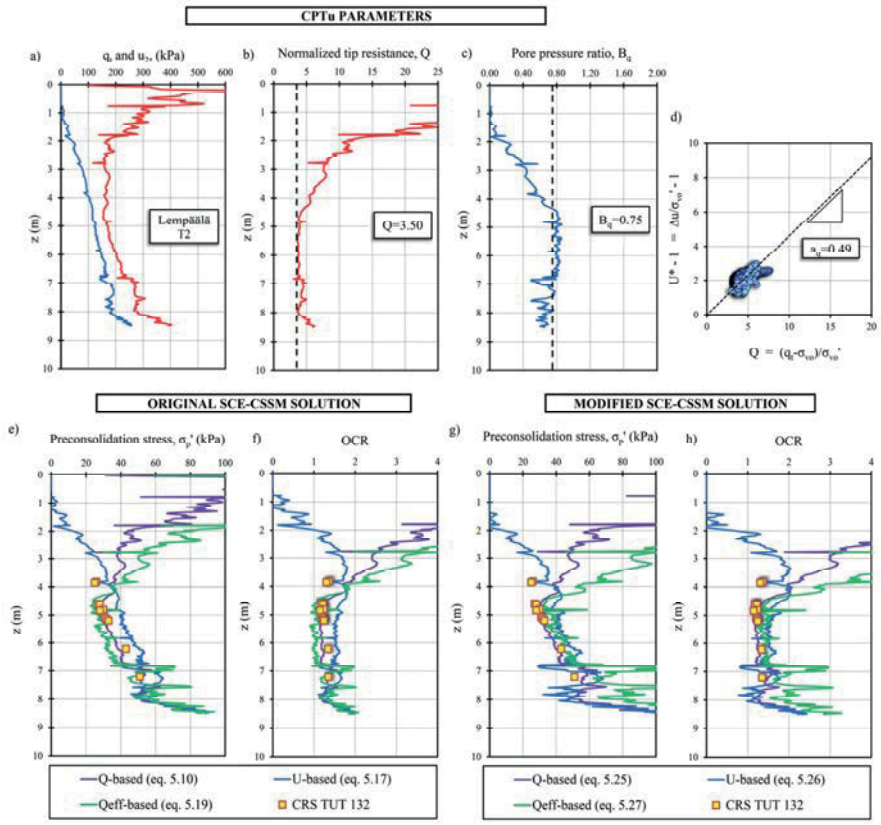

Figure 5.8. Implementation of the modified SCE-CSSM analytical solution on Lempäälä clay: a) CPTu soundings; b) normalized tip resistance (Q) versus depth; c) normalized pore pressure ratio (B_q) versus depth; d) evaluation of the slope parameter a_q; e) and f) implementation of the original SCE-CSSM for evaluating σ'_p and OCR, respectively; g) and h) implementation of the original SCE-CSSM for evaluating σ'_p and OCR, respectively.

5.5.3 Masku

The laboratory testing program conducted on Masku clay has been performed on undisturbed samples taken at three depth levels (3, 5, and 8 m) using the TUT 132 sampler. For this site, the comparison between the SCE-CSSM models and experimental test results is performed on a limited amount of data. The effective friction angles are evaluated based on two CIUC tests from samples taken at 2.5 and 2.9 m depth (Table 5.3, Fig. 5.9), giving values of $\phi'_{PEAK} = 30°$ and $\phi'_{MO} = 36.9°$. The NTH solution (eq. 5.30) provides $\phi' = 35.9°$ based on $Q = 6.50$ and $B_q = 0.65$. The original solution is implemented by assuming $\phi' = 36°$, $I_R = 124$ (eq. 5.31), and $\Lambda = 1$ and provides a rather good estimation of σ'_p and OCR (Fig. 5.10e and 5.10f). Conversely, it has been observed that for Masku clay, the modified solution provides the best fitting with the experimental data only when $\phi'_{PEAK} = \phi'_{MO} = 36°$, which corresponds to the original analytical solution. One of the main reasons that may explain these observations is the low sensitivity of Masku clay, which makes the original SCE-CSSM model more suitable for deriving σ'_p and OCR. These aspects will be analyzed in detail later in the thesis.

Table 5.3. Triaxial tests, Masku.

Test ID	Type	Depth (m)	In situ stress state			Consolidation state		
			σ'_{v0} (kPa)	σ'_p (kPa)	OCR	σ'_1 (kPa)	σ'_3 (kPa)	OCR (test)
C1	CIUC	2.5	20	50	2.50	100	100	1.00
C2	CIUC	2.9	20	53	2.65	51	51	1.00

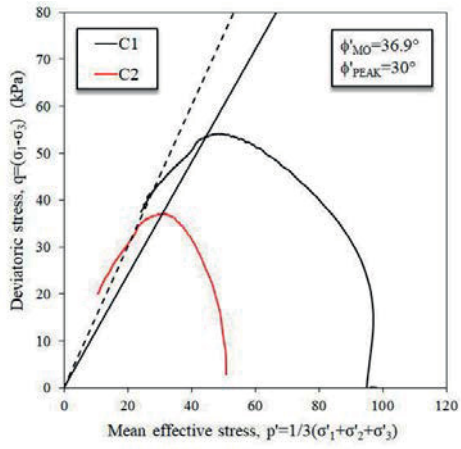

Figure 5.9. Effective stress paths from CIUC TX tests, Masku.

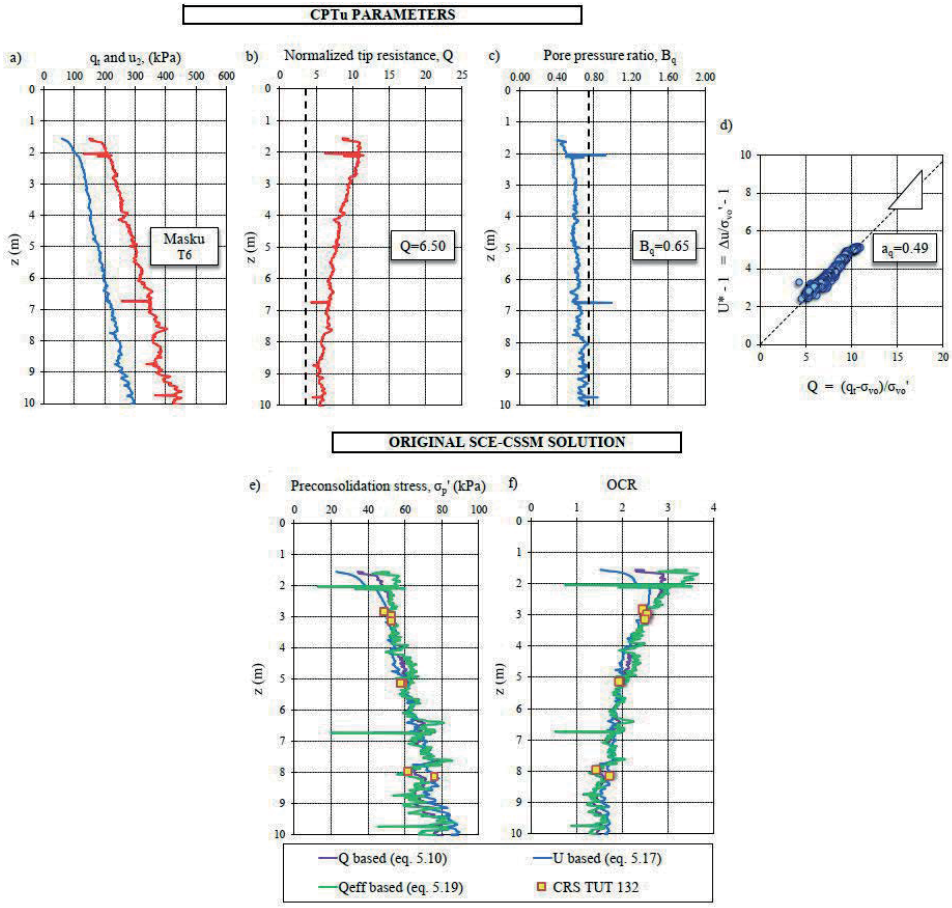

Figure 5.10. Implementation of the modified SCE-CSSM analytical solution on Masku clay: a) CPTu soundings; b) normalized tip resistance (Q) versus depth; c) normalized pore pressure ratio (B_q) versus depth; d) evaluation of the slope parameter a_q; e) and f) implementation of the original SCE-CSSM for evaluating σ'_p and OCR, respectively.

5.5.4 Paimio

Results obtained from the implementation of the SCE-CSSM models for Paimio clay are shown in Fig. 5.12. As for the other sites, the friction angles are determined based on the available TX test results, which are summarized in Table 5.4 and illustrated in Fig. 5.11. The effective stress paths suggest ϕ'_{PEAK} = 27.5° and ϕ'_{MO} = 33.7°. Assuming Q = 4.50 and B_q = 0.80, the NTH solution gives an effective friction angle ϕ' = 33.7°, which is consistent with the friction angle at maximum obliquity evaluated

from the experimental results. The best fitting with the CRS consolidation test results is obtained by assuming $\phi' = 28°$, $I_R = 580$ (eq. 5.31), and $\Lambda = 1$ in the original SCE-CSSM solution. Although an overall good prediction is obtained, the equation based on the excess pore pressure overestimates the stress history parameters below 6-m depth (Fig. 5.12e and 5.12f). As discussed in section 4.5, the bottom layer is characterized by higher plasticity, which may explain the different applicability of the model. The modified SCE-CSSM solution, however, provides the best data fitting by assuming $\phi'_{PEAK} = 31°$ and $\phi'_{MO} = 34°$, which are then used to evaluate $I_R = 138$ (eq. 5.33). As observed for Perniö clay, both solutions provide fairly good prediction. It is observed that the *U*-based equation from the original solution (eq. 5.17) slightly overestimate the σ'_p while the three verticals derived from the modified solution are more consistent and in agreement with the experimental data.

Table 5.4. Triaxial tests, Paimio.

Test ID	Type	Depth (m)	In situ stress state			Consolidation state		
			σ'_{v0} (kPa)	σ'_p (kPa)	OCR	σ'_1 (kPa)	σ'_3 (kPa)	OCR (test)
D1	CIUC	4.5	32.3	65	2.01	126	126	1
D2	CIUC	4.7	33.3	65	1.95	97	97	1
D3	CIUC	4.4	31.8	65	2.04	65	65	1

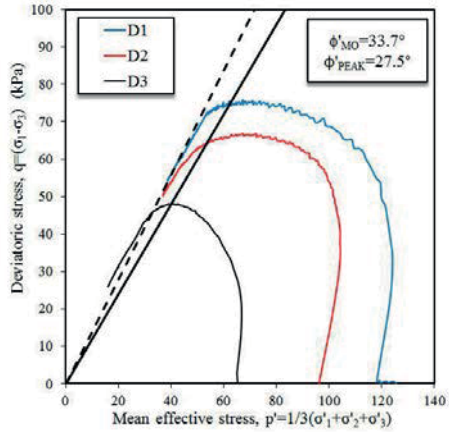

Figure 5.11. Effective stress paths from CIUC TX tests, Paimio.

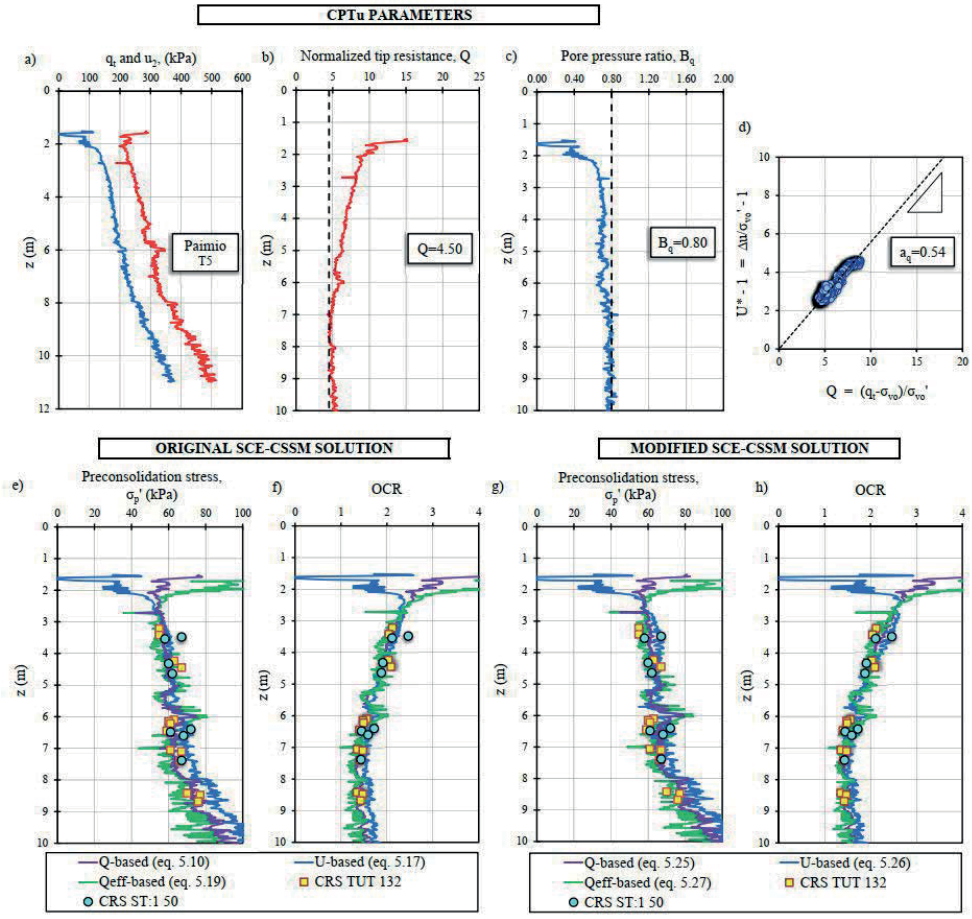

Figure 5.12. Implementation of the modified SCE-CSSM analytical solution on Paimio clay: a) CPTu soundings; b) normalized tip resistance (Q) versus depth; c) normalized pore pressure ratio (B_q) versus depth; d) evaluation of the slope parameter a_q; e) and f) implementation of the original SCE-CSSM for evaluating σ'_p and OCR, respectively; g) and h) implementation of the original SCE-CSSM for evaluating σ'_p and OCR, respectively.

5.5.5 Sipoo

Three available triaxial CIUC tests performed on undisturbed samples at 5.85-m depth (Fig. 5.13, Table 5.5) suggest a mobilized effective friction angle at peak ϕ'_{PEAK} = 25.4° and ϕ'_{MO} = 33.7°, whereas ϕ' = 36.3° is obtained from the NTH solution (Q = 6.30; B_q = 0.70). The curve-fitting procedure between the original SCE-CSSM solution and experimental data indicates the following set of parameters: ϕ' = 34°, I_R = 332, and Λ = 1. In contrast, the modified solution provides a good estimation of σ'_p and OCR for $\phi'_{PEAK} = \phi'_{MO}$ = 34°, thus matching the original SCE-CSSM equations. As observed for the Masku site, the modified SCE-CSSM solution appears to not be suitable when applied to low sensitive clays. Results are illustrated in Fig. 5.14.

Table 5.5. Triaxial tests, Sipoo.

Test ID	Type	Depth (m)	In situ stress state			Consolidation state		
			σ'_{v0} (kPa)	σ'_p (kPa)	OCR	σ'_1 (kPa)	σ'_3 (kPa)	σ'_{v0} (kPa)
E1	CIUC	5.85	34.6	53	1.531792	150	150	1.00
E2	CIUC	5.85	34.6	53	1.531792	111	111	1.00
E3	CIUC	5.85	34.6	53	1.531792	70	70	1.00

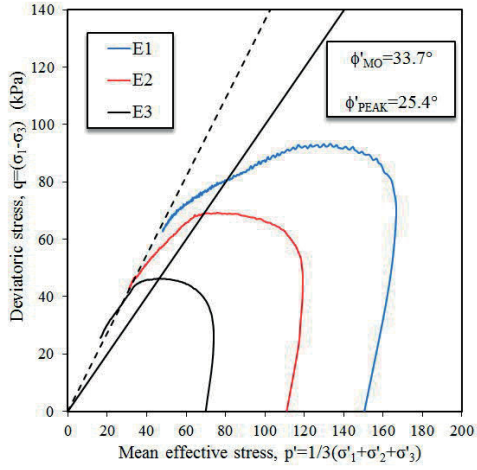

Figure 5.13. Effective stress paths from CIUC TX tests, Sipoo.

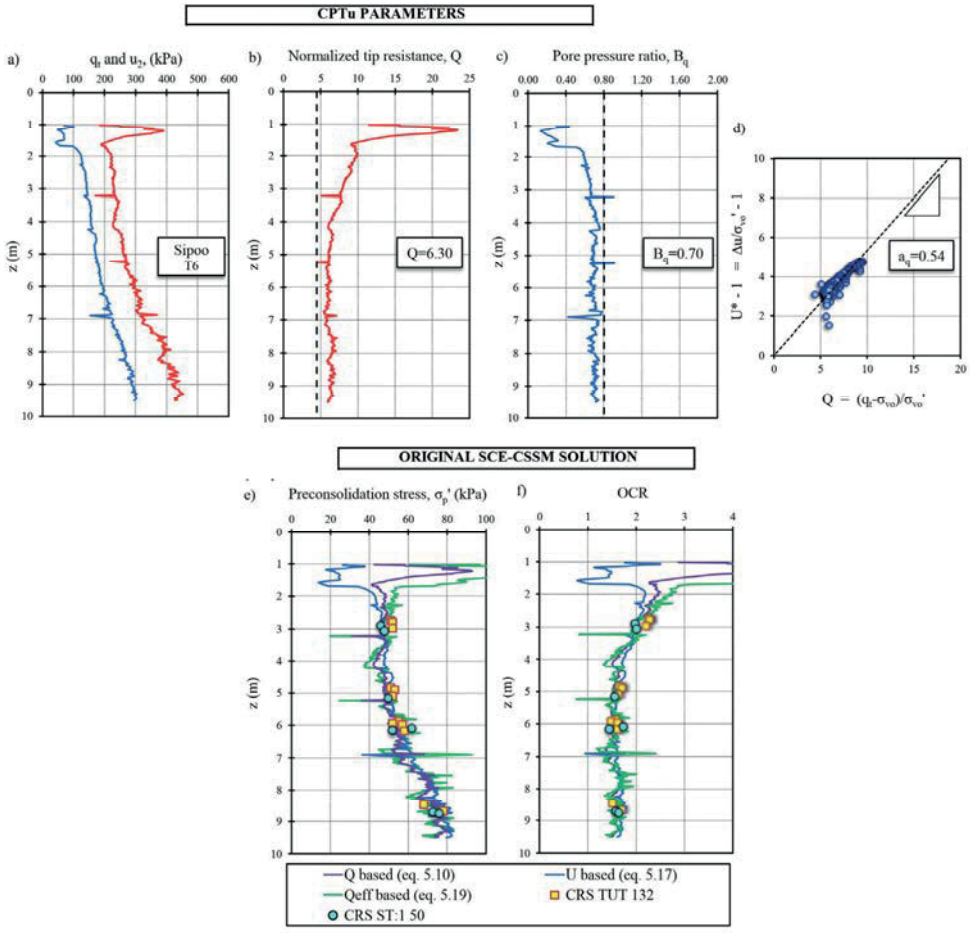

Figure 5.14. Implementation of the modified SCE-CSSM analytical solution on Sipoo clay: a) CPTu soundings; b) normalized tip resistance (Q) versus depth; c) normalized pore pressure ratio (B_q) versus depth; d) evaluation of the slope parameter a_q; e) and f) implementation of the original SCE-CSSM for evaluating σ'_p and OCR, respectively.

5.6 Validation of the SCE-CSSM analytical solutions

As observed in the previous sections, the SCE-CSSM framework provides a reliable methodology to estimate the values of σ'_p and OCR, which are generally in reasonable agreement with the experimental results. Table 5.6 summarizes the parameters adopted in the implementation of the analytical solutions as well as the effective friction angles evaluated from the NTH solution and CIUC/CAUC triaxial tests. The obtained results demonstrate that the three equations derived from the original SCE-CSSM framework (eq. 5.10, eq. 5.17, and eq. 5.19) are suitable for predicting the σ'_p in low sensitive clay sites ($S_t < 20$, e.g., Masku and Sipoo), whereas a slight disagreement between the three CPTu-based equations is observed in highly sensitive clays ($S_t > 20$, e.g., Perniö, Lempäälä, and Paimio). In contrast, the modified analytical solution (eq. 5.25, eq. 5.26, and eq. 5.27) overcomes the issues related by assuming two effective friction angle values (ϕ'_{PEAK} and ϕ'_{MO}). However, the obtained results revealed that the differences between the implementation of the original and modified SCE-CSSM methodologies in Finnish clays are not as evident as those observed in Leda and Haney clays (Agaiby 2018; Mayne et al. 2019). These aspects are discussed in detail in the following section.

It is worth observing that the friction angles that give the best fit between the model prediction and experimental results are not always consistent with the results from TX compression tests. As an example, for Perniö and Paimio clay, the ϕ'_{PEAK} adopted in the modified solution is higher than that evaluated from the laboratory tests. These disagreements can be justified in several possible ways. First, the value of ϕ'_{PEAK} is evaluated on samples consolidated beyond the in situ stress before shearing, thus altering their initial structure. Next, sample disturbance may also play a crucial role. Herein, it is difficult to provide further explanations of these aspects owing to the limited amounts of available TX compression tests from the investigated clays.

The validity of the implemented analytical solutions is assessed by conducting a statistical analysis on the model prediction with respect to the target values represented by the experimental test results. In particular, the goodness of each equation derived from the SCE-CSSM framework is evaluated based on four different parameters: coefficient of determination (R^2), bias factor (b), coefficient of variation (COV), and standard error (SE). R^2 expresses the proportion of the variance in the dependent variable that is predictable from the independent variable. It gives information about the goodness of fit of a model with the measured data points. It ranges between 0 and 1, where 0 indicates that the dependent variable

cannot be predicted from the independent variable while 1 indicates that the dependent variable can be predicted without error from the independent variable (ideal case). The bias factor is expressed as the mean of the ratio of the measured target value over the predicted target value, as detailed by Ching and Phoon (2014). The prediction is considered unbiased when $b = 1$ (ideal case). COV is defined as the ratio of the standard deviation (SD) gives information about the dispersion of data points around the mean. If COV = 0, no data scatter exists for the transformation model, meaning that the prediction is deterministic. SE is the standard deviation of the sampling distribution and measures the accuracy with which a sample represents the population. In particular, it provides information of the deviation of the sample mean from the actual mean of a population. The choice of considering different statistical tools is justified by the fact that they provide different information related to prediction accuracy, robustness, and dispersion of the analyzed estimator in comparison with the dataset.

Table 5.6. Summary of the SCE-CSSM parameters adopted in the implementation.

Site	NTH solution			TX tests		SCE-CSSM solutions					
	B_q	Q	ϕ'	ϕ'_{PEAK}	ϕ'_{MO}	TYPE	ϕ'_{PEAK}	ϕ'_{MO}	Λ	a_q	I_R
Perniö	0.80	4.50	33.7	28	36	ORIG.	28	–	1.00	0.54	580
						MOD.	31	33	1.00		191
Lempäälä	0.75	3.50	30	n.a.		ORIG.	30	–	1.00	0.47	142
						MOD.	28	30	1.00		88
Masku	0.65	6.50	35.9	30	36.9	ORIG.	36	–	1.00	0.49	124
						MOD.	not suitable				
Paimio	0.80	4.50	33.7	27.5	33.7	ORIG.	28	–	1.00	0.54	580
						MOD.	31	34	1.00		138
Sipoo	0.70	6.30	36.3	25.4	33.7	ORIG.	34	–	1.00	0.54	332
						MOD.	not suitable				

The results of the statistical analysis conducted on OCR and σ'_p are summarized in Table 5.7 and Table 5.8. As previously observed, the Lempäälä site is characterized by the lowest model accuracy, as demonstrated by the low values of the coefficient of determination. It is worth observing that there is an evident difference between the prediction of σ'_p and OCR even when the same model is implemented. As an example, the U-based prediction is characterized by $R^2 = 0.07$ when implemented to evaluate OCR while the same equation provides $R^2 = 0.90$ in case of σ'_p. As shown in APPENDIX 6, this inconsistency can be justified by the limited variability of the OCR values at Lempäälä site ($1 < OCR < 1.40$). In contrast, the σ'_p range is wider, thus giving higher value of R^2. Therefore, despite R^2 is generally a reliable indicator of the prediction goodness, in the aforementioned cases it may provide misleading

information. All the other sites are characterized by relatively high accuracy for both OCR and σ'_p, with R^2 ranging between 0.70 and 0.95. However, the prediction based on the Q_{eff} is generally characterized by higher uncertainties (e.g., Paimio).

Results from the statistical analysis do not provide significant differences between the predictions provided by the original and modified solutions. This is consistent with the observations made in the previous sections. In particular, it has been pointed out how the disagreement shown by the original SCE-CSSM equations applied for sensitive Finnish clays (Perniö, Lempäälä, and Paimio) is not as evident as that for Canadian and Norwegian clays (Agaiby and Mayne 2018; Mayne et al. 2019). Possible reasons that justify these findings are discussed in section 5.7.

From a theoretical point of view, the adoption of the modified equations is suggested for clays of $S_t > 30$ to avoid misleading prediction owing to the stress-strain incompatibility. Finally, b varying between 0.74 and 1.05, with a COV from 0.05 to 0.26 are observed. This would suggest that the values predicted by the analytical solutions are characterized by reasonably low variability.

Table 5.7. Summary of the statistical analysis of the SCE-CSSM equations for deriving OCR.

Site	Model	Statistical Analysis								
		R^2			b, (COV)			SE		
		Q	U	Q_{eff}	Q	U	Q_{eff}	Q	U	Q_{eff}
Perniö	ORIG.	0.80	0.83	0.74	1.00 (0.10)	0.91 (0.06)	1.03 (0.14)	0.17	0.11	0.21
	MOD.	0.80	0.83	0.75	0.99 (0.10)	0.97 (0.08)	1.01 (0.13)	0.17	0.14	0.20
Lempäälä	ORIG.	0.31	0.05	0.32	0.93 (0.13)	0.79 (0.07)	1.04 (0.23)	0.20	0.04	0.39
	MOD.	0.32	0.05	0.32	0.87 (0.16)	0.78 (0.09)	0.74 (0.08)	0.27	0.08	0.67
Masku	ORIG.	0.96	0.96	0.92	0.99 (0.05)	0.98 (0.07)	1.01 (0.07)	0.10	0.07	0.14
Paimio	ORIG.	0.85	0.85	0.75	1.01 (0.07)	0.95 (0.08)	1.05 (0.09)	0.12	0.10	0.15
	MOD.	0.85	0.85	0.78	0.95 (0.07)	0.92 (0.07)	0.98 (0.09)	0.13	0.14	0.15
Sipoo	ORIG.	0.86	0.78	0.86	1.05 (0.06)	1.02 (0.07)	1.03 (0.06)	0.08	0.09	0.08

Table 5.8. Summary of the statistical analysis of the SCE-CSSM equations for deriving σ'_p.

Site	Model	Statistical analysis								
		R^2			b, (COV)			SE		
		Q	U	Q_{eff}	Q	U	Q_{eff}	Q	U	Q_{eff}
Perniö	ORIG.	0.80	0.89	0.60	1.00 (0.10)	0.91 (0.07)	1.02 (0.14)	3.03	3.27	3.35
	MOD.	0.80	0.85	0.64	0.98 (0.10)	0.96 (0.08)	1.00 (0.13)	3.08	3.32	3.33
Lempäälä	ORIG.	0.74	0.93	0.17	0.93 (0.13)	0.78 (0.07)	1.03 (0.23)	3.44	2.53	7.60
	MOD.	0.56	0.90	0.07	0.87 (0.16)	0.78 (0.09)	0.74 (0.26)	5.09	3.22	13.62
Masku	ORIG.	0.85	0.86	0.67	0.99 (0.05)	0.97 (0.07)	1.01 (0.08)	3.08	4.66	4.03
Paimio	ORIG.	0.47	0.55	0.25	1.01 (0.07)	0.94 (0.08)	1.05 (0.09)	4.08	5.49	5.37
	MOD.	0.47	0.51	0.29	0.95 (0.07)	0.92 (0.07)	0.98 (0.09)	4.34	4.67	5.35
Sipoo	ORIG.	0.91	0.91	0.87	1.05 (0.06)	1.02 (0.07)	1.02 (0.06)	3.31	3.87	3.33

5.7 Simplified CPTu-based correlations for Finnish clays

The applicability of the SCE-CSSM framework in predicting the OCR and σ'_p from CPTu data has been extensively discussed in the previous sections. In particular, it has been shown that the original SCE-CSSM model provides good stress history prediction in low sensitive clays (e.g., Masku and Sipoo), whereas the modified solution fits reasonably well with the experimental data for clays with $S_t > 30$ (e.g., Perniö, Lempäälä, and Paimio). That said, the boundary of $S_t = 30$ should be regarded as the limit for the applicability of the original and modified SCE-CSSM methods in Finnish clays.

Although these analytical models offer a reliable and accurate methodology, they are impracticable from a computational point of view because a number of parameters are required. Therefore, in this section, simplified CPTu-based correlations valid for Finnish clays are derived based on the results obtained at the investigated sites.

For the clays with $S_t < 30$ (e.g., Masku and Sipoo), the ϕ' adopted in the original SCE-CSSM solution ranges between 34° and 36°, while I_R varies from 124 to 332 (Table 5.6). Based on this, simplified expressions can be derived from the original SCE-CSSM formulations, assuming an average operational effective friction angle ϕ' = 35° (i.e., $M_{c1} = 1.42$), $I_R = 230$, and $\Lambda = 1$. Using this set of parameters, equations (5.10), (5.17), and (5.19) can be expressed as follows.

$$\sigma'_p = 0.25\ (q_t - \sigma_{v0}) = 0.25\ q_{net} \quad (5.34)$$

$$\sigma'_p = 0.39\ (u_2 - u_0) = 0.39\ \Delta u_2 \quad (5.35)$$

$$\sigma'_p = 0.53\ (q_t - u_2) = 0.53\ q_{eff} \quad (5.36)$$

Similarly, for clays with $S_t > 30$, the following average parameters are assumed: $\phi'_{PEAK} = 31°$, $\phi'_{MO} = 34°$ (i.e., $M_{c1} = 1.24$, $M_{c2} = 1.37$), $I_R = 160$, and $\Lambda = 1$. Such parameters are evaluated based on the results obtained at Perniö and Paimio, which appear to be more reliable compared with those obtained at Lempäälä. Therefore, three simplified equations can be obtained from equations (5.25), (5.26), and (5.27).

$$\sigma'_p = 0.30\ (q_t - \sigma_{v0}) = 0.30\ q_{net} \quad (5.37)$$

$$\sigma'_p = 0.55\ (u_2 - u_0 - \sigma'_{v0}) = 0.55\ (\Delta u_2 - \sigma'_{v0}) \quad (5.38)$$

$$\sigma'_p = 0.6\ (q_t - \sigma_{v0}) - 0.54\ (\Delta u_2 - \sigma'_{v0}) \quad (5.39)$$

However, from a practical point of view, it may be convenient to rely on a single set of equations that are representative of the entire population of Finnish clays presented in this study, regardless of S_t. Therefore, equations (5.34) and (5.37) can be combined into one unique expression as follows:

$$\sigma'_p = 0.275\ (q_t - \sigma_{v0}) = 0.275\ q_{net}. \quad (5.40)$$

Equations (5.35), (5.36), (5.38), (5.39), and (5.40) are validated for the entire dataset of Finnish clays comprising n = 99 high-quality data points, and the results are presented in Fig. 5.15.

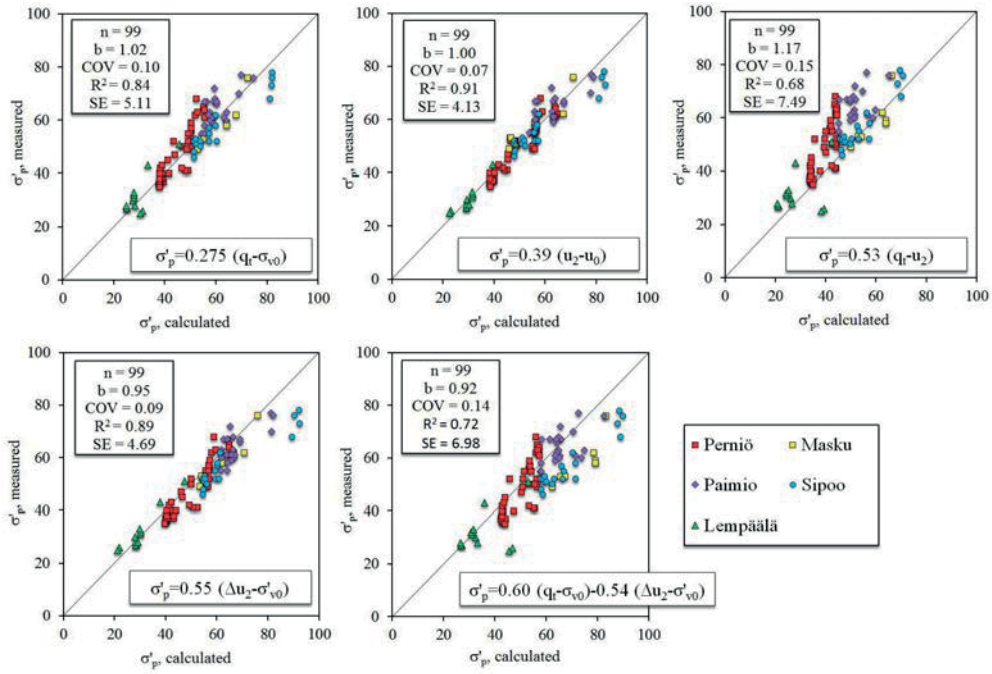

Figure 5.15. CPTu-based correlations for predicting σ'_p in Finnish clays derived from the SCE-CSSM theoretical solution.

The goodness of each correlation is evaluated based on *b* and COV. Based on these results, a calibration process is performed by correcting the above correlations using their b to obtain the following.

$$\sigma'_p = 0.28\,(q_t - \sigma_{v0}) = 0.28\,q_{net} \tag{5.41}$$

$$\sigma'_p = 0.39\,(u_2 - u_0) = 0.39\,\Delta u_2 \tag{5.42}$$

$$\sigma'_p = 0.62\,(q_t - u_2) = 0.62\,q_{eff} \tag{5.43}$$

$$\sigma'_p = 0.52\,(u_2 - u_0 - \sigma'_{v0}) = 0.52\,(\Delta u_2 - \sigma'_{v0}) \tag{5.44}$$

$$\sigma'_p = 0.55\,(q_t - \sigma_{v0}) - 0.50\,(\Delta u_2 - \sigma'_{v0}) \tag{5.45}$$

A summary of the calibrated equations, b, and COV is shown in Table 5.9, whereas the comparison between the experimental data and correlation-based predictions is shown in Fig. 5.16. Overall, the correlations provide a reasonably good estimation

of the σ'_p, as COV varies between 0.07 and 0.15. In addition to the CPTu measurements, the in situ effective stress (σ'_{v0}) and stationary pore water pressure (u_0) are needed.

Table 5.9. Calibrated correlations for predicting σ'_p in Finnish clays.

Equation	Correlation	n	*b*	*COV*	Calibrated correlation
5.40	$\sigma'_p = 0.275(q_t - \sigma_{v0})$	99	1.02	0.10	$\sigma'_p = 0.28(q_t - \sigma_{v0})$
5.35	$\sigma'_p = 0.39(u_2 - u_0)$	99	1.00	0.07	$\sigma'_p = 0.39(u_2 - u_0)$
5.36	$\sigma'_p = 0.53(q_t - u_2)$	99	1.17	0.15	$\sigma'_p = 0.62(q_t - u_2)$
5.38	$\sigma'_p = 0.55(\Delta u_2 - \sigma'_{v0})$	99	0.95	0.09	$\sigma'_p = 0.52(\Delta u_2 - \sigma'_{v0})$
5.39	$\sigma'_p = 0.6(q_t - \sigma_{v0}) - 0.54(\Delta u_2 - \sigma'_{v0})$	99	0.92	0.14	$\sigma'_p = 0.55(q_t - \sigma_{v0}) - 0.50(\Delta u_2 - \sigma'_{v0})$

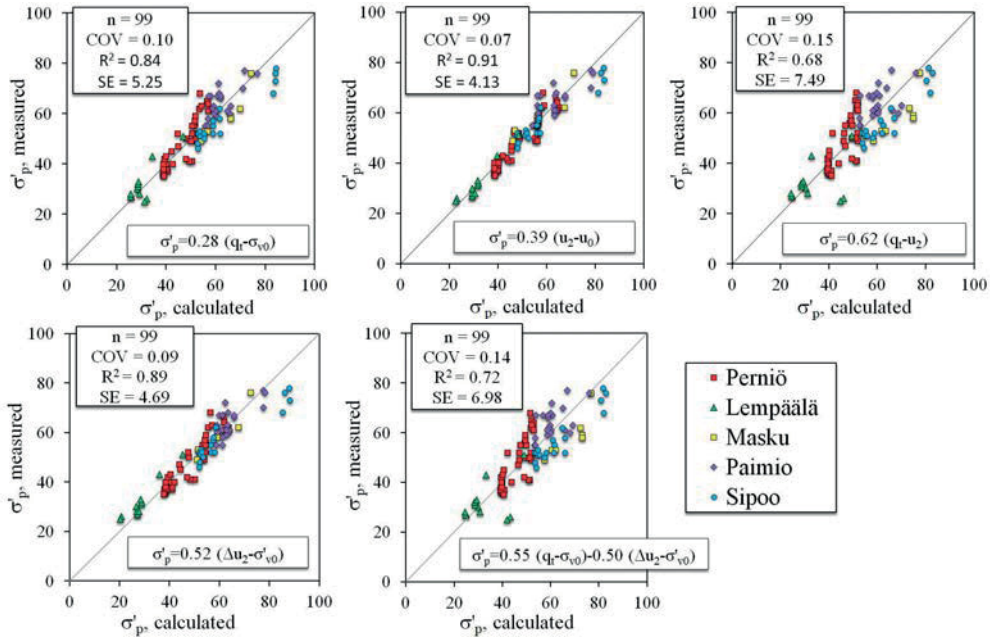

Figure 5.16. Calibrated CPTu-based correlations for predicting σ'_p in Finnish clays derived from the SCE-CSSM theoretical solution.

5.8 Discussion

Overall, the implementation of the SCE-CSSM analytical solutions at the investigated sites revealed that reliable estimations of OCR and σ'_p can be obtained when the proper soil parameters are assumed. As observed in previous studies (Agaiby 2018), a slight disagreement between the three CPTu-based equations is

observed when the original solution is adopted in clays with $S_t > 30$. The modified SCE-CSSM solution, however, is more suitable for highly sensitive clays by assuming two "operational" friction angles (ϕ'_{PEAK} and ϕ'_{MO}). In particular, for the investigated clays, the SCE-CSSM models provided the best fitting by adopting friction angle ratio ϕ'_{MO}/ϕ'_{peak} between 0.9 and 1. In contrast, lower values were observed for different worldwide sensitive soils, as detailed by Agaiby (2018). A possible reason for this lies in the magnitude of the slope parameter a_q: Finnish clays are characterized by a_q ranging between 0.45 and 0.55 while data obtained from other sensitive clay test sites (e.g. Gloucester and Tiller-Flotten) indicate higher a_q values. Figure 5.17 shows the friction angle ratio ϕ'_{MO}/ϕ'_{PEAK} as a function of the slope parameter a_q, highlighting the aforementioned differences between Finnish clays and well-documented sensitive clays. These aspects require further investigation by conducting additional investigation which would confirm the observed trend.

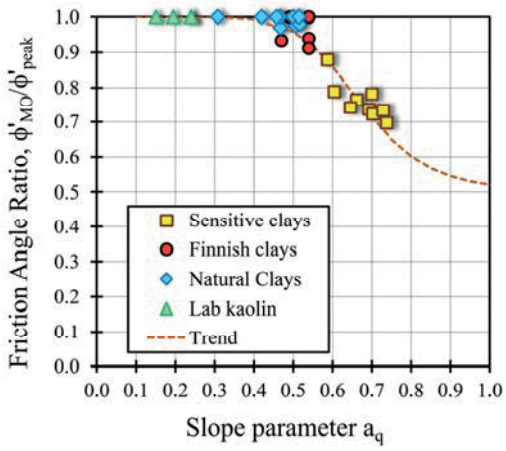

Figure 5.17. Friction angle ratio (ϕ'_{MO}/ϕ'_{PEAK}) as a function of a_q for different clays.

Simplified correlations valid for Finnish clays are derived by assuming average values of ϕ' and I_R, which have been evaluated from the results obtained at the investigated sites. These correlations have been further calibrated based on their bias to match the mean trend of the collected data. Although a relatively small database has been used to derive these correlations, they can be reliably used for the preliminary evaluation of OCR and σ'_p in the absence of site-specific data or when the available data is suspected to be unreliable. Finally, it is worth pointing out that the SCE-CSSM analytical framework provides a rational approach for the interpretation of CPTu data, which is more effective than "stand-alone" empirical methods.

6 DEFORMATION PROPERTIES OF FINNISH CLAYS

6.1 Introduction

The evaluation of soil settlement represents one of the key factors to guarantee safe design and ensure the validation of the SLS. In clayey soils, and particularly in soft sensitive clays, the load application may induce severe damages to the structure and infrastructure owing to the high compressibility of these soils. The soil settlement is the result of the delayed volumetric response owing to the interaction between the soil skeleton and pore water. This process is generally referred to as "consolidation" and indicates the time-dependent volume change phenomenon induced by the excess pore water pressure dissipation.

It has been observed (section 2.4.2) that existing settlement calculation methods may result in an inaccurate description of the soil stress-strain response. Therefore, the compression index method is not suitable for predicting the settlement in soft sensitive clays because the assumption of constant values of C_c is not representative for describing the highly nonlinear stress-strain behavior in the entire NC region. In contrast, both Janbu's method and Sällfors' methods are more suitable in predicting the settlement of soft sensitive clays.

Laboratory tests, such as oedometer or triaxial tests, commonly performed on undisturbed samples are considered the most reliable tests for determining the deformation characteristics of clays. However, as observed within this study, a proper laboratory investigation program is time consuming and the trustworthiness of the test results can be highly affected by sample disturbance. Therefore, many researchers have made considerable efforts to determine the soil deformation characteristics from the soil index properties (e.g., w and e_0) and field testing data (e.g., CPTu).

Traditionally, the piezocone has revealed to be a reliable tool for estimating the undrained strength and the stress history (OCR, σ'_p) of fine-grained soils, whereas its applicability for predicting deformation characteristics has shown more uncertainties. However, several authors (Sanglerat 1972; Mayne 2007; Robertson 2009) have proposed reliable correlations for evaluating the soil stiffness based on

CPTu parameters. Nevertheless, such equations are derived based on a database including soils characterized by different properties than Finnish clays; therefore, their validity should be assessed. In relation to this, studies conducted at Tampere University have revealed that these existing correlations require proper calibration when applied to Finnish clays (Di Buò et al. 2018). Herein, the main objective is not to replace the laboratory testing approach with empirical and analytical correlations based on CPTu tests but to provide a reliable methodology to perform preliminary settlement analysis using both field and laboratory data. Clearly, in the case of high-risk projects, an advanced laboratory testing program is needed along with the careful use of empirical correlations.

In this section, the deformation properties of Finnish clays are investigated on the basis of CRS consolidation test results. Moreover, the applicability of CPTu in predicting soil stiffness in terms of the constrained modulus (M) and compressibility is assessed. Finally, issues related to the application of the Tangent modulus method and CRS Swedish method in predicting the soil settlement in soft clays are discussed.

6.2 Deformation properties of Finnish clays

The typical stress-strain behavior of Finnish clays observed in 1D consolidation tests has been extensively analyzed in section 4. The soil exhibits a stiff response in the OC region, followed by a significant drop when σ'_p is reached, and subsequent nonlinear stress-strain relationship in the log σ'_v–ε_v plot. This behavior has been observed for all the tested samples, and it is the typical behavior of marine clays described by Janbu (1985).

As observed in section 2.4.2, the evaluation of the deformation characteristics of sensitive clays is rather challenging owing to the nonlinearity in terms of log σ'_v–ε_v observed from CRS consolidation test results. While both Janbu's method and Sällfors' method provide suitable representation of the compressibility of Finnish clays, difficulties arise in the application of the compression index method. For example, the assumption of a linear stress-strain relationship in terms of log σ'_v–ε_v leads to uncertainties in the definition of a unique value of C_c. These limitations can be partially overcome by considering a limited stress range within which differences between model prediction and experimental results are not significant.

In the following, the deformation parameters of Finnish clays are investigated, and the validity of the existing empirical correlations is assessed based on the available CRS consolidation test results.

6.2.1 Constrained modulus (M_0)

The soil stress-strain behavior obtained from the experimental CRS consolidation tests is characterized by nearly elastic response in the OC region, which can be approximated by assuming a constant value of the constrained modulus (M_0). For Finnish clays, results suggest that M_0 ranges between 1 and 2.5 MPa. However, several authors have pointed out that in sensitive clays, the effects of sample disturbance appear as a very significant reduction in the constrained modulus (M_0) (Lunne et al. 2006; Karlsrud and Hernandez–Martinez 2013; Amundsen et al. 2016; Di Buò et al. 2019b). This has also been observed from the comparison of different sampling techniques adopted for obtaining undisturbed samples in Finnish clays, indicating that the mini-block samples are characterized by higher M_0 than TUT 132 and ST:1 50 samples (section 4.8). Therefore, it is fundamental to rely on high-quality samples when establishing correlations for evaluating M_0. In the literature, existing correlations between M_0 and cone tip resistance typically have the following form:

$$M_0 = \alpha(q_t - \sigma_{v0}) = \alpha\, q_{net}, \tag{6.1}$$

where α is the constrained modulus cone factor. Exploiting the data from fine-grained soils, Mayne (2007) indicated values of α varying between 1 and 10, where the lowest values apply to soft clays. Di Buò et al. (2018) suggested values varying from 5 to 10 for Finnish clays by exploiting data from the experimental program presented herein. Fig. 6.1 illustrates the relationship between M_0 and q_{net} for the clays investigated in this study, confirming the variability of α between 5 and 10. However, based on the analyzed results, there is no evident influence of natural water content or soil plasticity on the parameter α.

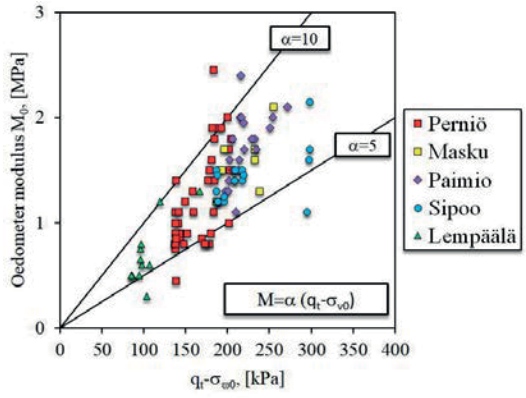

Figure 6.1. Evaluation of the constrained modulus cone factor (α) for Finnish clays.

Furthermore, the relationship between M_0 and v_s is investigated. Based on data from 28 Norwegian clay sites, L'Heureux and Long (2017) suggested the following equation.

$$M_0 = 0.0001\, v_s^{2.212} \tag{6.2}$$

Di Buò et al. (2018) investigated the applicability of equation (6.2) for Finnish clays, observing a significant data scatter. This is mainly attributable to the differences between Finnish and Norwegian clays in terms of PI, S_t, and OCR. Therefore, an analytical equation is theoretically derived based on the correlation linking M_0 and G:

$$M = \frac{2\,(\upsilon-1)}{(2\upsilon-1)} G, \tag{6.3}$$

where υ is Poisson's ratio, which can be assumed equal to 0.1 for small-strain stiffness (G_{max}). Considering a scale factor equal to 10 to account for the modulus degradation with increasing strain and expressing $G_{max} = \rho v_s^2$, where ρ is the soil density, the following equation is obtained.

$$M_0 = \frac{1}{10}\frac{2\,(\upsilon-1)}{(2\upsilon-1)} \rho v_s^2 = 0.225\, \rho v_s^2 \tag{6.4}$$

Assuming ρ = 1500 kg/m^3, equation (6.4) can be expressed as follows:

$$M_0 = 0.000375\, v_s^2, \tag{6.5}$$

where M and v_s are expressed in MPa and m/s, respectively. Fig. 6.2a shows the comparison between the measured versus estimated values of M_0 based on equation (6.6). Despite the significant data scatter (COV = 0.31), the theoretical solution seems to fit the mean trend of the data points (n = 51). However, equation 6.6 tends to overestimate M_0. Therefore, further calibration is performed based on the bias factor (b = 0.87) to obtain the following.

$$M_0 = 0.000326\, v_s^2 \tag{6.6}$$

Equation (6.6) is plotted in Fig. 6.2b. Note that these correlations are similar to those proposed by L'Heureux and Long (2017) for Norwegian clays.

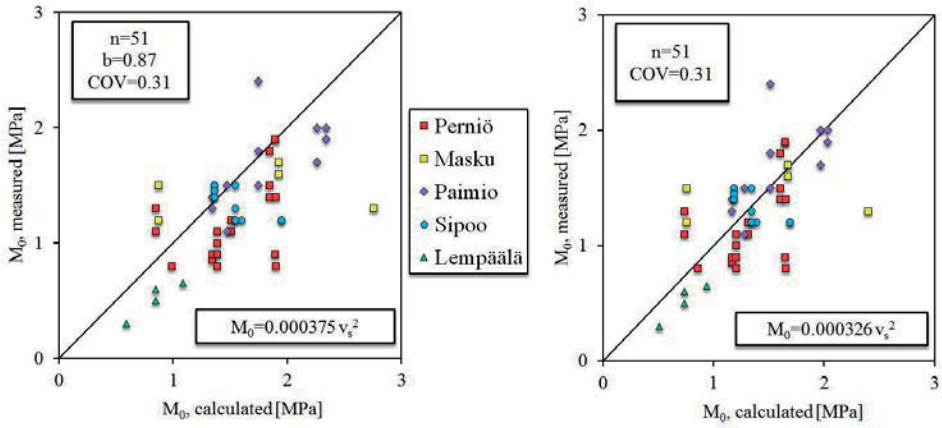

Figure 6.2. Evaluation of the constrained modulus (M_0) based on shear wave velocities (v_s): a) theoretical solution; b) calibrated correlation for Finnish clays.

Figure 6.3 presents the relationship between M_0 and v_s for all sites in the database together with the analyzed equations. It is worth observing that both solutions fit fairly well the experimental data points even though the equation proposed by L'Heureux and Long (2017) appears to slightly underestimate the value of M_0. However, at this stage, the database is limited and additional data points are needed to further improve these equations.

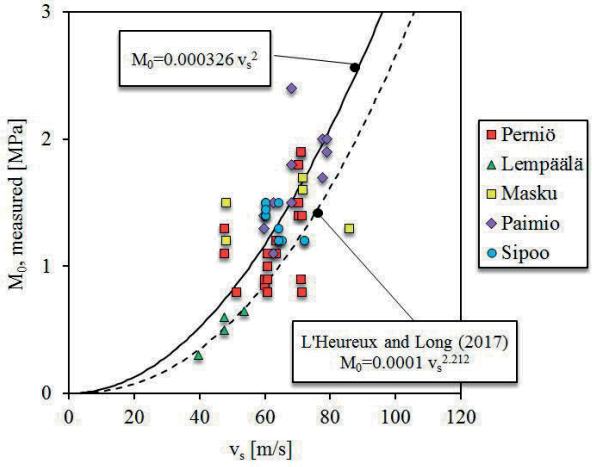

Figure 6.3. Relationship between the constrained modulus (M_0) and shear wave velocities (v_s) for Finnish clays.

Another approach for deriving CPTu-based correlations for evaluating M_0 can be established based on the SCE-CSSM analytical framework discussed in section 5. In particular, the simplified correlations derived for Finnish clays can be used herein for obtaining M_0. Experimental results show that for high-quality samples, σ'_p is generally reached at 4% of the vertical deformation (ε_v). Therefore, assuming linear stress-strain relationship in the OC region, the following equation can be established between M_0 and σ'_p:

$$M_0 = \frac{\sigma'_p}{0.04}. \tag{6.7}$$

Based on equation (6.7), following three CPTu-based equations for deriving M_0 can be obtained from equations (5.41), (5.42), and (5.43).

$$M_0 = 7\,(q_t - \sigma_{v0}) = 7\,q_{net} \tag{6.8}$$

$$M_0 = 9.75\,(u_2 - u_0) = 9.75\,\Delta u_2 \tag{6.9}$$

$$M_0 = 15.5\,(q_t - u_2) = 15.5\,q_{eff} \tag{6.10}$$

Fig. 6.4 shows the comparison between the estimations provided by equations (6.8), (6.9), and (6.10) with the CRS oedometer test results for each investigated site; the measured versus calculated values for all the sites are plotted in Fig. 6.5. Overall, the proposed correlations are characterized by R^2 ranging between 0.44 and 0.65, while COV varies between 0.20 and 0.25. Although only high-quality samples have been considered in the interpretation, the evaluation of M_0 from CRS consolidation tests is characterized by significant variability. However, the proposed CPTu-based correlations provide relatively good prediction and can be adopted to perform preliminary evaluation of M_0.

Table 6.1. Summary of the statistical analysis on the CPTu-based correlations for evaluating M_0.

Eq.	Correlation	Statistical analysis		
		R^2	***b*, (COV)**	**SE**
6.8	$M_0 = 7\,(q_t - \sigma_{v0})$	0.56	1 (0.24)	0.22
6.9	$M_0 = 9.75\,(u_2 - u_0)$	0.65	1 (0.21)	0.20
6.10	$M_0 = 15.5\,(q_t - u_2)$	0.44	1 (0.27)	0.25

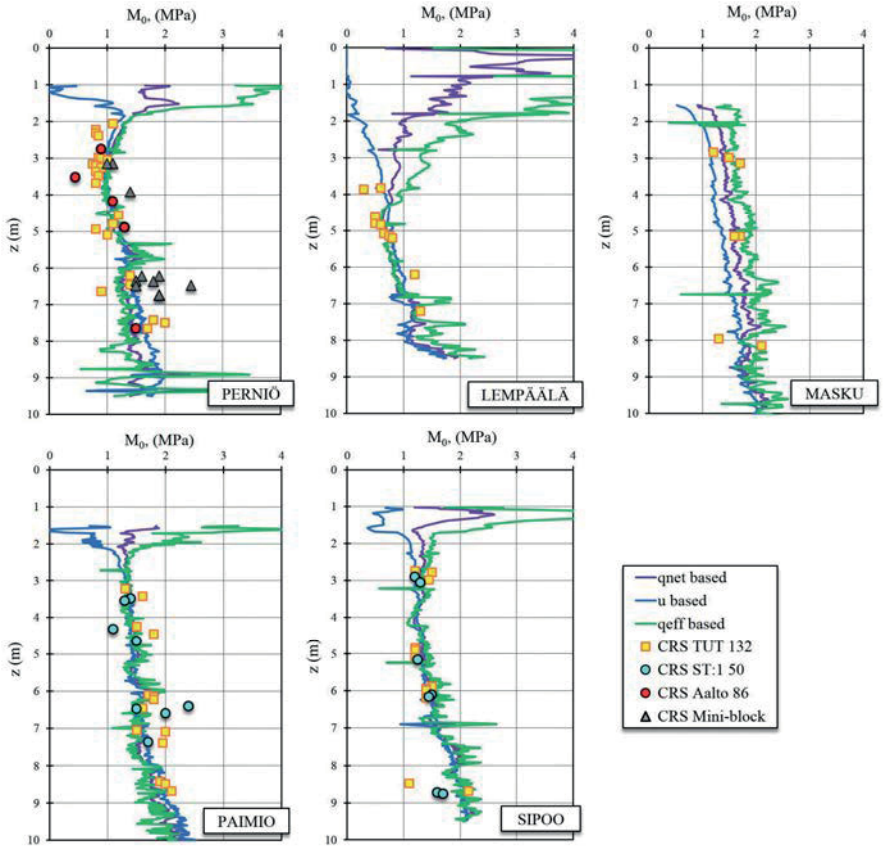

Figure 6.4. CPTu-based correlations for evaluating *M0* in Finnish clays.

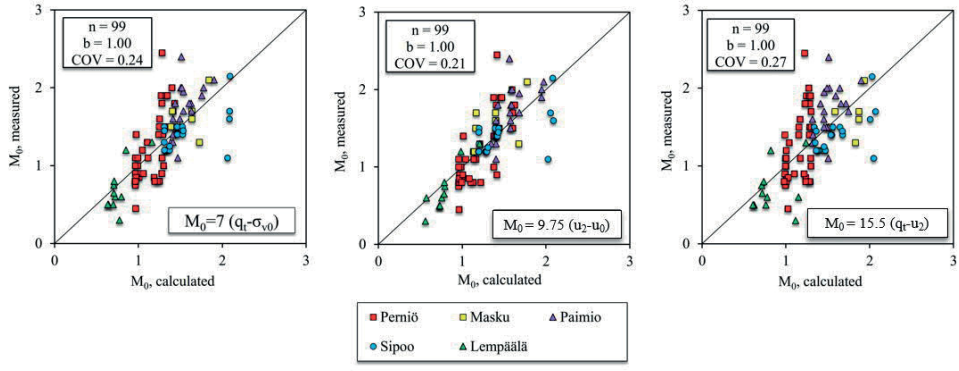

Figure 6.5. Proposed CPTu-based correlations for predicting *M0* in Finnish clays.

6.2.2 Compression indices C_r and C_c

Several studies have pointed out that the compressibility of natural clays is mainly influenced by the sedimentation state induced by the deposition environment (Schmertmann 1955; Burland 1990). Therefore, empirical correlations based on the state variables, such as the natural w and initial void ratio (e_0), are more effective than those based on intrinsic variables (e.g., w_L and PI). Table 6.2 presents a summary of some selected existing correlations based on soil index properties. Among them, the correlations proposed by Helenelund (1951) and Janbu (1985) are largely used in sensitive clays. These correlations suggest that samples characterized by higher w tend to be more compressible. With regard to this, some CRS consolidation test results from Finnish clays have been grouped by water content ranges and shown in Fig. 6.6, confirming these observations.

Table 6.2. Empirical correlations for evaluating the compressibility of natural clays.

Proposed Equation	Reference
$C_c = 0.007(w_L - 10)$	Skempton and Jones (1944)
$C_c = 0.017(w_L - 20)$	Shouka (1964)
$C_c = (w_L - 13)/109$	Mayne (1980)
$C_c = 0.01w$	Koppula (1981)
$C_c = 0.85(w/100)^{1.5}$	Helenelund (1951)
$C_c = 0.01(w - 7.549)$	Herrero (1983)
$m = 700/w$ (±30%)	Janbu (1985)

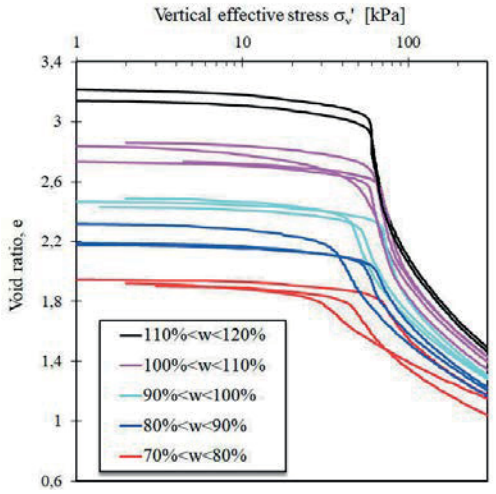

Figure 6.6. CRS consolidation test results grouped by water content ranges.

In this section, the deformation properties of Finnish clays are investigated in terms of the compressibility indices C_r and C_c. In particular, the recompression index (C_r) is evaluated from the CRS consolidation test results considering the stress range defined by the in situ vertical stress (σ'_{v0}) and σ'_p. In contrast, as discussed earlier, the value of C_c depends on the considered stress range. Therefore, three different compression index parameters are defined: $C_{c,1}$, $C_{c,2}$, and $C_{c,3}$ are referred to as σ'_p + 10 kPa, σ'_p + 20 kPa, and σ'_p + 50 kPa, respectively. The graphical method adopted for the determination of these parameters is illustrated in Fig. 6.7. Results indicate that C_c ranges between 2 and 7; in natural clays, C_r assumes values lower than the unit. That said, it is clear that when, as a result of the applied load, the effective vertical stress overcomes the preconsolidation stress, the soil settlement represents an important issue.

Fig. 6.8 shows the outcomes of the regression analysis between C_r and C_c and the water content. C_r varies between 0.10 and 0.55, while C_c ranges between 1 and 7. Two outlier data points from the Lempäälä site (tests B1.3 and B1.4) can be observed from the results. Because these tests are performed on samples taken from the upper layer of the site, they cannot be considered as sensitive clay; therefore, they are not included in the analysis. A clear trend between C_c and w can be noticed while C_r is characterized by high data scatter. Based on these experimental results, the following correlations are derived.

$$C_r = 0.0041\, w^{0.8969} \tag{6.8}$$

$$C_{c,1} = 8 \times 10^{-6}\, w^{2.8236} \tag{6.9}$$

$$C_{c,2} = 2 \times 10^{-5}\, w^{2.598} \tag{6.10}$$

$$C_{c,3} = 1 \times 10^{-8}\, w^{2.1786} \tag{6.11}$$

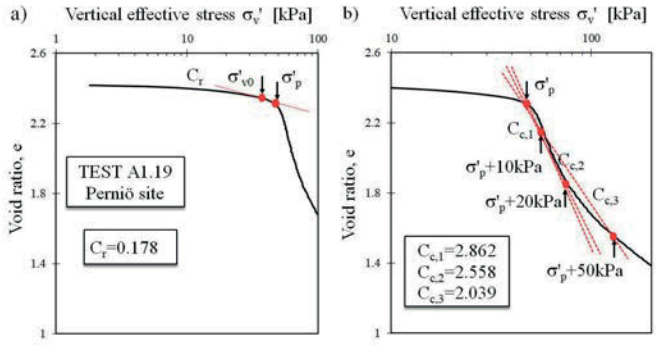

Figure 6.7. CRS consolidation test from Perniö clay: a) graphical method for evaluating C_r; b) graphical method for the evaluation of compression indices $C_{c,1}$, $C_{c,2}$, and $C_{c,3}$.

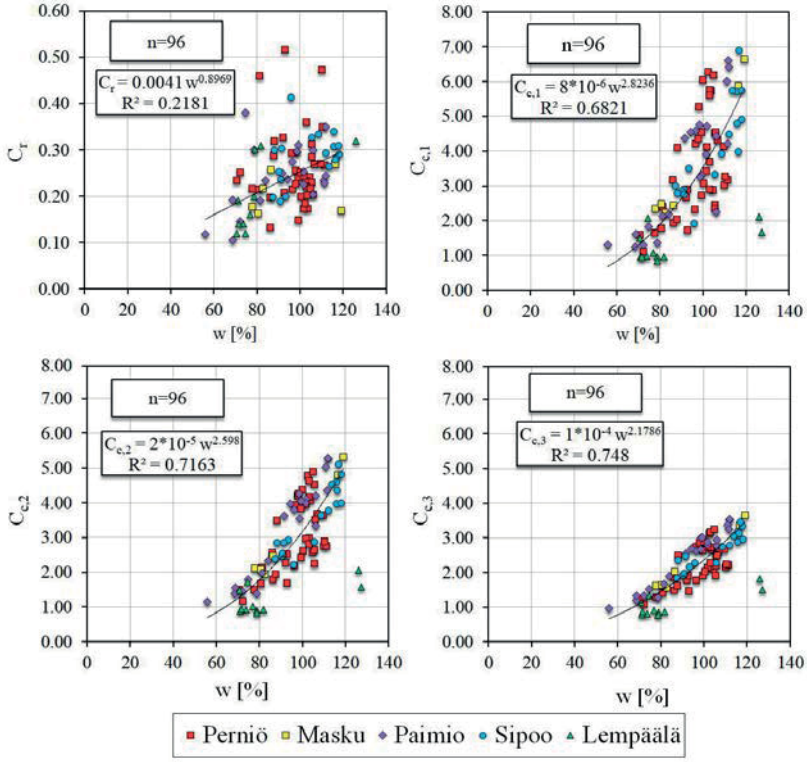

Figure 6.8. Regression analysis between C_c and C_r and w for Finnish clays.

Similarly, the influence of w_L on soil compressibility is investigated (Fig. 6.9). Although a trend can be observed, the significant data scatter does not allow robust correlations to be derived for estimating the compressibility indices based on w_L. The obtained results suggest that the natural water content is the most suitable parameter for evaluating C_c, while significant data scatter is observed for C_r.

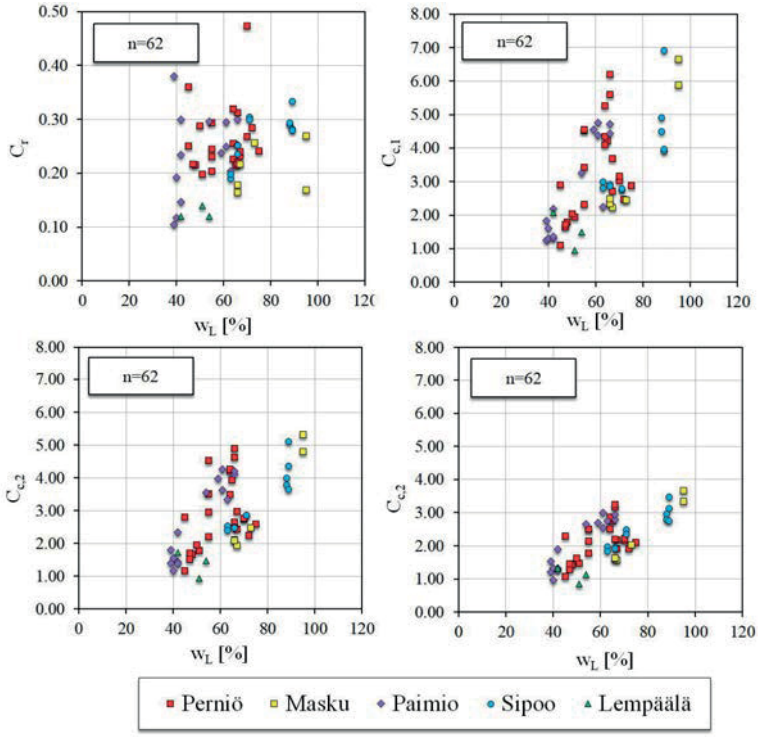

Figure 6.9. Regression analysis between the compression indices (C_c and C_r) and the liquid limit (w_L) for Finnish clays.

6.3 CPTu applicability in deriving the soil deformation characteristics

The CPTu has shown high applicability in evaluating the strength and the in situ stress state of clayey soil, whereas difficulties are encountered in the evaluation of the compressibility parameters beyond the σ'_p. In particular, it has been observed that C_c can be estimated based on the natural water content for a limited stress range. Therefore, the possibility of estimating the water content from the CPTu data would provide a direct link to predict the soil deformation characteristics in the NC range. To this end, the possibility of establishing CPTu-based correlations using soil conductivity is investigated. Several authors have indicated that the soil conductivity measurement can be used to estimate the pore-water salinity; therefore, it has been mainly used for quick clay mapping (Rankka et al. 2004; Donohue et al. 2012;

Sandven et al. 2017). In contrast, the use of the conductivity measurement for estimating geotechnical properties is currently considered unreliable. In particular, Haikola (2018) conducted an extensive study on Finnish clays aimed to derive the soil index properties from electrical conductivity measurements. The study revealed that a reliable correlation can be established between soil conductivity and pore-water salinity (Fig. 6.10), whereas correlations with other geotechnical parameters (e.g., PI, w, w_L, S_t, and s_u) could not be established, thus confirming what has been observed for Scandinavian clays (e.g., Montafia 2013).

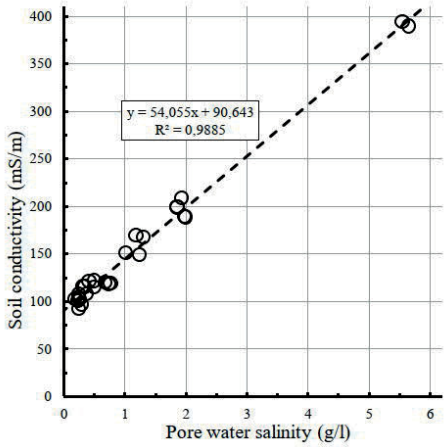

Figure 6.10. Relationship between soil conductivity and pore-water salinity for Finnish clays (Haikola 2018).

The relationship between conductivity and natural water content for the investigated clays is shown in Fig. 6.11. Results indicate that no correlation can be established between the two parameters because the water content increases while the conductivity remains nearly constant. Moreover, Masku clay is characterized by significantly higher conductivity than the other clays, probably owing to the higher pore-water salinity of the Masku clay.

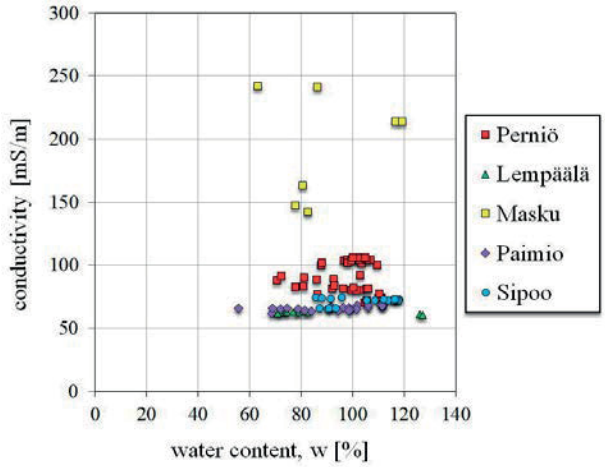

Figure 6.11. Relationship between soil conductivity and water content for Finnish clays.

A further attempt of estimating soil compressibility based on CPTu data is illustrated in Fig. 6.12. Note that a clear trend is observed between Janbu's modulus number (m_1) and cone tip resistance. However, to have a complete description of the stress-strain behavior, the stress exponent (β_1) is needed.

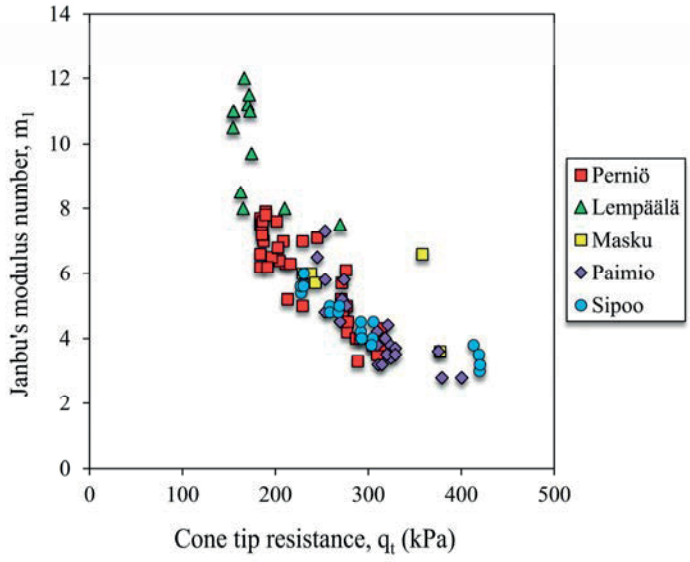

Figure 6.12. Relationship between cone tip restance and Janbu's modulus number m_1.

6.4 Aspects related to primary settlement calculation using Janbu's and Sällfors' methods

The present study highlighted that Janbu's and Sällfors' models provide a fairly good description of the stress-strain behavior observed during 1D consolidation tests; therefore, they are suitable for predicting the soil settlement in soft sensitive clay deposits. A summary of the deformation properties obtained on the basis of the curve-fitting procedure between these models with experimental CRS stress-strain curves is shown in Table 6.3. Overall, the modulus number in the NC region (m_1) varies between 3 and 7, with values up to 12 observed for Lempäälä clay. In contrast, the stress exponent (β_2) ranges between −1 and −1.5, even though few samples from Perniö and Sipoo deposits showed lower values ($\beta < -2$), thus indicating significant destructuration when passing σ'_p. As previously observed, the constrained modulus in the OC region (M_0) assumes values between 0.8 and 2 MPa. However, lower values can be observed for Lempäälä clay, which is probably due to the sample disturbance effect (section 4.8). The curve-fitting procedure performed based on Sällfors' method indicates that the lowest value of the constrained modulus just beyond σ'_p (M_L) ranges between 100 and 200 kPa, which is significantly lower than those observed for Scandinavian clays (e.g., Norwegian clay). This value remains approximately constant for a stress range of 5–15 kPa. Finally, once σ'_L is reached, the modulus increases linearly with an average value of $M' = 12–14$.

Table 6.3. Deformation characteristics of Finnish clays evaluated based on Janbu's and Sällfors' methods.

SITE	z (m)	Janbu's method				Sällfors' method			
		m_1	β_1	m_2	β_2	M_0 (MPa)	M_L (MPa)	$\sigma'_L-\sigma'_P$ (kPa)	M'
Perniö	2–3	5–7	(−0.8)–(−1.2)	8–11	1	0.8–1.1	0.09–0.14	4–7	11.5–12.5
	3–6	6–8	(−0.6)–(−1.2)	7.5–12	1	0.75–1.2	0.1–0.2	6.5–15	13–14
	6–8	3–5	(−1.3)–(2.5)	10–25	1	1–2.5	0.1–0.2	6–15	13–14.5
Lempäälä	3–8	7–12	(−0.4)–(−1)	3–13	1	0.3–1.3	0.1–0.2	6–17	10–16
Masku	3–8	4–6	(−0.9)–(−1.4)	12–21	1	1.2–2.1	0.1–0.2	7–11	12–13
Paimio	3–6	5–7	−1	13–16	1	1.3–1.6	0.2–0.3	5–15	13–17
	6–9	3–6	(−1)–(−1.8)	13–21	1	1.3–2.1	0.1–0.2	6–15	12–14
Sipoo	2–4	5.5	(−1)–(−1.4)	12–15	1	1.2–1.5	0.12–0.14	5–8	12–13
	4–9	3–5	(−1)–(−2)	12–20	1	1.2–2.0	0.10–0.20	6–15	12–13

As previously observed, both methods performed well for all the tested samples. However, difficulties are encountered when fitting the Janbu model in highly structured clays. In such cases, β is set to values lower than −2 to best-fit the significant strain increase beyond σ'_p. Although a good fitting between the model and experimental curve can be achieved, the inaccuracy of the model becomes more evident at a higher strain. In contrast, the Sällfors model overcomes these issues and provides a more accurate description of the stress-strain curve. These aspects have been partially discussed in section 4.7.1 and summarized Fig. 6.13, which shows the fitting provided by both models considering a CRS consolidation test performed on a Perniö clay sample (A3.11).

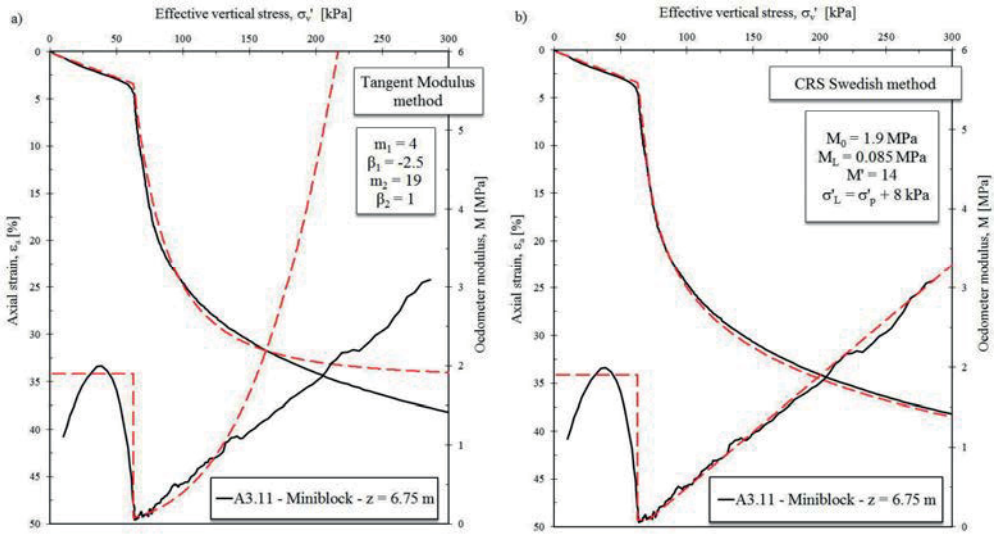

Figure 6.13. Comparison between CRS consolidation test and best-fit stress-strain curves provided by (a) Janbu's method and (b) Sällfors' method.

One relevant aspect to consider when performing settlement calculation in soft sensitive clays is that the deformation parameters have to be corrected based on the preconsolidation stress level. The common mistake in practice is to assume constant deformation parameters to model the entire soft clay layer. Such parameters are generally evaluated from representative CRS consolidation test results, without considering that the in situ applied stress range differs from the test. Therefore, when this set of parameters is related to a different σ'_p than the one obtained from the oedometer test, it provides an unrealistic stress-strain response and therefore a misleading soil settlement prediction. To overcome these issues, a mathematical

modification method when performing settlement analysis using Janbu's method was introduced by Länsivaara (1999; 2000; 2010):

$$m_{calc} = m_{test}\left(\frac{\sigma'_{p,test}}{\sigma'_{p,calc}}\right)^{-\beta}, \quad (6.12)$$

where m_{calc} is the modulus number to be used in settlement calculation, m_{test} is the modulus number evaluated from the oedometer test, $\sigma'_{p,test}$ is the preconsolidation stress obtained from the oedometer test, and $\sigma'_{p,calc}$ is the preconsolidation stress used in the calculation. The proposed modification is clearly more relevant in the case of highly structured clays ($\beta < -2$) while no change is applied when $\beta = 0$.

To explain the main principles of the proposed correction method, an example of settlement calculation analysis is performed at the Perniö site (Fig. 6.14). The settlement induced by a uniform load of 20 kPa is estimated using the soil deformation properties evaluated based on the result of the CRS consolidation test performed on undisturbed sample taken at 6.36-m depth (A3.6; σ'_p = 52 kPa; m_1 = 5.7; $\beta_1 = -2$). The in situ stress is given (σ_{v0} = 92.9 kPa; σ'_{v0} = 40.3 kPa; u_0 = 52.5 kPa). The CRS consolidation test result indicates a value of OCR = 1.30, which is considered constant within the deposit. The stress-strain path corresponding to a 20 kPa stress increase (Fig. 6.14c) induces an increase in the vertical deformation $\Delta\varepsilon_v$ = 9%. Using this set of parameters for the entire soil layer, Janbu's method provides an unrealistic value of the vertical deformation in the upper layer, as shown in Fig. 6.14e. The reasons for this are illustrated in Fig. 6.14d and 6.14f. It can be observed that the stress-strain response for smaller stresses is extrapolated along the path where destructuration occurs, resulting in significantly high compressibility. In contrast, the soil stress-strain behavior should be derived considering the virgin compression curve, as correctly shown in Fig. 6.14f. This error can be avoided by considering that the deformation properties depend on the σ'_p, as suggested by Länsivaara (2000). Finally, Fig. 6.14e shows the value of the vertical deformation estimated using the original and corrected modulus number. As expected, the analysis performed based on m_{calc} provides reasonable estimation of the soil settlement.

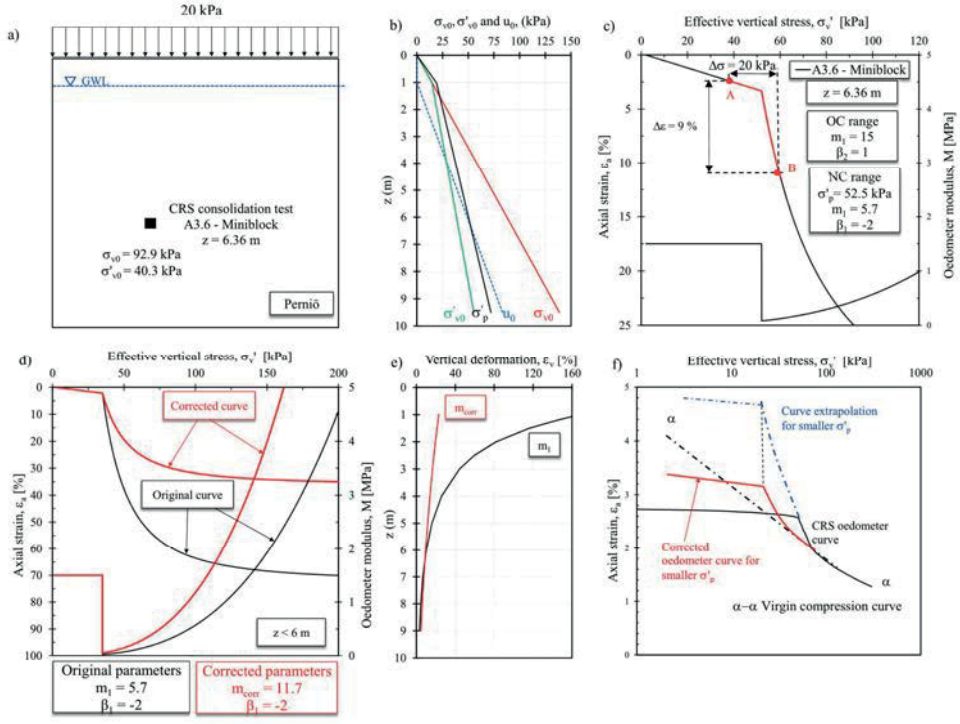

Figure 6.14. Principles of the modulus number correction when applying Janbu's method in settlement calculation: a) schematization of the case study; b) in situ stress of Perniö deposit; c) CRS oedometer test result; d) application of the modulus number correction on the stress-strain curve extrapolated for z = 4 m; e) effect of the modulus number reduction on the calculated vertical deformation; f) principles of the modulus number correction in the *e*-log σ'_v scale.

The same principles should also be applied when performing the settlement calculation based on Sällfors' method. However, because the minimum value of the constrained modulus (M_L) is given, the overall error is somehow limited. A correction parameter (k_1) has been introduced by Länsivaara (2000), defined as follows.

$$k_1 = \frac{\sigma'_{p,test}}{\sigma'_{p,calc}} \tag{6.13}$$

Based on this factor, Sällfors' method's parameters are corrected as follows.

$$M_{0,calc} = \frac{M_{0,test}}{k_1} = M_{0,test} \frac{\sigma'_{p,calc}}{\sigma'_{p,test}} \quad (6.14)$$

$$M_{L,calc} = \frac{M_{L,test}}{k_1} = M_{L,test} \frac{\sigma'_{p,calc}}{\sigma'_{p,test}} \quad (6.15)$$

$$\sigma'_{L,calc} = \frac{\sigma'_{L,test}}{k_1} = \sigma'_{L,test} \frac{\sigma'_{p,calc}}{\sigma'_{p,test}} \quad (6.16)$$

$$M'_{calc} = M'_{test} \quad (6.17)$$

To investigate the settlement prediction accuracy, the same case study illustrated in Fig. 6.14 has been analyzed using Sällfors' method. Considering the CRS consolidation test results from 6.36-m depth (test A3.6), the deformation parameters for the entire soil layer have been derived based on the original and corrected method formulations. The comparison between the stress-strain responses is shown in Fig. 6.15a, whereas the calculated vertical deformation is illustrated in Fig. 6.15b. In this case, the differences between the extrapolated curves are limited, with an overall difference of less than 10% in terms of the vertical deformation.

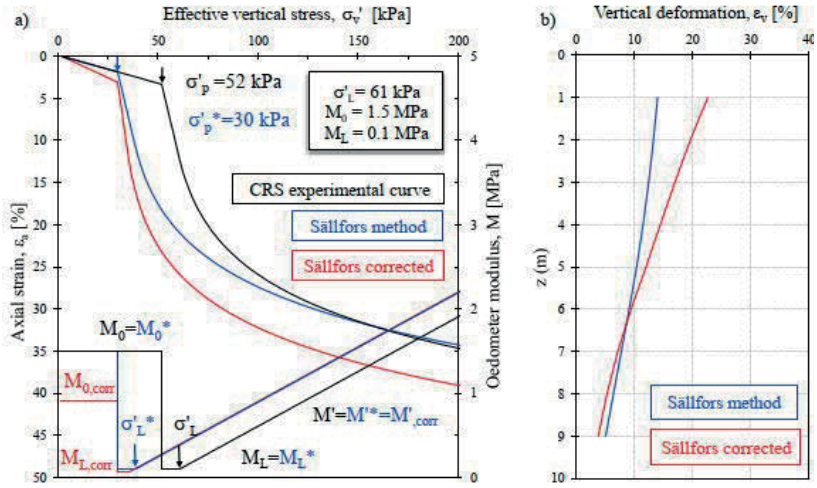

Figure 6.15. Application of Sällfors' method correction: a) stress-strain response comparison; b) estimation of the vertical deformation induced by load application.

Finally, the comparison between both methods is shown in Fig. 6.16; the settlement prediction is summarized in Table 6.4. Results indicate that the difference between the corrected Janbu's and Sällfors' methods is basically negligible as they both

provide similar vertical deformation prediction. The correction procedure must always be applied to Janbu's modulus number, whereas the error related to Sällfors' method is less significant. However, in conventional practice, it is always suggested to correct the deformation parameters when these are extrapolated from a representative CRS oedometer test to avoid inaccurate settlement prediction, as previously shown.

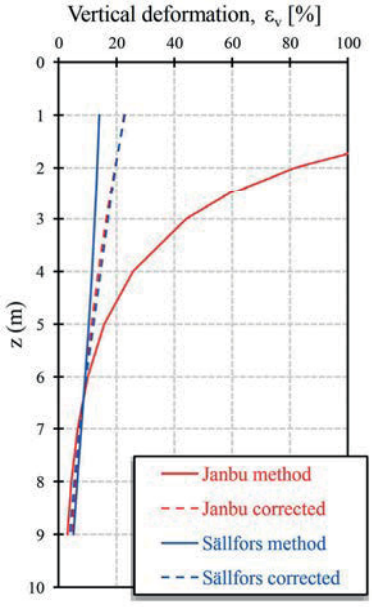

Figure 6.16. Comparison between Janbu's and Sällfors' methods for settlement prediction.

Table 6.4. Total settlement prediction provided by the different calculation methods.

Total settlement prediction (cm)			
Janbu method	**Corrected Janbu method**	**Sällfors method**	**Corrected Sällfors method**
248	98	81	99

7 CONCLUSIONS

7.1 Concluding remarks

The presented study investigated the applicability of piezocone testing in evaluating the preconsolidation stress and the deformation properties of Finnish clays. In order to build an extensive database of high-quality data, five soft sensitive clay test sites were extensively investigated. The experimental program comprised both field and laboratory tests on high-quality undisturbed samples. The collected data has been exploited to establish CPTu-based correlations for evaluating the stress history and deformation properties of Finnish clays. Most of the objectives have been fulfilled even though further studies are needed to clarify few issues which have been raised within the study.

The major findings of the study are presented below.

- The geological origin of Finnish clay sediments is rather complex owing to the different environmental stages related to the Baltic Sea. Different from marine clays located in Norway and in the coastal area of Sweden, the depositional environment of Finnish clays is mostly characterized by fresh to brackish water, depending to the connection with the Atlantic Ocean during its geological history. Therefore, the development of soil sensitivity in such clays is probably not strictly connected to salt leaching as, for example, Norwegian clays but more likely dependent to other post-depositional processes.
- The sample quality is one of the most relevant factors affecting the interpretation of laboratory tests, especially in soft sensitive clays. In order to build a high-quality dataset and establish reliable correlations, particular effort has been paid to the soil sampling. In particular, the study investigated the performances of different sampling techniques in retrieving undisturbed samples from the investigated sites. Results indicated that the mini-block and TUT 132 tube samplers provide overall the highest sample quality, while several issues were encountered when using the traditional piston samplers, especially in low-plastic clays. As an example, the use of rotation to cut-off

the sampled soil from the deposit appeared to be less invasive compared with apparatus lifting suggested by the Finnish guidelines. Moreover, proper maintenance should always be guaranteed when using the piston samplers to avoid additional disturbance. However, it was observed that good quality samples can be achieved using the traditional ST:1 50 piston sampler when the proper sampling procedure is adopted. The use of the TUT 132 tube and mini-block samplers is highly suggested, particularly in low-plastic clays. Finally, the influence of storage time on sample quality was investigated for the TUT 132 tube sampler. Results showed that high sample quality can be maintained up to three years after the sampling.

- A well-established hybrid analytical method based on SCE-CSSM theoretical framework was implemented to predict the σ'_p and OCR profiles from CPTu data. The statistical analysis conducted using R^2, b, COV, and SE indicated a fairly good agreement between the experimental data from CRS consolidation tests and the model prediction for each investigated site. Based on these results, simplified CPTu-based correlations for Finnish clays were derived by assuming average analytical parameters, which are considered representative of the Finnish subsoil condition. In particular, the implementation of the analytical models revealed some inconsistencies in the evaluation of the effective friction angles. These aspects have been analyzed in the thesis.

- Three different settlement calculation methods have been employed in this study to investigate the deformation characteristics. In particular, it was observed that the compression index method is not suitable for describing the stress-strain behavior in the entire NC region. In contrast, both Janbu's and Sällfors' models match relatively well with the CRS consolidation test results. Correlations for evaluating M_0 based on the cone tip resistance and shear wave velocities are presented, whereas difficulties were encountered in deriving CPTu-based correlations for the NC range deformation characteristics. However, empirical correlations between the compression indices with the natural water content were established. An attempt to correlate the soil resistivity measurements with the modulus number has been made, resulting in considerably high data scatter. In contrast, a clear trend between the cone tip resistance (q_t) and Janbu's modulus number (m_1) was observed. Finally, the study investigated several issues related to the Janbu's and Sällfors' models applied to highly sensitive clays.

7.2 Recommendations for future work

The results obtained from this study represent the first step toward an effective introduction of CPTu for field investigation in Finnish geotechnical practice. It has been shown that the piezocone data can be successfully implemented to predict the soil properties. However, it would be beneficial to extend the database by including additional sites that are considered representative of the Finnish subsoil condition and further validating the proposed CPTu-based correlations.

As previously noted, the study showed that the adopted sampling operations clearly affect the achieved sample quality and, therefore, the interpretation of laboratory tests. However, it was not possible to conduct an effective study to assess the performance of the different samplers and procedures for all the sites. Therefore, a more detailed study on this topic would clarify the issues related to the ST:1 50 piston samplers in low-plastic clays, the influence of rotation and lifting on the achieved sample quality, and the storage effect on both piston and mini-block samples.

Although the implementation of the SCE-CSSM model provided reliable prediction of σ'_p for all the investigated sites, the inconsistencies between the operational friction angles (ϕ'_{PEAK}, ϕ'_{MO}) providing the best-fit and the effective friction angles evaluated on the basis of TX compression tests requires additional examination.

Finally, in this study, a proper methodology to predict the deformation characteristics from the CPTu data could not be established. Although the constrained modulus in the OC region can be estimated fairly well based on the net cone tip resistance, difficulties were encountered in the evaluation of the deformation properties in the NC region. Therefore, as future work, the applicability of piezocone testing for estimating the soil compressibility should be investigated in detail, with particular emphasis on Janbu's and Sällfors' deformation parameters.

REFERENCES

Agaiby, S. 2018. Advancements in the interpretation of seismic piezocone tests in clays and other geomaterials. Doctoral dissertation, School of Civil & Environmental Engineering, Georgia Institute of Technology, Atlanta.

Agaiby, S., and Mayne, P.W. 2018. Evaluating undrained rigidity index of clays from piezocone data. *In* Cone Penetration Testing 2018: Proceedings of the 4th International Symposium on Cone Penetration Testing (CPT'18), 21-22 June, 2018, Delft, The Netherlands (p. 65). CRC Press.

Amundsen, H. A., Thakur, V., and Emdal, A. 2016. Sample disturbance in block samples of low plastic soft clays. *In* 17th Nordic Geotechnical Meeting, Island.

Amundsen, H.A., Dang, H., Adamson, M., Emdal, A., and Thakur, V. 2017. A New Laboratory Procedure to Study Stress Relief in Soil Samples. *In* Landslides in Sensitive Clays. pp. 121-131. Springer, Cham.

Andresen, A. and Kolstad, P. 1979. The NGI 54-mm Sampler for Undisturbed Sampling of Clays and Representative Sampling of Coarser Materials. *In* Proc. of the Int. Conf. on Soil Sampling, Singapore, 1-9.

Baligh, M. M., and Levadoux, J. N. 1986. Consolidation after undrained piezocone penetration. II: Interpretation. Journal of geotechnical engineering, **112**(7): 727-745.

Baligh, M.M., Azzouz, A.S., and Chin, C.T. 1987. Disturbances due to "ideal" tube sampling. Journal of geotechnical engineering, **113**(7): 739-757.

Bazin, S., and Pfaffhuber, A.A. 2013. Mapping of quick clay by electrical resistivity tomography under structural constraint. Journal of Applied Geophysics, **98**: 280-287.

Becker, D.E., Crooks, J.H.A., Been, K., and Jefferies, M.G. 1987. Work as a criterion for determining in situ and yield stresses in clays. Canadian Geotechnical Journal, **24**(4): 549-564.

Begemann, H.K.S. 1965. The friction jacket cone as an aid in determining the soil profile. *In* Proceedings of the 6th International Conference on Soil Mechanics and Foundation Engineering, ICSMFE, Montreal, September. pp. 8-15.

Bishop, A. W. 1971. The influence of progressive failure on the choice of the method of stability analysis. Géotechnique, **21**(2): 168-172.

Bjerrum, L. 1954. Geotechnical properties of Norwegian marine clays. Géotechnique, **4**(2): 49-69.

Bjerrum, L. 1973. Problems of soil mechanics and construction on soft clays and structurally unstable soils. *In* Proc. 8th ICSMFE, Vol. 3, pp. 111-159.

Boone, S.J. 2010. A critical reappraisal of "preconsolidation pressure" interpretations using the oedometer test. Canadian Geotechnical Journal, **47**(3): 281-296.

Burland, J.B. 1990. On the compressibility and shear strength of natural clays. Géotechnique, **40**(3): 329-378.

Butterfield, R. 1979. A natural compression law for soils (an advance on e-log p'). Géotechnique, **29**(4).

Campanella, R.G., Gillespie, D.G., and Robertson, P.K. 1982. Pore pressures during cone penetration testing. *In* ESOPT 2nd European Symposium on Penetration Testing, Amsterdam, The Netherlands.

Campanella, R.G., Robertson, P.K., and Gillespie, D. 1986. A seismic cone penetrometer for offshore applications. *In* Oceanology, Springer, Dordrecht, pp. 479-486.

Casagrande, A. 1936. The determination of pre-consolidation load and its practical significance. *In* Proc. Int. Conf. Soil Mech. Found. Eng. Cambridge, Mass., 1936 (Vol. 3, p. 60).

Chandler, R.J. 1988. The in-situ measurement of the undrained shear strength of clays using the field vane. Vane shear strength testing in soils: field and laboratory studies, 13-44.

Chen, B.S., and Mayne, P.W. 1994. Profiling the overconsolidation ratio of clays by piezocone tests. Rep. No. GIT-CEEGEO-94, 1.

Chen, B.S. and Mayne, P.W. 1996. Statistical relationships between piezocone measurements and stress history of clays. Canadian Geotechnical Journal, **33**(3): 488-498.

Ching, J., and Phoon, K. K. 2014. Correlations among some clay parameters—the multivariate distribution. Canadian Geotechnical Journal, **51**(6): 686-704.

D'Ignazio, M. 2016. Undrained shear strength of Finnish clays for stability analyses of embankments. PhD thesis, Department of Civil Engineering, Tampere University of Technology, Tampere, Finland.

D'Ignazio, M., Lunne, T., Andersen, K. H., Yang, S., Di Buò, B., & Länsivaara, T. 2019. Estimation of preconsolidation stress of clays from piezocone by means of high-quality calibration data. AIMS Geosciences, 5(2); 104-116.

Demers, D., and Leroueil, S. 2002. Evaluation of preconsolidation pressure and the overconsolidation ratio from piezocone tests of clay deposits in Quebec. Canadian Geotechnical Journal, **39**(1): 174-192.

Di Buò, B., D'Ignazio, M., Selänpää, J., and Länsivaara, T. 2016. Preliminary results from a study aiming to improve ground investigation data. *In* Proceedings of the 17th Nordic Geotechnical Meeting, Reykjavik (pp. 25-28).

Di Buò, B., Selänpää, J., D'Ignazio, M., and Lansivaara, T. 2018. Evaluation of existing CPTu-based correlations for the deformation properties of Finnish soft clays. *In* Cone Penetration Testing IV, Proceedings of the 4th International Symposium on Cone Penetration Testing (CPT 2018), Delft (pp. 185-191).

Di Buò, B., D'Ignazio, M., Selänpää, J., Haikola, M., Länsivaara, T., and Di Sante, M. 2019a. Investigation and geotechnical characterization of Perniö clay, Finland. AIMS Geosciences, **5**(3): 591-616.

Di Buò, B., Selänpää, J., Länsivaara, T., and D'Ignazio, M. 2019b. Evaluation of sample quality from different sampling methods in Finnish soft sensitive clays. Canadian Geotechnical Journal, **56**(8): 1154-1168.

Di Buò, B., Franza, A., Länsivaara, T., and Mayne, P.W. 2019c. Compressibility of Finnish clays. *In* Proceedings of the XVII European Conference on Soil Mechanics and Geotechnical Engineering (ECSMGE 2019), Reykjavik, Iceland.

Di Buò, B., D'Ignazio, M., Selänpää, J., Länsivaara, T., and Mayne, P.W. 2019d. Yield stress evaluation of Finnish clays based on analytical CPTu models. Canadian Geotechnical Journal. (accepted for publication).

Di Buò, B., Haikola, M., Länsivaara, T., and Pagani, E. 2020. Influence of the piezocone sleeve sensor inaccuracy on the interpretation of geotechnical parameters. *In* Proceedings of the 18th Nordic Geotechnical Meeting (NGM), Helsinki (in submission).

Donohue, S., Long, M., O-Connor, P., Eide Helle, T., Aspmo Pfaffhuber, A., & Rømoen, M. (2012). Multi-method geophysical mapping of quick clay. Near Surface Geophysics, **10**(3): 207-219.

Emdal, A., Gylland, A., Amundsen, H. A., Kåsin, K., and Long, M. 2016. Mini-block sampler. Canadian Geotechnical Journal, **53**(8): 1235-1245.

Eronen, M., Gluckert, G., Hatakka, L., Plassche, O. V. D., Plicht, J. V. D., and Rantala, P. (2001). Rates of Holocene isostatic uplift and relative sea-level lowering of the Baltic in SW Finland based on studies of isolation contacts. Boreas, **30**(1): 17-30.

Gardemeister, R. 1975. On engineering-geological properties of fine-grained sediments in Finland. Dissertation. Technical Research Center of Finland, Building Technology and Community Development, Publication 9. 91 p.

Graham, J., Kwok, C.K., and Ambrosie, R.W. 1987. Stress release, undrained storage, and reconsolidation in simulated underwater clay. Canadian Geotechnical Journal, **24**(2): 279–288.

Haikola, M. 2018. Water content determination of soft Finnish clays using electrical conductivity measurements. M.Sc. Thesis. Department of civil engineering. Tampere University of Technology, Tampere, Finland.

Helenelund, K.V. 1951. Om konsolidering och sättning av belastade marklager. Doctoral dissertation, Tekijä, Finland.

Herrero, O. 1983. Closure to "universal compression index equation". Journal of Geotechnical Engineering, **109**(5): 755–761.

Hight, D. W. 2003. Sampling effects in soft clay: an update on Ladd and Lambe. Soil behavior and soft ground construction, pp. 86-121, ASCE.

Hight, D., and Leroueil, S. 2003. Characterization of soils for engineering purposes. Characterization and Engineering Properties of Natural Soils, Vol.1, Swets and Sitlinger, Lisse, pp. 255-360.

Hvorslev, M.J. 1949. Subsurface exploration and sampling of soils for civil engineering purposes. Waterways Experimental Station, Vicksburg, Miss., USA

ISO/TS 17892-5, 2004. Geotechnical investigation and testing - laboratory testing of soil - part 5: *incremental loading oedometer test*. ISO, Geneva, Switzerland

ISO, E. 22476-1, 2009: Geotechnical investigation and testing. *Field testing. Part*, *1*.

ISO, S. 22476-1: 2012. Geotechnical investigation and testing–Field testing–Part, 1.

ISO. 2012. Geotechnical investigation and testing - field testing - part 1: Electrical cone and piezocone penetration test. ISO 22476-1. 2012.

Jacobsen, H.M. 1992. Bestemmelse af forbelastningstryk i laboratoriet. In *11. Nordiske Geoteknikerm de (NGM-92)* (pp. 455-460). Dansk Geoteknisk Forening.

Jamiolkowski, M., Ladd, C.C., Germaine, J.T. and Lancellotta, R. 1985. New developments in field and laboratory testing of soils. *In* Proc. 11th Int. Conf. on Soil Mech. and Found. Engrg., San Francisco, Vol. 1, pp. 57-153.

Janbu, N. 1967. Settlement calculations based on the tangent modulus concept. Three guest lectures at Moscow State University, Bulletin No. 2, Soil Mechanics. Norwegian Institute of Technology, pp. 1–57.

Janbu, N. 1969. The resistance concept applied to deformations of soils. In Proceedings of the 7th International Conference on Soil Mechanics and Foundation Engineering, Mexico City (Vol. 2529, pp. 191-196).

Janbu, N. 1985. Soil models in offshore engineering. Géotechnique, **35**(3): 241-281.

Janbu, N., and Senneset, K. 1974. Effective stress interpretation of in situ static penetration tests. *In* Proceedings of the 1st European symposium on penetration testing (Vol. 2, pp. 181-93).

Jefferies, M.G., and Davies, M.P. 1993. Use of CPTU to estimate equivalent SPTN 60. Geotechnical Testing Journal, **16**(4): 458-468.

Karlsrud, K. 1991. Sammenstilling av noen erfaringer med prøvetaking og effekt av prøveforstyrrelse i norske marine leire. NGI report, 521500-6.

Karlsrud, K., Lunne, T., and Kort, D.A. 2005 CPTU correlations for clays. *In* Proceedings of the International Conference on Soil Mechanics and Geotechnical Engineering, Balkema Publishers 16: 693.

Karlsrud, K., and Hernandez-Martinez, F.G. 2013. Strength and deformation properties of Norwegian clays from laboratory tests on high-quality block samples. Canadian Geotechnical Journal, **50**(12): 1273-1293.

Karlsson, M., Emdal, A., and Dijkstra, J. 2016. Consequences of sample disturbance when predicting long-term settlements in soft clay. Canadian Geotechnical Journal, **53**(12): 1965-1977.

Keaveny, J. 1985. In-Situ Determination of Drained and Undrained Soil Strength Using the Cone Penetration Test. PhD Dissertation, University of California, Berkeley

Keaveny, J. M., and Mitchell, J. K. 1986. Strength of fine-grained soils using the piezocone. *In* Use of In Situ Tests in Geotechnical Engineering (pp. 668-685). ASCE.

Kirkpatrick, W.M., and Khan, A.J. 1984. The reaction of clays to sampling stress relief. Géotechnique, **34**(1): 29-42.

Kolisoja, P., Sahi, K., and Hartikainen, J. 1987. Automated oedometer device. *In* European conference on soil mechanics and foundation engineering. 9 (pp. 67-70).

Konrad, J. M., and Law, K. T. 1987. Undrained shear strength from piezocone tests. Canadian Geotechnical Journal, **24**(3), 392-405.

Koppula, S.D. 1981. Statistical estimation of compression index. Geotechnical Testing Journal **4**(2): 68-73.

L'Heureux, J. S., and Long, M. 2017. Relationship between shear-wave velocity and geotechnical parameters for Norwegian clays. Journal of Geotechnical and Geoenvironmental Engineering, **143**(6)

La Rochelle, P., Sarrailh, J., Roy, M., and Tavenas, F.A. 1976. Effect of storage and reconsolidation on the properties of champlain clays. *In* Soil specimen preparation for laboratory testing. ASTM International.

La Rochelle, P. L., Sarrailh, J., Tavenas, F., Roy, M., and Leroueil, S. 1981. Causes of sampling disturbance and design of a new sampler for sensitive soils. Canadian Geotechnical Journal, **18**(1):52-66.

Ladd, C.C., and DeGroot, D.J. 2003. Recommended practice for soft ground site characterization: Arthur Casagrande Lecture. *In* 12th panamerican conference on soil mechanics and geotechnical engineering (Vol. 1, pp. 1-57). Essen, Germany: Verlag GmbH.

Larsson, R., and Mulabdic, M. 1991 Shear moduli in Scandinavian clays. Measurement of initial shear modulus with seismic cones. Empirical correlations for the initial shear modulus in clay. Rapport / Statens Geotekniska Institut, 40.

Larsson, R. 2011. Metodbeskrivning för SGI:s 200 mm diameter 'blockprovtagare' - Ostörd provtagning i finkornig jord. Swedish Geotechnical Institute (SGI). Göta River Commission, GAU. Subreport 33. Linköping. [In Swedish].

Lefebvre, G., and Poulin, C. 1979. A new method of sampling in sensitive clay. Canadian Geotechnical Journal, **16**(1): 226-233.

Lehtonen, V. 2015. Modelling undrained shear strength and pore pressure based on an effective stress soil model in limit equilibrium method. PhD thesis, Department of Civil Engineering, Tampere University of Technology, Tampere, Finland.

Lehtonen, V. J., Meehan, C. L., Länsivaara, T., & Mansikkamäki, J. 2015. Full-scale embankment failure test under simulated train loading. Géotechnique, **65**(12): 961-974.

Leroueil, S. 1991. Exploration of soft soil and determination of design parameters. *In* Proc. of Geo-Coast'91, 2, 969-998.

Leroueil, S., and Hight, D.W. 2003. Behaviour and properties of natural soils and soft rocks. Characterisation and engineering properties of natural soils, 1, 29-254.

Levadoux, J.N., and Baligh, M. 1986. Consolidation after undrained piezocone penetration. I: Prediction. Journal of Geotechnical Engineering, **112** (7): 707-726.

Liao, T., and Mayne, P.W. 2006. Automated post-processing of shear wave signals. *In* Proceedings of the 8th US National Conference on Earthquake Engineering, San Francisco (pp. 460-1).

Lunne, T., Christoffersen, H., Tjelta, T. 1985. Engineering use of Piezocone Data in North Sea Clays. *In* proc. ICSMFE-11; San Francisco, 2, 907- 912.

Lunne, T., Berre, T., and Strandvik, S. 1997. Sample disturbance effects in soft low plastic Norwegian clay. *In* Symposium on Recent Developments in Soil and Pavement MechanicsCAPES-Fundacao Coordenacao do Aperfeicoamento de Pessoal de Nivel Superior; CNPq-Conselho Nacional de Desenvolvimento Cientifico a Tecnologico; FAPERJ-Fundacao de Ampora a Pesquisa do Estado do Rio de Janeiro; FINEP-Financiadora de Estudos e Projetos.

Lunne, T., Berre, T., Andersen, K. H., Strandvik, S., and Sjursen, M. 2006. Effects of sample disturbance and consolidation procedures on measured shear strength of soft marine Norwegian clays. Canadian Geotechnical Journal, **43**(7): 726-750.

Länsivaara, T. 1999. A study of the mechanical behavior of soft clay. PhD Dissertation, Norwegian University of Science and Technology, Norway.

Länsivaara, T. 2000. *Painumalaskentamenetelmien käyttökelpoisuuden arviointi*. Technical report. Tielaitos, tiehallinto.

Länsivaara, T. 2010. Failure induced pore pressure by simple procedure in LEM. *In Numerical Methods in Geotechnical Engineering* (pp. 525-530). CRC Press.

Länsivaara, T. 2017. Preconsolidation pressure of natural soil deposits [Video Lecture Moodle]. https://moodle.tuni.fi

Mansikkamäki, J. 2015. Effective stress finite element stability analysis of an old railway embankment on soft clay. PhD thesis, Department of Civil Engineering, Tampere University of Technology, Tampere, Finland.

Mataić, I. 2016. On structure and rate dependence of Perniö clay. PhD thesis, Aalto University, Helsinki.

Mayne, P.W. 1980. Cam-clay predictions of undrained strength. Journal of Geotechnical Engineering, ASCE **106**(11): 1219–1242.
Mayne, P. W. 1986. CPT indexing of in situ OCR in clays. *In* Use of In Situ Tests in Geotechnical Engineering (pp. 780-793). ASCE.

Mayne, P.W. 1988. Determining OCR in clays from laboratory strength. Journal of Geotechnical Engineering, **114**(1): 76-92.

Mayne, P.W. 1991. Determination of OCR in clays by piezocone tests using cavity expansion and critical state concepts. Soils and foundations, **31**(2): 65-76.

Mayne, P.W. 2001. Stress-strain-strength-flow parameters from enhanced in-situ tests. *In* Proc. Int. Conf. on In Situ Measurement of Soil Properties and Case Histories, Bali (pp. 27-47).

Mayne, P.W. 2005. Keynote: Integrated ground behavior: in-situ and lab tests. Deformation Characteristics of Geomaterials, Vol. 2. (Proc. IS-Lyon), Taylor and Francis Group, London: 155-177.

Mayne, P.W. 2007. In-situ test calibrations for evaluating soil parameters. In Characterization & Engineering Properties of Natural Soils, Vol. 3 (Proc. Singapore 2006), Taylor & Francis Group, London, pp. 1602–1652.

Mayne, P.W. 2008. Piezocone profiling of clays for maritime site investigations. *In* Proceedings of the 11th Baltic Sea Geotechnical Conference, Gdansk, Poland (pp. 15-18).

Mayne, P.W., and Bachus, R.C. 1988. Profiling OCR in clays by piezocone soundings. In Proceedings, International Symposium on Penetration Testing. Edited by JD Ruiter. AA Balkema, Rotterdam, The Netherlands (Vol. 2, pp. 857-864).

Mayne, P. W., and Holtz, R.D. 1988. Profiling stress history from piezocone soundings. Soils and Foundations, **28**(1): 16-28.

Mayne, P.W., Coop, M.R., Springman, S., Huang, A.B., and Zornberg, J. 2009. SOA-1: Geomaterial behavior and testing. In Proc. 17th Intl. Conf. Soil Mechanics & Geot. Engrg (Vol. 4, pp. 2777-2872).

Mayne, P.W., Peuchen, J., and Bouwmeester, D. 2010. Soil unit weight estimation from CPTs. *In* 2nd International Symposium on Cone Penetration Testing, Huntington Beach, CA, USA, May 2010.

Mayne, P.W., Cargill, e., Miller, B. 2019. Geotechnical characteristics of sensitive Leda clay at Canada test site in Gloucester, Ontario. AIMS Geosciences, 5(3): 390-411.

Molle, J. 2005. The accuracy of the interpretation of CPT-based soil classification methods in soft soils. M.Sc. Thesis, Section for Engineering Geology, Department of Applied Earth Sciences, Delft University of Technology Report no. 242, Report AES/IG/05-25, December.

Montafia, A. 2013. Influence of physical properties of marine clays on electric resistivity and basic geotechnical parameters. M.Sc. thesis, Institutt for bygg, anlegg og transport, NTNU, Trondheim, Norway.

NGF. 2013. Veiledning for prøvetaking. Communication nr. 11 of the Norwegian Geotechnical Society Available from http://www4.databasehuset.no/ngf/wpcontent/uploads/2015/03/NGF-Melding-11-Provetaking-2014.pdf. [In Norwegian. Title in English: "Guidelines for sampling".]

Onitsuka, K., Hong, Z., Hara, Y., and Yoshitake, S. 1995. Interpretation of oedometer test data for natural clays. Soils and Foundations, **35**(3): 61-70.

Pacheco Silva, F. 1970. A new graphical construction for determination of the preconsolidation stress of a soil sample. *In* Proceedings of the 4th Brazilian Conference on Soil Mechanics and Foundation Engineering, Rio de Janeiro, Brazil (Vol. 2, No. 1, pp. 225-232).

Randolph, M.F., Steenfelt, J.S. and Wroth, C.P. 1979. The effect of pile type on design parameters for driven piles. Proc. Seventh European Conf Soil Mech. Fdn Engng 2, 107-114.

Rankka, K., Andersson-Sköld, Y., Hultén, C., Larsson, R., Leroux, V., and Dahlin, T. 2004. Quick-clay in Sweden: Swedish Geotechnical Institute, Technical report No. 65, p. 137.

Robertson, P.K. 1990. Soil classification using the cone penetration test. Canadian Geotechnical Journal, **27**(1), 151-158.

Robertson, P.K. 1998. Risk-based site investigation. Geotechnical News, **16**(3):45-47.

Robertson, P. K. 2009. Interpretation of cone penetration tests - a unified approach. Canadian geotechnical journal, **46**(11): 1337-1355.

Robertson, P.K. 2013a. CPT QAQC with Worked Examples [Gregg Drilling Webinar]. http://www.greggdrilling.com/webinars/cpt-qaqc-with-worked-examples/

Robertson, P. K. 2013b. CPT Interpretation: fine grained soils [Gregg Drilling Webinar]. http://www.greggdrilling.com/webinars/cpt-interpretation-fine-grained-soils/

Robertson, P. K., Campanella, R. G., Gillespie, D., and Greig, J. 1986. Use of piezometer cone data. *In* Use of in situ tests in geotechnical engineering (pp. 1263-1280). ASCE.

Robertson, P.K., and Campanella, R.G. 1988. Guidelines for geotechnical design using CPT and CPTU. *University of British Columbia, Vancouver, Department of Civil Engineering, Soil Mechanics Series*, *120*.

Robertson, P.K., and Wride, C.E. 1998. Evaluating cyclic liquefaction potential using the cone penetration test. Canadian geotechnical journal, **35**(3): 442-459.

Rosenqvist, I.T. 1953. Considerations on the sensitivity of Norwegian quick-clays. Géotechnique, **3**(5), 195-200.

Rosenqvist, I. T. 1978. Alternative sources for acidification of river water in Norway. Science of the total environment, **10**(1): 39-49.

Sandven, R. 1990. Strength and deformation properties obtained from piezocone tests. Doctoral dissertation, Norwegian University of Science and Technology, Trondheim.

Sandven, R., Senneset, K., and Janbu, N. 1988. Interpretation of piezocone tests in cohesive soils. Proceedings of the International Symposium on Penetration Testing, ISOPT-1, Orlando, 2, 939-953, Balkema Pub., Rotterdam.

Sandven, R., and Watn, A. 1995. Theme lecture: interpretation of test results. Soil classification and parameter evaluation from piezocone tests. Results from Oslo airport. In Proceedings of the International Symposium on Cone Penetration Testing, Vol. 3, Swedish Geotechnical Society Report SGF 3:95, Linköping, pp. 35–55.

Sandven, R., Gylland, A. S., Montafia, A., Pfaffhuber, A. A., Kåsin, K., and Long, M. 2017. Future Strategy for Soil Investigations in Quick Clay Areas. *In* Landslides in Sensitive Clays (pp. 497-507). Springer, Cham.

Sanglerat, G. 1972. The Penetrometers and Soil Exploration. Elsevier, Amsterdam, 488p.

Schmertmann, J.H. 1955. The undistrubed consolidation behaviour of clay. Trans. ASCE 120: 1201-1233.

Schmertmann, J. H. 1978. Guidelines for cone penetration test: performance and design (No. FHWA-TS-78-209). United States. Federal Highway Administration.

Schnaid, F., Sills, G.C., Soares, J.M., and Nyirenda, Z. 1997. Predictions of the coefficient of consolidation from piezocone tests. Canadian Geotechnical Journal, **34**(2): 315-327.

Selänpää, J. 2020. Strength and anisotropy evaluation of Finnish soft sensitive clays. PhD thesis, Tampere University, Tampere, Finland (in submission).

Selänpää, J., Di Buò, B., Länsivaara, T. and D'Ignazio, M. 2017. Problems related to field vane testing in soft soil conditions and improved reliability of measurements using an innovative field vane device. *In* Landslides in Sensitive Clays (pp. 109-119). Springer, Cham.

Selänpää, J., Di Buò, B., Haikola, M., Länsivaara, T., and D'Ignazio, M. 2018. Evaluation of existing CPTu-based correlations for the undrained shear strength of soft Finnish clays. In Cone Penetration Testing IV: Proceedings of the 4th International Symposium on Cone Penetration Testing (CPT 2018), June 21-22, 2018, Delft, The Netherlands.

Senneset, K., and Janbu, N. 1985. Shear strength parameters obtained from static cone penetration tests. *In* Chaney, R. C. and K. R . Demars, eds. Strength testing of marine sediments: laboratory and in-situ measurements. Philadelphia, PA, American Society for Testing and Materials, 41-54. (Special Technical Publication 883.)

Senneset, K., Janbu, N. and Svanø, G. 1982. Strength and deformation parameters from cone penetration tests. *2nd European Conference on Penetration Testing* (ESOPT II) 2: 863-870.

Senneset, K., Sandven, R., and Janbu, N. 1989. Evaluation of soil parameters from piezocone tests. Transportation Research Record, (1235), 24-37.

SFS. 2004. Geotechnical investigation and testing. Sampling methods and groundwater measurements. Part 1. Technical principles for execution. SFS-EN ISO 22475-1:2006E. Finnish Standards

Skempton, A.W., and Jones, O.T. 1944. Notes on the compressibility of clays. Quarterly Journal of the Geological Society, **100**(1-4), 119-135.

Shouka, H. 1964. Relationship of compression index and liquid limit of alluvial clay. *In* Proceedings of the 19th Japan Civil Engineering Conference. Touhoku (pp. 30-31).

Schroeder, K., Andersen, K.H., Tjok K. 2006. Laboratory testing and detailed geotechnical design of the Mad Dog Anchors. Offshore Technology Conference, 17949.

Shouka, H. 1964. Relationship of compression index and liquid limit of alluvial clay. *In* Proceedings of the 19th Japan Civil Engineering Conference. Touhoku (pp. 30-31).

Smits, F.P. 1982. Penetration pore pressure measured with piezometer cones. *In* Proceedings of the Second European Symposium on Penetration Testing (ESOPT II) (Vol. 2, pp. 871-876).

Solberg, I.L., Rønning, J.S., Dalsegg, E., Hansen, L., Rokoengen, K., and Sandven, R. (2008). Resistivity measurements as a tool for outlining quick-clay extent and valley-fill stratigraphy: a feasibility study from Buvika, central Norway. Canadian Geotechnical Journal, **45**(2): 210-225.

Skempton, A.W., and Jones, O.T. 1944. Notes on the compressibility of clays. Quarterly Journal of the Geological Society, **100**(1-4): 119-135.

Sully, J. P., Campanella, R. G., and Robertson, P.K. 1988. Overconsolidation ratio of clays from penetration pore pressures. Journal of Geotechnical Engineering, **114**(2): 209-216.

Sällfors, G. 1975. Preconsolidation pressure of soft, high-plastic clays. Doctoral dissertation, Chalmers University of technology, Sweden.

Tavenas, F., and S. Leroueil. 1987. Laboratory and its stress–strain-time behavior of soft clays: A STATE-OF-THE-ART. *In* Proceedings of the symposium on geotech. Engineering of soft soils, Mexico City.

Tavenas, F., Flon, P., Leroueil, S., and Lebuis, J. 1983. Remolding energy and risk of slide retrogression in sensitive clays. *In* Proceedings of the Symposium on Slopes on Soft Clays, Linköping, Sweden. SGI Report (No. 17, pp. 423-454).

Thakur, V., Degago, S. A., Selänpää, J., and Länsivaara, T. 2017. Determination of remoulding energy of sensitive clays. *In* Landslides in Sensitive Clays (pp. 97-107). Springer, Cham.

Torrance, J. K. 1974. A Laboratory Investigation of the Effect of Leaching on the Compressibility and Shear Strength of Norwegian Maring Clays. Norwegian Geotechnical Institute Publication, (104).

Tumay, M. T., Acar, Y. B., Deseze, E., & Yilmaz, R. 1982. Soil exploration in soft clays with the quasi-static electric cone penetrometer. *In* Proceedings, 2nd European Symposium on Penetration Testing, Amsterdam (Vol. 2, pp. 915-921).

Vesic, A.S. 1972. Expansion of cavities in infinite soil mass. Journal of Soil Mechanics & Foundations Div, 98(sm3).

Vesic, A.S. 1977. Design of pile foundations. NCHRP synthesis of highway practice, (42).

Wroth, C. P. 1984. The interpretation of in situ soil tests. Géotechnique, **34**(4): 449-489.

Wroth P. 1988. Penetration testing – A More Rigorous Approach to Interpretation. Proc. of the International Symposium on Penetration Testing, ISOPT-1, Orlando, 303-311, Balkema Pub., Rotterdam.

Wroth, C.P., and Houlsby, G.T. 1985. Soil mechanics-property characterization and analysis procedures. In Proc. 11th Int. Conf. Soil Mech. Found. Eng., San Francisco, Vol. 1, pp 1-50.

Zhang, G., Robertson, P. K., and Brachman, R. W. 2002. Estimating liquefaction-induced ground settlements from CPT for level ground. Canadian Geotechnical Journal, **39**(5): 1168-1180.

APPENDIX 1: CRS consolidation test results, Perniö

Site	Test code	Depth (m)	Sampler	Storage (days)	Unit weight (γ)	w (%)	e_0	σ'_p (kPa)	OCR	$\Delta e/e_0$	Janbu parameters		Sällfors parameters			
											m_1	β_1	M_0 (MPa)	M_L (MPa)	M'	$\sigma'_L - \sigma'_p$ (kPa)
PERNIO	A1.1	2.05	TUT 132	204	14.2	104.6	2.87	52	2.65	0.02	5.2	-1.1	1.1	0.14	11.5	7
	A1.2	2.22	TUT 132	182	14.2	105.5	2.91	41	2.00	0.03	6.3	-0.8	0.8	0.11	11.5	4
	A1.3	2.31	TUT 132	1	13.8	110	2.76	41	1.97	0.03	7	-1.2	0.8	0.10	12	5
	A1.4	2.38	TUT 132	182	14	111.3	3.04	42	1.98	0.03	6.4	-1.1	0.85	0.11	12	7
	A1.5	2.98	TUT 132	47	14.4	103.1	2.95	37	1.53	0.03	7	-1.2	0.85	0.09	13	7
	A1.6	2.99	TUT 132	198	14.5	99.4	2.79	38	1.57	0.03	7.2	-1.1	0.9	0.10	12.5	6.5
	A1.7	3.04	TUT 132	154	14.3	101.6	2.73	40	1.64	0.03	7.2	-1.2	1	0.11	13	10
	A1.8	3.15	TUT 132	10	14.5	96.3	2.78	36	1.44	0.04	7.7	-1	0.75	0.15	13.5	15
	A1.9	3.20	TUT 132	160	14.3	92.2	2.34	36	1.43	0.04	7.5	-1	0.8	0.10	13.5	7
	A1.10	3.25	TUT 132	16	14.6	100.4	2.92	38	1.50	0.03	7.5	-1.2	0.9	0.10	13	8
	A1.11	3.36	TUT 132	8	15.1	80.8	2.2	36	1.39	0.05	7.6	-0.8	0.8	0.15	14	12
	A1.12	3.48	TUT 132	220	15.3	77.7	2.11	37	1.40	0.04	7.9	-0.8	0.85	0.14	13.5	8
	A1.13	3.68	TUT 132	182	14.9	86.3	2.37	37	1.35	0.04	7.6	-0.8	0.8	0.13	13	6.5
	A1.14	4.55	TUT 132	149	15	92.7	2.66	45	1.42	0.03	6.3	-1.1	1.2	0.13	13.5	9
	A1.15	4.80	TUT 132	16	15.8	70.7	2	47	1.43	0.04	7	-0.9	1.1	0.20	14	11
	A1.16	4.94	TUT 132	230	15.4	72.3	1.94	50	1.49	0.06	7.1	-0.6	0.8	0.28	13	12
	A1.17	5.10	TUT 132	7	14.9	87.7	2.42	49	1.43	0.04	6.1	-0.9	1	0.20	13	14
	A1.18	6.20	TUT 132	49	14.1	109.6	2.99	50	1.26	0.04	5	-1.3	1.4	0.14	13	15
	A1.19	6.46	TUT 132	7	14.3	106.8	3.02	49	1.20	0.04	5.2	-1.3	1.4	0.09	12.7	6
	A1.20	6.64	TUT 132	4	14.2	105.6	2.87	56	1.34	0.06	5	-1.3	0.9	0.18	13	16
	A1.21	7.42	TUT 132	211	14.6	96.5	2.7	62	1.37	0.03	4	-1.9	1.8	0.11	14	9
	A1.22	7.50	TUT 132	175	15.1	97.9	2.46	65	1.42	0.03	3.5	-1.8	2	0.13	14.5	12
	A1.23	7.66	TUT 132	7	14.5	98.1	2.46	64	1.37	0.04	3.8	-2	1.7	0.10	13.5	6.5
	A2.1	3.04	ST:1 50	20	14.3	102.5	2.83									
	A2.2	3.04	ST:1 50	10	14.3	100.7	2.73									
	A2.3	4.90	ST:1 50	10	14.9	84.6	2.28				DISTURBED SAMPLES					
	A2.4	6.32	ST:1 50	18	14.1	111.2	3.07									
	A2.5	6.50	ST:1 50	10	14.1	103.5	2.71	56	1.37	0.07	4.6	-1	0.85	0.18	13	16

A2.6	7.34	ST:1 50	21	14.2	101.4	2.71									
A2.7	7.48	ST:1 50	51	14.6	91.1	2.46	DISTURBED SAMPLES								
A3.1	3.15	Mini-block	92	14.5	105.6	3.05	38	1.53	0.03	6.6	-1.2	1.1	0.07	13	6
A3.2	3.15	Mini-block	92	14.5	106	3.2	40	1.61	0.03	6.2	-1.1	1	0.08	13	6
A3.3	3.92	Mini-block	3	15	86.1	2.44	42	1.47	0.03	6.5	-1.1	1.4	0.09	14	6
A3.4	6.22	Mini-block	244	14.7	103.6	2.95	55	1.39	0.03	4.8	-1.7	1.9	0.10	13	7
A3.5	6.23	Mini-block	244	14.7	103.2	2.91	55	1.39	0.03	5	-2	1.6	0.10	13	7
A3.6	6.36	Mini-block	250	14.9	101.7	3.25	52	1.29	0.04	5.7	-2	1.5	0.10	13	9
A3.7	6.37	Mini-block	250	14.6	102.5	3.05	57	1.41	0.03	4.2	-1.8	1.8	0.10	13	9
A3.8	6.48	Mini-block	3	14.5	99.4	2.83	59	1.44	0.02	4.5	-1.8	2.45	0.10	13.5	7
A3.9	6.49	Mini-block	3	14.5	100.1	2.81	62	1.51	0.04	4	-1.7	1.5	0.10	13	6
A3.10	6.74	Mini-block	3	14.3	103	2.87	68	1.61	0.03	3.3	-2.2	1.9	0.10	13	6.5
A3.11	6.75	Mini-block	7	14.5	104.9	3.08	63	1.49	0.03	4	-2.5	1.9	0.08	14	8
A4.1	2.75	Aalto 86		13.9	110.3	2.87	40	1.79	0.03	6.2	-1	0.9	0.1	12	7
A4.2	3.52	Aalto 86		14.6	92.9	2.53	35	1.35	0.08	7.8	-0.7	0.45	0.15	13	9
A4.3	4.18	Aalto 86		15.1	81.3	2.22	43	1.49	0.04	6.8	-1.1	1.1	0.12	13	6
A4.4	4.90	Aalto 86		14.2	103	2.74	52	1.62	0.03	5	-1	1.3	0.12	12	8
A4.5	7.66	Aalto 86		14.6	88.1	2.3	61	1.37	0.04	4.3	-2	1.5	0.11	14	8

APPENDIX 2: CRS consolidation test results, Lempäälä

Site	Test code	Depth (m)	Sampler	Storage (days)	Unit weight (γ)	w (%)	e_0	σ'_p (kPa)	OCR	$\Delta e/e_0$	Janbu parameters		Sällfors parameters			
											m_1	β_1	M_0 (MPa)	M_L (MPa)	M'	$\sigma'_L - \sigma'_p$ (kPa)
LEMPÄÄLÄ	B1.1	3.64	TUT 132	220	13	121.2	2.63				DISTURBED SAMPLES					
	B1.2	3.65	TUT 132	210	13.6	120.9	3.17									
	B1.3	3.82	TUT 132	26	13.4	126.1	3.22	26	1.36	0.06	8	-0.5	0.6	0..12	10	6
	B1.4	3.86	TUT 132	1	13	127.2	2.86	25	1.30	0.13	8.5	-0.4	0.3	0.18	11	12
	B1.5	4.60	TUT 132	228	15.1	78.9	2.1	27	1.17	0.11	11	-0.5	0.5	0.2	15	10
	B1.6	4.61	TUT 132	235	15.2	81.9	2.3	27	1.17	0.12	11	-0.6	0.5	0.2	16	12
	B1.7	4.62	TUT 132	235	15.1	82.9	2.3	28	1.22	0.14	10.5	-0.5	0.5	0.2	16	14
	B1.9	4.80	TUT 132	230	15.4	78.8	2.26	30	1.24	0.11	12	-0.6	0.5	0.21	17	7
	B1.10	4.84	TUT 132	41	15.3	77	2.11	28	1.14	0.10	11.2	-0.6	0.6	0.18	16	9
	B1.11	5.08	TUT 132	41	15.6	73.8	2.07	31	1.20	0.08	11.5	-0.6	0.65	0.2	16.5	7
	B1.12	5.14	TUT 132	29	15.6	71.2	1.96	32	1.22	0.07	11	-0.6	0.75	0.2	16	6
	B1.13	5.20	TUT 132	19	15.5	71.7	1.93	33	1.24	0.07	9.7	-0.5	0.8	0.26	16.5	17
	B1.14	6.21	TUT 132	2	15.5	74.6	2.08	43	1.34	0.04	8	-1.1	1.2	0.15	15	8
	B1.15	7.21	TUT 132	6	15.6	70.8	1.95	51	1.35	0.04	7.5	-1	1.3	0.2	16	7
	B2.1	3.74	ST:1 50	86	13.7	116	3.04				DISTURBED SAMPLES					
	B2.2	3.75	ST:1 50	79	13.9	112.7	3		1.00	0.06	8.2	-0.4	0.4	0.2	12	19
	B2.3	5.14	ST:1 50	79	15.6	69.3	1.87				DISTURBED SAMPLES					
	B2.4	5.15	ST:1 50	86	15.5	71.8	1.94									
	B2.5	5.30	ST:1 50	84	15.5	74.1	2.07	32	1.01	0.06	11	-0.6	0.65	0.25	16	12.5
	B2.6	6.14	ST:1 50	2	15.4	74.7	2.02				DISTURBED SAMPLES					

APPENDIX 3: CRS consolidation test results, Masku

Site	Test code	Depth (m)	Sampler	Storage (days)	Unit weight (γ)	w (%)	e_0	σ'_p (kPa)	OCR	$\Delta e/e_0$	Janbu parameters		Sällfors parameters			
											m_1	β_1	M_0 (MPa)	M_L (MPa)	M'	$\sigma'_L - \sigma'_p$ (kPa)
MASKU	C1.1	2.84	TUT 132	224	15.1	82.7	2.22	49	2.45	0.03	6	-0.9	1.2	0.18	13	11
	C1.2	2.99	TUT 132	226	15.3	77.8	2.15	53	2.55	0.03	6	-1.3	1.5	0.15	13.5	7
	C1.3	3.15	TUT 132	6	15.2	80.7	2.22	53	2.50	0.02	5.7	-1	1.7	0.18	13	10
	C1.4	5.15	TUT 132	1	14	116.5	3.26	59	1.96	0.02	3.8	-1.6	1.7	0.1	12	8
	C1.5	5.15	TUT 132	1	13.8	119.1	3.23	58	1.92	0.03	3.8	-1.6	1.6	0.09	12.5	8
	C1.6	7.96	TUT 132	226	15.9	63.2	1.69	62	1.43	0.07	6.6	-0.6	1.3	0.3	13	8
	C1.7	8.15	TUT 132	3	14.9	86.4	2.39	76	1.72	0.03	3.6	-1.4	2.1	0.22	12.5	11

APPENDIX 4: CRS consolidation test results, Paimio

Site	Test code	Depth (m)	Sampler	Storage (days)	Unit weight (γ)	w (%)	e_0	σ'_p (kPa)	OCR	$\Delta e/e_0$	Janbu parameters		Sällfors parameters			
											m_1	β_1	M_0 (MPa)	M_L (MPa)	M'	$\sigma'_L - \sigma'_p$ (kPa)
PAIMIO	D1.1	3.22	TUT 132	214	16.2	68.7	2.06	55	2.12	0.03	6.5	-1	1.3	0.27	15	16
	D1.2	3.42	TUT 132	28	16.4	55.9	1.51	55	2.04	0.02	7.3	-1	1.6	0.21	17	6
	D1.3	4.24	TUT 132	223	15.1	84	2.37	63	2.03	0.03	4.5	-1.2	1.5	0.2	13	13
	D1.4	4.45	TUT 132	28	15.5	72.2	1.96	67	2.09	0.03	5.2	-0.8	1.8	0.24	14	9
	D1.5	6.10	TUT 132	720	14.2	112.1	3.23	63	1.56	0.03	3.4	-2	1.7	0.1	13	10
	D1.6	6.15	TUT 132	509	14.2	111	3.22	60	1.48	0.03	3.8	-1.8	1.8	0.11	13.5	12
	D1.7	6.22	TUT 132	224	14.2	111.9	3.23	61	1.49	0.03	4.4	-2.5	1.8	0.1	14	11
	D1.8	6.45	TUT 132	30	14.4	101.8	2.95	59	1.40	0.03	4.2	-1.8	1.6	0.1	13.5	8
	D1.9	7.06	TUT 132	515	14.8	96.4	2.88	61	1.35	0.04	4	-1.5	1.5	0.135	14	12
	D1.10	7.10	TUT 132	264	14.6	101.6	3	67	1.48	0.03	3.5	-1.8	2	0.135	13	11
	D1.11	7.40	TUT 132	30	14.6	94.3	2.61	66	1.41	0.03	3.7	-1.6	1.95	0.1	14.5	6.7
	D1.12	8.42	TUT 132	720	14.9	91.7	3.65	70	1.35	0.03	3.6	-1.4	1.9	0.12	13	6
	D1.13	8.48	TUT 132	214	14.6	98.5	2.81	77	1.48	0.03	2.8	-1.5	2	0.13	14	10
	D1.14	8.68	TUT 132	30	14.3	99.3	2.68	76	1.43	0.03	2.8	-1.7	2.1	0.1	14	7.1
	D2.1	3.48	ST1:50	273	15.8	74.7	2.22	67	2.46	0.03	4.8	-1	1.4	0.23	13	11
	D2.2	3.54	ST1:50	24	15.6	68.8	1.84	58	2.11	0.03	5.8	-1.1	1.3	0.18	13.2	5
	D2.3	4.32	ST1:50	90	15.2	78.8	2.17	60	1.91	0.04	5.8	-0.8	1.1	0.28	13	14
	D2.4	4.64	ST1:50	24	15	81.4	2.19	62	1.88	0.03	5	-1	1.5	0.18	12	5
	D2.5	6.40	ST1:50	267	14.4	106.2	3.14	72	1.72	0.02	3.2	-1.3	2.4	0.18	12	15
	D2.6	6.48	ST1:50	33	14.2	106.2	2.83	61	1.45	0.04	3.8	-1.5	1.5	0.1	13	7
	D2.7	6.60	ST1:50	186	14.6	111.5	3.68	68	1.59	0.03	3.2	-1.8	2	0.1	12	6
	D2.8	7.38	ST1:50	35	14.6	98.7	2.74	67	1.43	0.04	3.5	-1.7	1.7	0.14	14	12

APPENDIX 5: CRS consolidation test results, Sipoo.

Site	Test code	Depth (m)	Sampler	Storage (days)	Unit weight (γ)	w (%)	e_0	σ'_p (kPa)	OCR	$\Delta e/e_0$	Janbu parameters		Sällfors parameters			
											m_1	β_1	M_0 (MPa)	M_L (MPa)	M'	$\sigma'_L - \sigma'_p$ (kPa)
SIPOO	E1.1	2.74	TUT 132	720	14.8	91.1	2.57	51	2.26	0.03	5.4	-1	1.2	0.12	12	5
	E1.2	2.78	TUT 132	240	14.6	90.3	2.41	52	2.29	0.02	5.6	-1.2	1.5	0.14	13	8
	E1.3	2.98	TUT 132	40	14.7	90.8	2.47	52	2.21	0.02	5.6	-1.3	1.45	0.13	12	6
	E1.4	4.84	TUT 132	720	14.5	105.6	3.11	51	1.66	0.03	5	-1	1.2	0.12	11	6
	E1.5	4.9	TUT 132	240	14	115.7	3.25	53	1.71	0.03	4.8	-1.5	1.2	0.12	12	10
	E1.6	5.1	TUT 132	42	13.9	118.1	3.29	52	1.64	0.03	4.8	-1.5	1.2	0.1	11.5	7
	E1.7	5.88	TUT 132	715	14.2	115.7	3.46	55	1.59	0.03	4.2	-1.5	1.5	0.09	12	7
	E1.8	5.94	TUT 132	515	14.2	113.7	3.33	52	1.49	0.03	4.5	-1.5	1.4	0.085	13.5	8
	E1.9	5.98	TUT 132	228	14	117.9	3.35	57	1.63	0.03	4	-1.6	1.4	0.11	12	11
	E1.10	6.18	TUT 132	48	13.9	116.8	3.19	58	1.62	0.03	4	-1.7	1.4	0.09	12	7
	E1.11	8.48	TUT 132	222	14.5	95.8	2.63	68	1.52	0.06	3.8	-1.2	1.1	0.2	12	15
	E1.12	8.68	TUT 132	80	14.9	85.9	2.34	78	1.71	0.03	3	-2	2.15	0.17	13	9
	E2.1	2.9	ST1:50	62	14.7	87.3	2.31	46	1.98	0.03	6	-1	1.2	0.11	12.5	5
	E2.2	3.06	ST1:50	30	14.4	93.4	2.45	48	2.00	0.02	6	-1.4	1.3	0.12	12	8
	E2.3	5.16	ST1:50	30	14	112.1	3.1	50	1.56	0.03	5	-1.4	1.25	0.1	12	7
	E2.4	6.1	ST1:50	255	14.6	108.7	3.43	62	1.75	0.03	3.8	-1.2	1.5	0.16	11	12
	E2.5	6.16	ST1:50	34	13.9	116.3	3.2	52	1.45	0.03	4.5	-1.3	1.45	0.09	12.5	7.5
	E2.6	8.72	ST1:50	60	14.8	91.4	2.57	73	1.59	0.04	3.5	-1.5	1.6	0.16	12.5	8
	E2.7	8.76	ST1:50	35	14.8	88.1	2.41	76	1.65	0.04	3.2	-1.5	1.7	0.15	12	6

APPENDIX 6: Statistical analysis results from the implementation of the SCE-CSSM models on Finnish clays

1. PERNIÖ

1a) Original SCE-CSSM solution

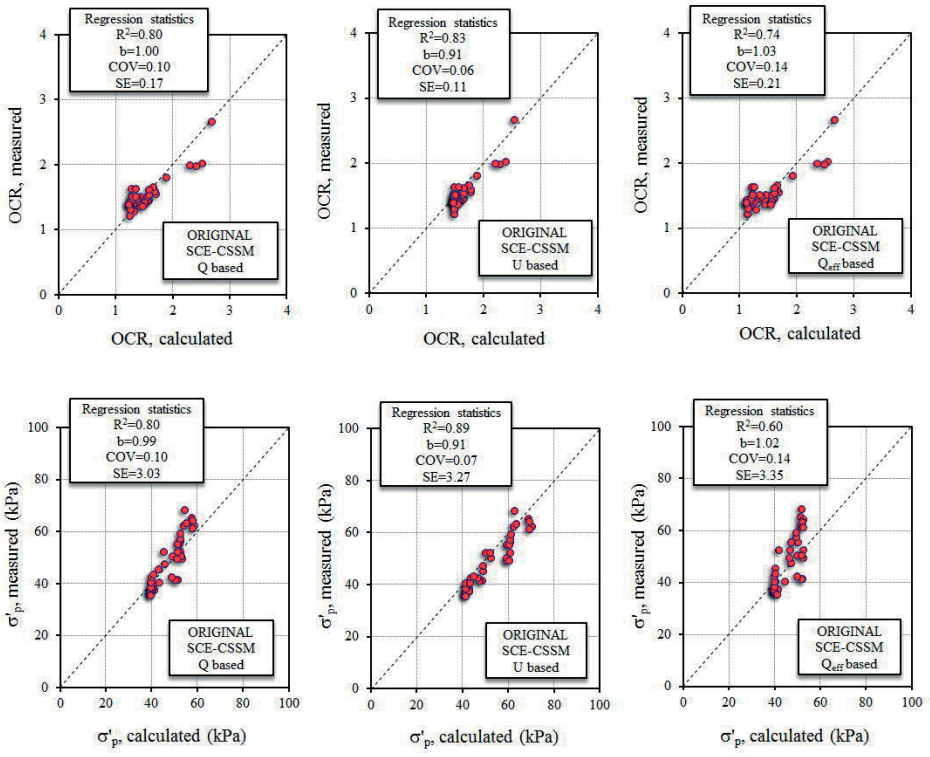

1b) Modified SCE-CSSM solution

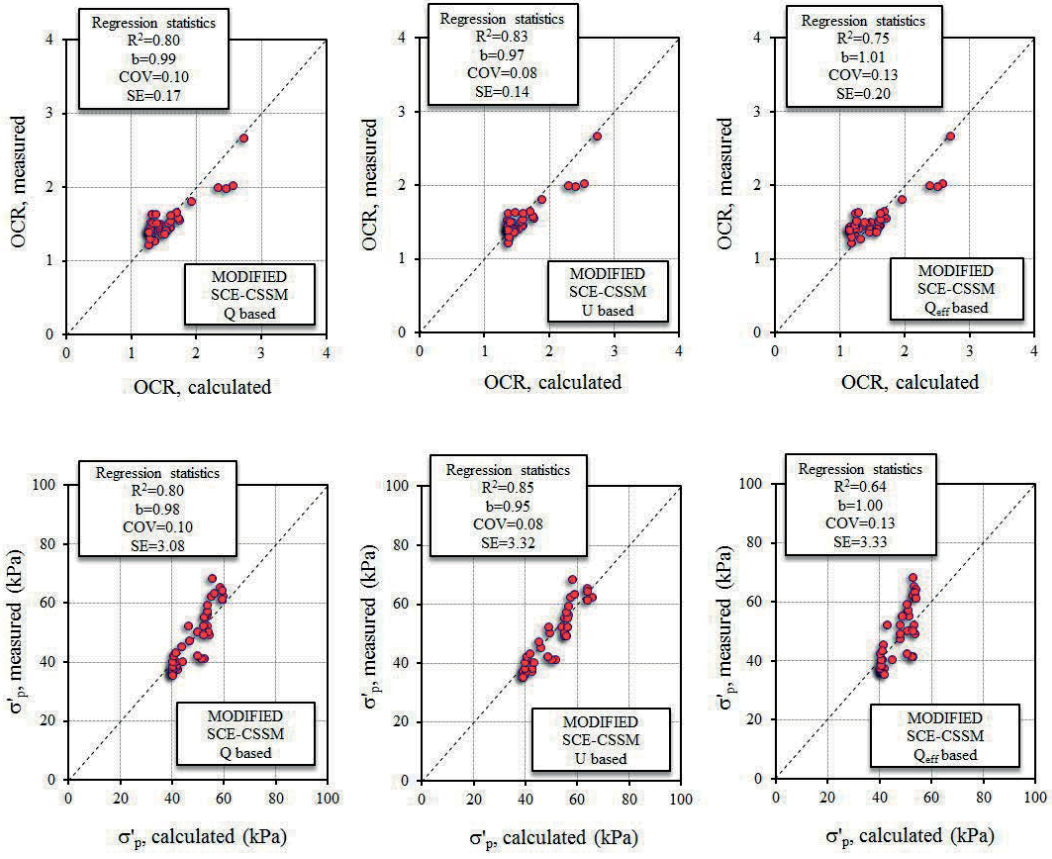

2. LEMPÄÄLÄ

2a) Original SCE-CSSM solution

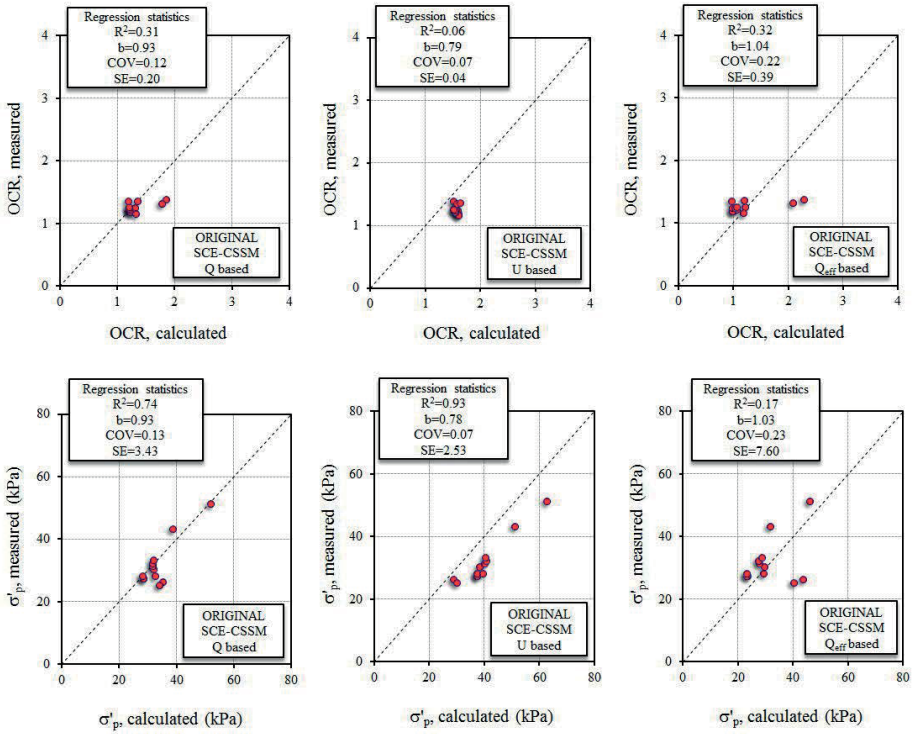

2b) Modified SCE-CSSM solution

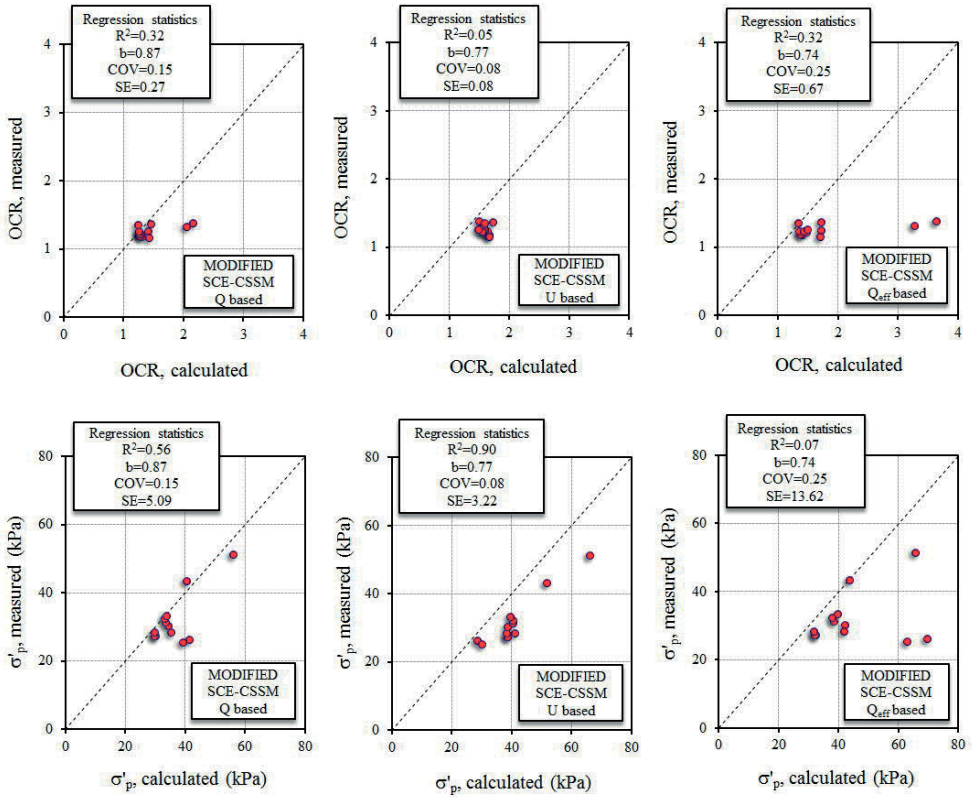

3. MASKU

3a) Original SCE-CSSM solution

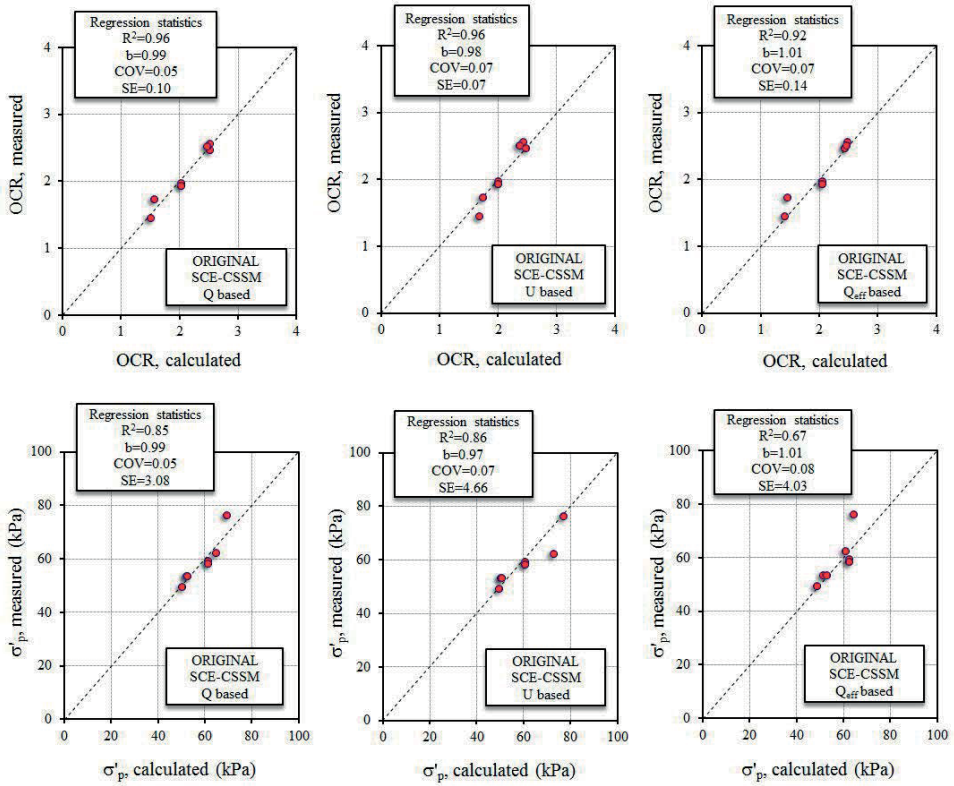

4. PAIMIO

4a) Original SCE-CSSM solution

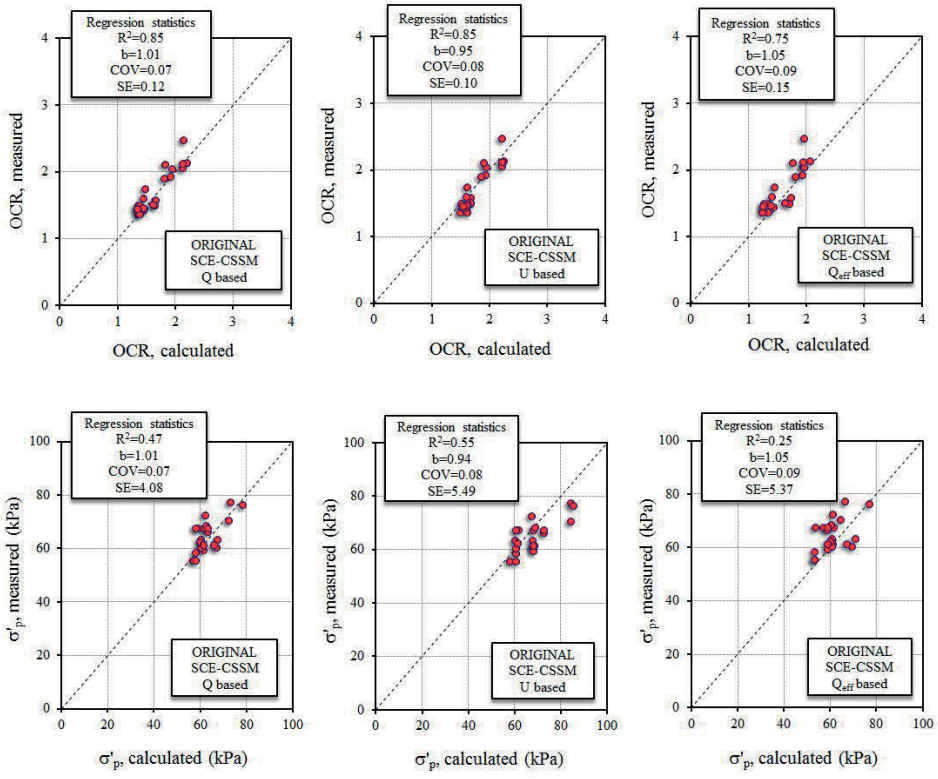

4b) Modified SCE-CSSM solution

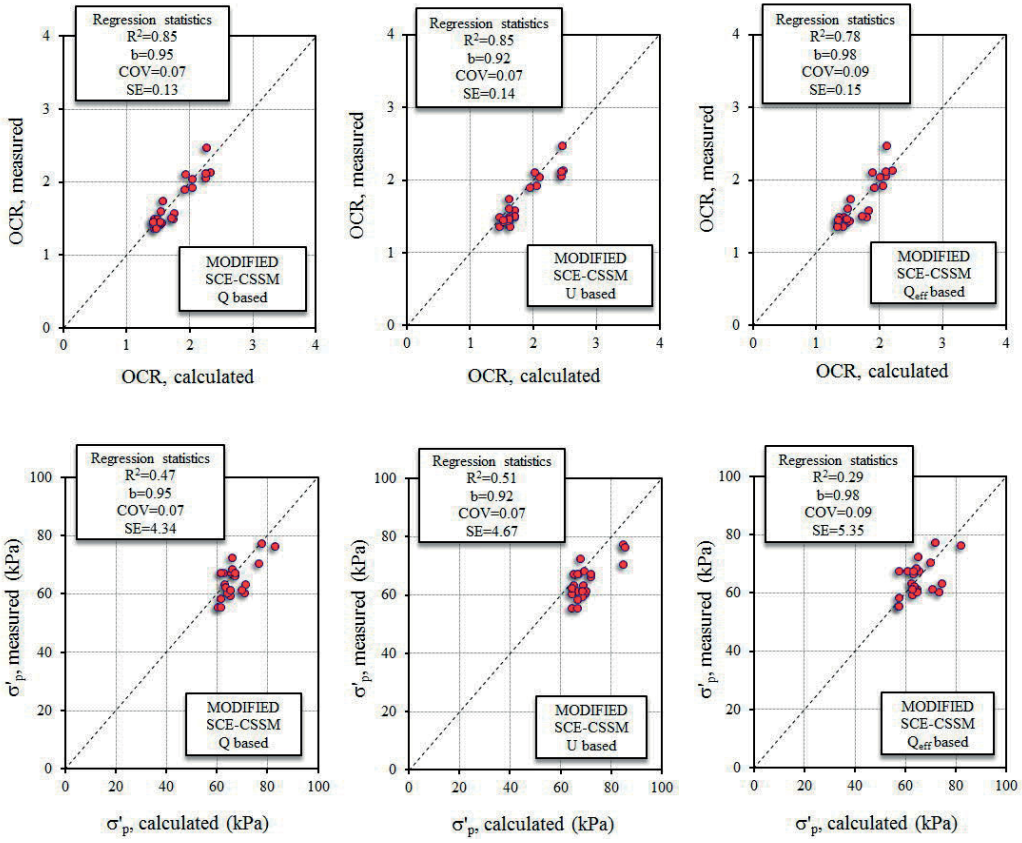

5. SIPOO

5a) Original SCE-CSSM solution